EVALUATION OF NON-SOLVENT METHODS TO CHARACTERIZE RECLAIMED ASPHALT PAVEMENT BINDER

by

Jennifer Elizabeth Michael

A thesis submitted to the Graduate Faculty of
Auburn University
in partial fulfillment of the
requirements for the Degree of
Master of Science

Auburn, Alabama
December 12, 2011

Approved by

Randy C. West, Chair, Director, National Center for Asphalt Technology
David H. Timm, Associate Professor, Civil Engineering
Rod E. Turochy, Associate Professor, Civil Engineering
J. Richard Willis, Assistant Research Professor, Civil Engineering

ABSTRACT

Increases in material costs have led many agencies to consider allowing higher percentages of reclaimed asphalt pavement (RAP) in asphalt mixes. However, as RAP percentages increase, the stiffness of the overall mix is likely to increase as well. Therefore, it is necessary to determine the properties of the RAP binder. Current procedures include conducting a solvent extraction to remove the aged binder from the RAP, distilling the aged binder from the solvent, and testing the recovered binder in accordance with standard binder grading tests. For high RAP content mixes, blending charts are then used to determine either the grade of virgin binder to add to the mixture or the amount of RAP that can be used. However, blending charts assume complete blending of the RAP and virgin binder. This research study examines the use of mix tests and prediction models as an alternative approach to characterizing the RAP mixtures.

Several materials were utilized in this investigation, including 100% virgin, 100% RAP, and plant produced mixtures containing up to 25% recycled materials. Each mix was subjected to dynamic modulus testing. The data from these tests, along with volumetric properties, were used with the Hirsch model and Christensen-Anderson model to backcalculate binder properties. These properties were then compared to measured values from standard binder grading tests. The results indicated that the backcalculation technique was feasible for characterizing RAP binders.

A sensitivity analysis was also performed using laboratory produced mixtures which varied by asphalt type, RAP source, and RAP content (20%, 35%, and 50%). Dynamic modulus tests were conducted and backcalculated binder properties were compared among the contributing factors. The trends were not as expected, with both the dynamic modulus and backcalculated properties exhibiting insensitivity to both binder grade and RAP percentage. It is recommended that further analysis be performed to determine the cause of these insensitivities.

ACKNOWLEDGEMENTS

TABLE OF CONTENTS

LIST OF TABLES

LIST OF FIGURES

CHAPTER 1
INTRODUCTION

1.1 Background

Increases in material costs and reduced availability of high quality aggregates have led

many agencies to consider allowing higher percentages of reclaimed asphalt pavement

(RAP) in asphalt mixes. RAP is a material comprised of both aggregate and aged asphalt

binder. Incorporating RAP as a component in an asphalt mixture requires accounting for

the RAP aggregate and asphalt properties during the mix design process.

There are several issues that must be considered when characterizing RAP for mix

design purposes. The RAP aggregate must be characterized to determine gradation,

aggregate specific gravity (G_{sb}), and other aggregate properties. These properties are

required in order to determine if the blended aggregate properties meet specification

according to AASHTO M 323, Standard Specification for Superpave Volumetric Mix

Design. However, there is concern as to how the aggregate properties are affected

depending on which method was chosen to extract the aggregate from the RAP. Also,

since RAP contains aged binder, the asphalt content of the RAP must first be determined

so that the overall optimum asphalt content (a combination of both aged binder and virgin

binder) can be used in the design. Additionally, the binder rheological properties are also

needed when including higher RAP percentages in the mixture since this will affect the

stiffness of the blended mix. In order to obtain the RAP binder for rheological testing,

only a solvent extraction allows for the binder to be recovered.

Procedures for incorporating RAP into a Superpave mixture were developed by NCHRP Project 9-12, *Incorporation of Reclaimed Asphalt Pavement in the Superpave System* (McDaniel, Soleymani, Anderson, Turner, and Peterson, 2000). These procedures include conducting a solvent extraction to remove the aged binder from the RAP, distilling the aged binder from the solvent, and testing the recovered binder in accordance with standard binder grading tests. For high RAP content mixes, blending charts are then used to determine either the grade of virgin binder to add to the mixture or the amount of RAP that can be used. However, blending charts assume complete blending of the RAP and virgin binder, which has been found to not always be true (e.g. Shah, McDaniel, Huber, and Gallivan, 2007; Huang, Li, Vukosavljevic, Shu, and Egan, 2005). It is thought that at high RAP contents only partial blending occurs. There is interest in revising the mix design process for mixes containing RAP that would better address the partial blending issue and provide a better method for characterizing RAP.

Using mix tests and predictive models to determine binder properties may be a better alternative to the extensive process associated with extracting and testing RAP binders. It may also provide a better indication of how the blended mix will contribute to the overall performance of the pavement. Previous studies have examined the use of mix tests, particularly dynamic modulus (E*), to determine binder characteristics (e.g. Bennert and Dongré, 2009; Tran, Taylor, West, Kvasnak, and Turner, 2009). They found that these mix tests are feasible for characterizing RAP mixes. This investigation focused on using results from mix tests to determine blended binder and RAP binder properties.

1.2 Objectives

Due to increased interest in binder blending of RAP mixes and the potential to characterize these mixtures with simple mix tests, the following objectives were established to further investigate non-solvent methods of characterizing RAP.

1. Determine the most appropriate extraction method to characterize RAP aggregate, specifically aggregate specific gravity (G_{sb}).

2. Find a suitable mix test and prediction model to backcalculate binder properties using two virgin mixes and six 100% RAP mixes.

3. Use the selected mix test to verify the backcalculation technique using plant produced mixes with varying percentages of RAP

4. Evaluate laboratory produced mixes with varying binder grades, RAP percentages, and RAP sources to assess the sensitivity of the method to changes in the binder properties.

1.3 Scope

To accomplish the first objective, four methods were utilized to determine the G_{sb} of virgin and RAP aggregates. Two of the four methods involved extracting the aggregate through either the ignition method or the solvent extraction method. The other two methods involved estimating the G_{sb} using other mix properties. The G_{sb} from the four different methods were statistically compared. To determine the effect of each testing methodology on properties related to G_{sb}, the voids in mineral aggregate (VMA) were computed and a similar comparison was made. An additional analysis was performed to see if the differences between the VMA values affected the calculation of E* using the

Hirsch model, which requires the binder shear modulus (G*), VMA, and voids filled with asphalt (VFA).

The second objective was achieved by performing two different mix tests on two virgin mixes and six 100% RAP mixes. The purpose of using these materials was to eliminate any variability due to the extent at which RAP and virgin binder blends. The two mix tests included relaxation modulus, E(t), and E*. E(t) was tested in accordance to a test method proposed by Alan Carter as part of his dissertation, *Development of a Non-Solvent Based Test Method for Evaluating Reclaimed Asphalt Pavement Mixes*, in 2004. E* was tested in accordance with AASHTO TP 62-07. The Hirsch model was used to backcalculate G* using measured E* data, along with the volumetric properties, VMA and VFA. The Christensen Anderson model (C-A) was used to develop G* master curves and predict the G* and phase angle (δ) at a specified frequency and reference temperature. This allowed high and intermediate critical temperatures to be determined. A comparison was made between the predicted critical temperatures and the actual critical temperatures as determined from standard binder grading test on a dynamic shear rheometer (DSR). Based on the results from the two mix tests, the remainder of the investigation utilized only E* testing as a probable mix test.

Five plant produced mixes containing various percentages of RAP were prepared and tested according to AASHTO TP 62-07. The properties of these mixes were used to verify the backcalculation process using the Hirsch and C-A models. Comparisons were made between the predicted and measured values to assess the accuracy of this procedure for mixes containing RAP.

The sensitivity analysis was performed on 27 laboratory produced mixes, which included three RAP sources, three RAP percentages, and three binder types. Specimens were prepared for E* testing and the results were used with both the Hirsch and C-A models to determine the high critical temperature. The sensitivity of this method to binder changes was assessed.

1.4 Organization of Thesis

The literature review in Chapter Two provides an explanation of current methods used to characterize RAP for the mix design process, a review of previous studies evaluating the extent of binder blending between virgin and RAP binders, and a summary of different mix tests and predictive models used to characterize RAP in lieu of solvent extractions and binder testing. Chapter Three explains the experimental plan that was followed for this investigation. It details two phases that were carried out in this project. Chapter Four describes all of the materials used in this study, including sampling locations and material properties. Chapter Five discusses the methods for determining material properties, sample preparation and test procedures for both E* and E(t) testing. Chapter Six provides results from the extraction method study for determining G_{sb}, E(t) and E* results from the virgin and 100% RAP mixes, and results from the backcalculation procedure using the Hirsch and C-A model. It also discusses the findings from the backcalculation procedure used with the plant produced mixtures and the comparisons between the 27 laboratory produced mixtures. Chapter Seven summarizes the results from this investigation and provides recommendations for using a non-solvent method for characterizing RAP and RAP mixtures.

CHAPTER 2
LITERATURE REVIEW

2.1 Introduction

Many agencies are allowing higher percentages of RAP in asphalt mixes. However, incorporating RAP as a component in an asphalt mixture requires accounting for the RAP properties during the mix design process. Some of the required properties include asphalt content, gradation, G_{sb}, other aggregate properties, and rheological data.

Currently, there are several methods used to extract the RAP binder from the aggregate to determine material properties. However, there is concern about how each extraction method affects those material properties. If the binder is required for rheological testing, a solvent extraction must be conducted in order to remove the aged binder from the RAP. The aged binder is then distilled from the solvent and the recovered binder is tested in accordance with standard binder grading tests. For high RAP content mixes, blending charts are then used to determine either the grade of virgin binder to add to the design mixture or the amount of RAP that can be used. Blending charts, however, assume complete blending of the RAP and virgin binder which does not necessarily occur at high RAP percentages. To address this partial blending issue, there has been an increased interest in developing new methods to characterize mixes containing RAP which may provide a better indication of how the blended mix will contribute to the overall performance of the pavement.

The following literature review summarizes the current mix design process for mixes containing RAP, focusing on methods and evaluations of characterizing the RAP materials and blended binders. It also summarizes several methods and evaluations of using mix tests and predictive models to determine binder properties in lieu of using solvent extractions and recoveries.

2.2 Mix Design for Mixes Containing RAP

2.2.1 Characterization of RAP Materials

The first step to designing a Superpave mix consists of selecting the appropriate materials. The binder, aggregate, and RAP must be selected so that the final mix will meet the climatic and traffic requirements applicable to the paving site.

When RAP is used in a Superpave mix, the RAP aggregate and the RAP binder reduces the amount of virgin aggregate and binder required for the design. Therefore, the RAP properties must be accounted for, specifically the asphalt content, aggregate gradation, specific gravity, and consensus properties. When RAP percentages in excess of 25% are used, it is also important to know the stiffness of the RAP binder so that an appropriate virgin binder can be selected (Shah et al., 2007).

2.2.1.1 Quantification of RAP Asphalt Content

The RAP binder contributes to the overall asphalt content of the mix. Therefore, it is necessary to first determine the asphalt content of the RAP. This can be done by either an ignition oven extraction or a solvent extraction.

2.2.1.1.1 Ignition Oven Extraction

AASHTO T 308, Determining the Asphalt Binder Content of Hot-Mix Asphalt by the Ignition Method, is one standard used for determining the asphalt content. The method

involves burning the binder off of the aggregate in an ignition furnace at 538°C (1000°F). The asphalt content is then calculated as the difference between the initial mass of the sample and the mass of the residual aggregate. This process takes 30 to 45 minutes and does not require the use of any chemical solvents. Because the ignition method burns the binder off of the aggregate, this method does not allow for binder to be recovered and tested.

Certain aggregates, such as dolomitic limestone, can break down in the high temperature furnace producing a higher percentage of fines. This can lead to inaccurate gradations and asphalt contents. If local aggregates obtain characteristics of aggregate breakdown, an analysis should be conducted to compare the mass of a virgin aggregate sample to the residual aggregate sample from the ignition oven in order to attain a correction factor. However, since RAP aggregate cannot be compared to the virgin aggregate, a correction factor cannot be accurately identified for RAP which may lead to erroneous results. Therefore, the correction factor must be estimated based on experience with local aggregates.

2.2.1.1.2 Solvent Extraction

AASHTO T 164, Quantitative Extraction of Asphalt Binder from Hot-Mix Asphalt, is another standard for determining the asphalt content. The solvent extraction method involves removing the binder from the aggregate using a chlorinated solvent, non-chlorinated solvent, or a biodegradable solvent in a centrifuge, reflux, or vacuum extractor. The asphalt content is determined by calculating the differences from the mass of the extracted aggregate, moisture content, and mineral matter in the extract. If a chlorinated or non-chlorinated solvent is used, the extracted asphalt can be recovered by

the Abson method or Rotavapor method following AASHTO T 170, Recovery of Asphalt Binder from Solution by Abson Method, or AASHTO T 319, Quantitative Extraction and Recovery of Asphalt Binder from Asphalt Mixes. Once the asphalt is recovered, additional binder tests can be performed. However, the extraction method takes longer than the ignition oven method and could require harmful solvents that can be expensive when considering the disposal costs.

One of the most common solvents used for the extraction of binder is Trichloroethylene (TCE) (Stroup-Gardiner and Nelson, 2000). This chlorinated solvent is classified as group A5 by the American Conference of Governmental Industrial Hygienist (ACGIH), as indicated in the Material Safety Data Sheet (Trichloroethylene MSDS, 2010). Group A5 is not suspected as a human carcinogen. The permissible exposure limits set by the Occupational Safety and Health Administration (OSHA) per million parts of air (ppm) as a time-weighted average (TWA) over an 8-hour work shift is set at an acceptable ceiling of 200 ppm. The maximum peak concentration above the acceptable ceiling (maximum duration of 5 minutes in any 2-hour period) is 300 ppm. Exposure to high levels of this chemical has been known to cause headaches, dizziness, unconsciousness, or even death (Occupational Safety and Health Guideline for Trichloroethylene Potential Human Carcinogen, 1988). Regulations placed on this solvent by the Clean Air Act of 1990 and the Resource Conservation and Recovery Act (RCRA) have made the use of TCE expensive and difficult (Halogenated Solvent Industry Alliance, 2001).

With the high risks and costs associated with TCE, biodegradable solvents were studied and introduced into the extraction process. A common biodegradable solvent

used for asphalt extraction is d-Limonene. This solvent is the main component of oil

extracted from citrus rinds. It is a safer alternative to the hazardous chemicals found in

chlorinated solvents. However, according to AASHTO T 319, biodegradable solvents are

not suitable when the recovered binder is required for additional testing.

Another alternative solvent is N-Propyl Bromide (nPB). nPB is a non-chlorinated

solvent that has been classified as non-carcinogenic and non-hazardous. The U.S. EPA

has approved nPB under the Significant New Alternatives Policy (SNAP) as a suitable

replacement for ozone depleting chemicals (Enviro Tech International, 2008). Even

though this chemical has been identified as non-carcinogenic, precautions are still

necessary to avoid headaches, dizziness, and nausea (Collins-Garcia, Tia, Roque, and

Choubane, 2000).

A comparison of TCE and four nPB solvents conducted at the National Center for

Asphalt Technology (NCAT) concluded that nPB could be used as a replacement for

TCE. However, one of the nPB solvents showed some incompatibility with polymer-

modified PG 76-22 asphalt. It was recommended that initial comparisons of results for

standard chlorinated solvents and a specific nPB product be evaluated before accepting

that product as a replacement (Stroup-Gardiner and Nelson, 2000).

2.2.1.1.3 Comparison of Extraction Methods in Determining Asphalt Contents

A recent study conducted by NCAT and the University of Nevada Reno evaluated three

methods of obtaining asphalt contents of simulated RAP mixtures. Asphalt contents were

determined using the centrifuge method, the reflux method, and the ignition method.

TCE was used for both the centrifuge and reflux methods; no correction factor was used

in the ignition method. The results showed that all results were significantly lower than

the known asphalt contents. However, the ignition oven produced results closest to the

true asphalt content compared to the other two solvent methods (Kvasnak, West,

Michael, Loria, Hajj, and Tran, 2009).

2.2.1.2 Quantification of RAP Aggregate Properties

2.2.1.2.1 RAP Aggregate Testing for Mix Designs

After the extraction process, the recovered aggregate can be used to determine the

gradation, consensus properties, and G_{sb}. The gradation of the RAP aggregate must be

determined so that the final blended aggregate gradation falls within the limits specified

by AASHTO M 323-07, Superpave Volumetric Mix Design. The consensus properties,

including fine and coarse aggregate angularity, flat and elongated particles, and sand

equivalency must also be determined. It should be noted that the Superpave

specifications for the consensus properties apply to the blended aggregate. However, the

individual RAP aggregate properties may be useful in determining how much RAP can

be used in a blend.   The G_{sb} is used to calculate the voids in mineral aggregate (VMA),

which is a limiting criterion in the Superpave mix design specifications. The G_{sb} is

calculated from the G_{sb} of each aggregate used in the blend. However, studies have

shown that these aggregate properties are affected by the various extraction methods.

2.2.1.2.2 Comparison of Extraction Methods on RAP Aggregate Properties

Research conducted for the Arkansas State Highway and Transportation Department

(AHTD) looked at changes in gradation and coarse aggregate G_{sb} caused from using the

ignition method. Results showed that there was little change in gradation and the

changes in coarse aggregate G_{sb} could be attributed to testing variability (Hall and

Williams, 1999).

Similar results were found in a study conducted for the Virginia Transportation Research Council (VTRC). An evaluation of ten mix designs, using nine aggregate sources, was conducted to compare the gradation, G_{sb}, and consensus property results of virgin aggregates recovered from the ignition method. The evaluation determined that results for aggregate recovered from the ignition oven were not significantly different from the original results for gradation, FAA, and flat and elongated particles. However, significant differences were found between the original and ignition oven recovered coarse and fine aggregates' G_{sb} for approximately half of the designs tested (Prowell and Carter, 2000). Since the G_{sb} is used to calculate VMA, it is important to determine which method of extraction produces the least amount of error.

Considering the differences found in G_{sb} of extracted aggregates, NCHRP Report 452 recommended using the calculated effective specific gravity (G_{se}) to estimate the G_{sb} for determination of VMA. The G_{se} is dependent on the asphalt content, maximum specific gravity (G_{mm}), and specific gravity of the binder (G_b). Results from the study conducted for the VTRC concluded that G_{sb} from the aggregate recovered from the ignition method produced lower error in VMA than the estimated G_{sb} using G_{se} (Prowell and Carter 2000).

The NCAT-UNR study also evaluated the effect of three extraction methods on G_{sb} of laboratory produced RAP. The G_{sb} of the original aggregate was compared to that of aggregate recovered from the centrifuge, reflux, and ignition oven extracted aggregate, as well as to the estimated G_{sb} from the G_{se}. The results indicated that the estimated G_{sb} was the most similar to the original G_{sb} value. However, for this particular experiment, the asphalt absorption used in the estimation was calculated using known values of G_{se},

G_{sb}, and G_b, which are unknowns for RAP aggregates. It was recommended that local asphalt absorption values be used in the estimation (Kvasnak et al., 2009).

2.2.1.2 RAP Binder Properties

In the Superpave mix design specification, AASHTO M323, it is necessary to determine the binder grade of the RAP asphalt when using more than 25% RAP. This process requires the RAP asphalt to be extracted, and recovered through either the Rotavapor or Abson Recovery method, then classified in accordance with AASHTO M320. Once the critical temperatures for the recovered RAP binder are determined, blending charts are used to determine the appropriate virgin binder grade or percentage of RAP to be used in the design.

2.2.2 Characterization of Blended Binders

Methods for creating blending charts are described in the NCHRP Report 452 (McDaniel and Anderson, 2001). There are two methods that can be employed; using a known RAP percentage, or using a known virgin binder grade. The first method requires a desired final blended binder grade, percentage of RAP, and recovered RAP properties. The high, intermediate, and low critical temperatures of the virgin binder can be determined separately by Equation 2.1.

$$T_{virgin} = \frac{T_{Blend} - (\% RAP * T_{RAP})}{(1 - \% RAP)}$$

Equation 2.1

where,

T_{Virgin} = critical temperature of the virgin asphalt binder

T_{Blend} = final desired critical temperature of the blended asphalt binder

$\% RAP$ = percentage of RAP expressed as a decimal

T_{RAP} = critical temperature of recovered RAP binder

The other method requires a desired final blended binder grade, virgin asphalt binder grade, and recovered RAP properties. The appropriate amount of RAP can be determined by Equation 2.2,

$$\% RAP = \frac{T_{Blend} - T_{Virgin}}{T_{RAP} - T_{Virgin}}$$
Equation 2.2

These linear blending equations were found to be appropriate if the RAP binder is tested in both an unaged and RTFO-aged condition as specified in NCHRP Report 452. However, blending charts assume complete binder blending which has not always been found to be true in previous studies (e.g. Shah et al., 2007; Huang et al., 2005).

2.2.2.1 Previous Studies on Binder Blending of Hot Mix Asphalt with RAP

There has been concern in the past that RAP asphalt does not contribute to the effective binder of a mix and acts basically as 'black rock'. In other words, the asphalt in the RAP does not blend with the new virgin binder. The other extreme case would be to assume that 100% blending occurs between both the RAP binder and virgin binder. Several research studies have evaluated the interaction of RAP in asphalt mixes to determine what actually occurs when using RAP in an asphalt mix. It is generally accepted that there is some blending of the RAP and virgin asphalt, however the extent of blending is still under investigation.

One study conducted as part of the NCHRP 9-12 project evaluated three blending scenarios. The first scenario simulated the actual practice of blending the RAP with the virgin materials as would occur at the plant. The second scenario involved extracting the binder from the RAP and combining only the RAP aggregate with the virgin materials, thereby treating the RAP as black rock. The third scenario involved extracting and

recovering the RAP binder and then completely blending the recovered binder with the virgin binder prior to mixing with the aggregates to simulate complete blending. Three RAP sources, two RAP percentages (10% and 40%), and two asphalt binders were evaluated in this study. Shear tests at high temperatures and indirect tensile creep and strength tests at low temperatures were performed on each of the mixtures to evaluate the effects of the different scenarios. In general, there were no significant differences found among the three scenarios for the 10% RAP mixtures. At the 40% RAP level, there was a significant difference found with the RAP mixtures treated as black rock compared to both the actual practice method and the complete blending method with the black rock having a lower stiffness at both high and low temperatures and higher deformations at high test temperatures. The results of the actual practice case and the complete blending case were not significantly different. These findings indicate that RAP does not act like black rock, and at least some blending occurs between the RAP binder and virgin binder (McDaniel et al., 2000).

A study conducted by Huang et al. in 2005 also evaluated how much aged RAP binder blended with virgin binder under normal mixing conditions. The fine fraction of a RAP source, material passing the No. 4 sieve, was blended with virgin aggregate retained on the No. 4 sieve so that the virgin and RAP particles could be distinguishable after mixing. An extreme case was first considered by dry mixing RAP at varying proportions (10%, 20%, and 30%) with virgin aggregate for approximately 3 minutes at an initial mixing temperature of 375°F. The virgin aggregate and RAP were then separated on a No. 4 sieve and the asphalt contents were determined for both fine and coarse portions. Regardless of the RAP percentage used, the asphalt content of the RAP was reduced by

about 11%, indicating that a small portion of the aged binder was available for blending (Huang et al., 2005).

In this same study, a second experiment consisted of mixing 20% of the fine RAP fraction with virgin aggregate retained on the No. 4 sieve and PG 64-22 binder for 3 minutes at 375°F. The mix was then sieved into the coarse and fine parts, where the fine part consisted of only RAP particles and virgin binder. Staged extractions were performed by soaking the fine part in TCE for only 3 minutes and then decanting the solution. The first soaking was considered to remove the outermost layer of blended binder. A second soaking obtained the asphalt binder of the second layer, and so on. This staged extraction was repeated four times to obtain four different asphalt layers. The Abson recovery method was used to recover the binder from the four layers and standard binder tests were performed. The results showed that the 3rd and 4th layer (closest to the RAP aggregate) was stiffer than the outer two layers, indicating that the RAP mixture forms a 3 layered composite material (RAP aggregate, coated with aged RAP binder, and then coated with new virgin binder) (Huang et al. 2005). These results indicate that RAP does not act like "black rock" nor does 100% blending between RAP and virgin binders occur.

A study jointly funded by seven north central states (Illinois, Indiana, Iowa, Michigan, Minnesota, Missouri, and Wisconsin) examined regional materials and higher RAP contents in the Superpave mix design method. Mixes were developed with RAP percentages from 0% to 50% RAP. The binders were extracted and their properties were determined in terms of critical temperatures. It was determined that blending the aged RAP binder and new virgin binder could be charted as an approximately linear relation.

A straight line connected the critical temperatures from 0% RAP to 100% RAP. The critical temperatures for RTFO and RTFO-PAV recovered binders from the 25% RAP mixtures fell on the straight line, however, linear blending did not occur in the unaged binder (McDaniel and Nantung, 2005). A later study conducted by one of the same researchers evaluated the binder extracted from plant-produced mixes. The plant produced mixes contained 0%, 15%, 25%, and 40% RAP and used two different virgin binders (PG 64-22 and PG 58-28). The PG grading indicated that the asphalt binder did not stiffen linearly with increasing RAP percentages, which is generally assumed when using blending charts. Although there were some changes in the measured properties at 40% RAP, it was not proportional to the amount of RAP added to the mixture (Shah et al., 2008).

Since many of the studies identified in the literature search have shown that 100% blending does not occur, there is some concern on whether or not blending charts are really the best method for designing high RAP mixes. Some researchers have proposed using E* or other mix properties and a predictive model to backcalculate the effective binder properties. These results would provide a better representation of the actual blending that occurs in mixtures. The following section describes the methods for backcalculating effective binder properties.

2.3 Methods for BackCalculation

2.3.1 Mix Tests

Considering the costs and health hazards of chemicals used in the extraction and recovery process, the time involved in obtaining RAP properties, and the false assumption of using linear blending charts, there has been an interest in developing other methods to

characterize mixes containing RAP. One method for determining effective binder

properties is using mix tests and predictive models to backcalculate the blended binder

stiffness. Two mix tests that have been explored are the E* and the indirect tension

relaxation modulus, E(t).

2.3.1.1 E* Definition

E* is a material property that is related to mixture performance. It is a measure of a

mixtures' stiffness when subjected to sinusoidal loading and can be defined as the

absolute value of the maximum stress amplitude divided by the maximum recoverable

axial strain amplitude. The E* test, AASHTO TP 62-07 Determining Dynamic Modulus

of Hot-Mix Asphalt, applies a sinusoidal load to the specimen at different frequencies and

temperatures. These frequencies and temperatures are used to simulate different traffic

speeds and climates. In addition to E* data, the phase angle (δ) is also measured which is

defined as the lag between the applied stress and the resulting strain. Specimens that

display a purely elastic response would have a δ equal to 0° and specimens that display a

purely viscous response would have a δ equal to 90°.

A useful tool for analyzing this data is through the use of master curves where E*

is plotted against the reduced frequency on a log-log scale. Master curves use the

principle of time-temperature superposition. The measured data at different temperatures

are shifted to a reference temperature with respect to the loading frequency until a single

smooth curve is constructed. This describes the material's dependency on the loading

rate. The modulus is expected to increase as the loading rate increases. At lower

frequencies, the material will be less stiff due to the viscoelastic nature of the material.

The following master curve development procedure follows the AASHTO Designation PP 61, Standard Practice for Developing Dynamic Modulus Master Curves for Hot Mix Asphalt Using the Asphalt Mixture Performance Tester (AMPT). The first step in constructing a master curve for E* data is to choose a standard reference temperature. This reference temperature is used to shift the data measured at different temperatures with respect to the loading frequency until the curve merges into a single, smooth line. The following equation describes the shifted E* data.

$$\log(E^*) = \delta + \frac{(Max - \delta)}{1 + e^{\beta + \gamma(\log \omega_r)}}$$
Equation 2.3

where,

E*   = dynamic modulus, psi

ω_r = reduced frequency, Hz

δ, β, and γ = the fitting parameters

Max   = the limiting maximum modulus, psi

The temperature shift factors are incorporated into the equation above through the reduced frequency variable as shown in Equation 2.4,

$$\log(\omega_r) = \log(\omega) + \log[a(T)]$$
Equation 2.4

where,

ω = loading frequency, Hz

a(T) = shift factor as a function of temperature

The shift factor is calculated using Equation 2.5,

$$\log[a(T)] = \frac{\Delta E_a}{19.14714}\left(\frac{1}{T} - \frac{1}{T_r}\right)$$
Equation 2.5

19

where,

ΔE_a = activation energy (treated as a fitting parameter)

T   = test temperature, °K

T_r = reference temperature, °K

The limiting maximum modulus is estimated from HMA volumetric properties using the

Hirsch model and a limiting binder modulus of 1 GPa as shown in Equation 2.6 and 2.7,

$$E^*_{Max} = P_C \left[4,200,000\left(1 - \frac{VMA}{100}\right) + 435,000\left(\frac{VFAxVMA}{10,000}\right) + \frac{1 - P_C}{\frac{\left(1 - \frac{VMA}{100}\right)}{4,200,000} + \frac{VMA}{435,000(VFA)}} \right]$$ **Equation 2.6**

where,

$$P_C = \frac{\left(20 + \frac{435,000(VFA)}{VMA}\right)^{0.58}}{650 + \left(\frac{435,000(VFA)}{VMA}\right)^{0.58}}$$ **Equation 2.7**

where,

E^*_{max} = the limiting maximum HMA dynamic modulus, psi

VMA = voids in mineral aggregate, %

VFA = voids filled with asphalt, %

To make the master curve development simpler, these functions can be set up in

an Excel spreadsheet. The δ, β, γ, and ΔE_a parameters can be obtained through numerical

optimization using the Excel Solver function. The sum of the squared errors (SSE)

should be calculated between the log of the measured E* values and the log of the E*

values predicted from Equation 2.3. The Solver function then minimizes the SSE by

changing the fitted parameters. The predicted E* can then be plotted against the log of the reduced frequency in order to obtain a fitted curve representing E* at different loading rates for one referenced temperature.

Since mix stiffness affects pavement performance, E* can be used for other applications besides just backcalculating effective binder properties for mix design purposes. For example, the Mechanistic-Empirical Pavement Design Guide (MEPDG) was developed in order to design pavements based on a mechanistic approach by evaluating the structural damage that is probable during its design life. The MEPDG uses E* data to predict rutting and fatigue cracking susceptibility for this purpose. Since E* testing shows promise for both mix design and pavement design applications, it is necessary to evaluate any sensitivities that certain factors may have on E*. Several researchers have already done this by evaluating the effects on E* due to different contributing factors.

2.3.1. 2 Sensitivities with E* testing

Several factors have been found to be sensitive in the E* tests. These factors include RAP percentage, asphalt content, asphalt type, gradation, VMA, VFA, and test temperature. A study conducted in 2005 by Daniel and Lachance evaluated E* of mixtures containing 0%, 15%, 25%, and 40% RAP contents. The 15% RAP mix was stiffer than the virgin mix, but the 25% and 40% RAP mixtures were more similar in stiffness to the virgin mixture. The authors explained that the results of the 25 and 45% RAP mixes were affected by finer gradations that resulted in higher VMA and VFA.

A similar study by Li et al. (2008) evaluated asphalt mixtures containing two RAP sources, two RAP percentages (20% and 40%), and two asphalt binders (PG 58-28 and

PG 58-34). One RAP came from a single source (SS) and the other RAP was a

combination of multiple sources (MS) milled in Minnesota. The SS RAP was found to

have a stiffer binder than the MS RAP. Control mixtures with no RAP were also mixed

with the two virgin asphalt binders resulting in ten different mixtures. The gradation of

each RAP mixture was designed to be as similar to the control mix as practically

possible. The asphalt contents varied from 5.05% to 5.38% on the RAP mixtures and the

control mix had an asphalt content of 5.85%. In general, the mixtures containing RAP

had a higher E* than the control mixture, especially at the lower frequencies. At the

same lower frequencies, the mixtures containing 40% RAP had an E* equal to or higher

than the 20% RAP mixture. This suggests that mixtures with high RAP percentages

would be less susceptible to rutting since lower frequencies correspond to slow traffic

loading. At the higher frequencies, almost all of the mixes with 20% RAP had a higher

E* compared to the 40% RAP mixes. This was attributed to difficulties of measuring E*

at low temperatures. An analysis of variance (ANOVA) to evaluate the effect of RAP

percentage, binder type, test temperature, RAP source, and test frequency found all

factors significant except for the RAP source. The results indicated that at lower

frequencies, the mixture with SS RAP had higher E* than mixtures containing MS RAP.

However, no clear trend between the RAP sources was observed at the higher

frequencies. This was most likely due to the stiffer binder in the SS RAP which typically

contributes more to the mix properties at lower frequencies, or higher temperatures (Li,

Marasteanu, Williams, and Clyne, 2008).

2.3.1.3 E(t) Definition

Another mix property that has been evaluated for estimating the effect of RAP binder is

relaxation modulus, E(t), which is the reciprocal of creep compliance where the time-

dependent strain is measured from an applied static load. Methods have been developed

to directly measure E(t) by applying a known strain to the specimen for a designated time

limit and measuring the stress as the specimen relaxes. Because of the viscoelastic

behavior of asphalt pavements, a target strain can first be determined so that the specimen

is not damaged during testing.

2.3.1.4 Sensitivities with E(t) testing

A study was conducted at Auburn University which measured E(t) of mixes prepared

with two aggregate sources, two RAP sources, two virgin binders, and varying RAP

percentages up to 100%. The initial E(t) and the curvature coefficient were determined

for each mix. The curvature coefficient is a measure of the ability of the mix to relax

over time. As expected, when more RAP was incorporated into the mix, the initial E(t)

increased and the curvature coefficient decreased. An ANOVA analysis determined that

the E(t) test was not sensitive to gradation, aggregate source, or RAP source. However,

both RAP sources had very similar PG grades and, therefore, an additional analysis was

performed on two virgin mixes to determine if the test was sensitive to binder grade using

a PG 64-22 and PG 76-22. As expected, a slight difference was found between the two

binders at warmer temperatures but the difference was not significant. An analysis

addressing the increase in RAP percentage was also evaluated. The tests that were

performed at 5°C showed that the addition of 15% RAP doubled the initial E(t) but there

were no significant increases observed with increasing RAP percentages beyond 15%.

The curvature coefficients of the 0% and 15% RAP mixes were similar and a significant difference was only observed in the higher RAP mixes compared to the control. However, there was no significant difference found between 50% and 100% RAP. At 22°C, there was a significant increase in initial E(t) with the 15% RAP design, but no significant difference between 15% and 25% RAP. Also, both the 50% and 100% RAP mixtures had statistically similar E(t) values but were significantly higher than the lower percentages. It was concluded that the E(t) test is sensitive to the addition of RAP and the relationship between modulus and RAP percentage is non- linear (Carter, 2004).

2.3.2 Predictive Models

Several predictive models have been developed so that binder testing results could be used to predict E* or vice versa. The following sections discuss the development, evaluation of fit, and the sensitivities of three current predictive models. Also discussed is how one of these models has been used to backcalculate the binder properties, specifically G* and δ. Additionally, a section is included on using E(t) to backcalculate the binder properties.

2.3.2.1 Development and Evaluation of Predictive Models

2.3.2.1.1 Witczak 1-37A Model

The Andrei, Witczak, and Mirza revised model, also known as the Witczak 1-37A model, developed in 1999 is shown in Equation 2.8. In this model, dynamic modulus is a function of aggregate gradation, mix volumetrics, loading frequency, and binder viscosity (Bari and Witczak 2006).

$$\log E^* = -1.25 + 0.029\rho_{200} - 0.0018(\rho_{200})^2 - 0.0028\rho_4 - 0.058V_a - 0.822\frac{V_{beff}}{V_{beff} + V_a}$$

$$+ \frac{3.872 - 0.0021\rho_4 + 0.004\rho_{38} - 0.000017(\rho_{38})^2 + 0.0055\rho_{34}}{1 + e^{(-0.603313 - 0.313351\log(f) - 0.393532\log(\eta))}}$$

Equation 2.8

where,

E*   = dynamic modulus of mix, 10^5 psi

η = viscosity of binder, 10^6 Poise

f   = loading frequency, Hz

ρ_{200} = % passing #200 (0.075 mm) sieve

ρ_4 = cumulative % retained on #4 (4.76 mm) sieve

ρ_{38} = cumulative % retained on 3/8 in. (9.5 mm) sieve

ρ_{34} = cumulative % retained on ¾ in. (19 mm) sieve

V_a = air voids, % by volume

V_{beff} = effective binder content, % by volume

      The binder viscosity variable used in this model is based on a linear relationship
between log log viscosity to log temperature as shown in Equation 2.9. When these
variables are plotted, the parameter VTS is found as the slope of the line and the
parameter A is the intercept. If the viscosity data is not available, viscosity can be
calculated from Equation 2.10 using G* and δ information (Bari and Witczak 2006).

$$\log \log \eta = A + VTS \log T_R \qquad\qquad \textbf{Equation 2.9}$$

$$\eta = \frac{G*}{10}\left(\frac{1}{\sin \delta}\right)^{4.8628} \qquad\qquad \textbf{Equation 2.10}$$

where,

η = binder viscosity, cP

A, VTS = regression parameters

T_R = temperature, Rankine

G*   = binder complex shear modulus, Pa

δ = binder phase angle, degree

During the validation of the 1-37A model, a database consisting of 2750 E*

values measured on 205 HMA mixtures were compared to the predicted values. The

comparison had a very high correlation with a correlation coefficient (R^2) of 0.94 in

logarithmic scale. However, when the E* database was expanded to include a total of

7400 E* values measured on 346 HMA mixtures, the correlation dropped to 0.88 (Bari

and Witczak, 2006).

A field evaluation of the Witzcak 1-37A model was conducted using the

Superpave binder properties and the relationship developed between those properties and

the binder viscosity. Five pavement construction locations across the United States were

considered and G* and δ values were measured for unaged, RTFO, and PAV aged

binders, as well as the volumetric mix properties. When comparing the predicted E*

values to the measured E* values, the RTFO binder data generally provided the highest

correlation. However, the model tended to overestimate E* at E* values below 125,000

psi for all three binder aging conditions. This was attributed to the Witzcak 1-37A

prediction model being developed using traditional viscosity measurements whereas this

evaluation used Superpave binder properties to calculate viscosities using Equation 2.9.

The difference in these parameters is most likely due to the fact that the A-VTS

relationship does not consider the effect of loading frequency. It was recommended that

actual E* measurements be made when the stiffness of the mix is anticipated to be below

125,000 psi (Dongré, Myers, D'Angelo, Paugh, and Gudimettla, 2005).

2.3.2.1.2 Witczak 1-40D Model

Since viscosity of the binder is not required in the Superpave Performance Grading

System and studies have indicated sensitivity to the relationship shown in Equation 2.10,

the Witczak 1-37A model was revised to incorporate the Superpave binder properties, G*

and δ, in lieu of frequency and viscosity. This model, developed in 2006 by Bari and

Witczak, is referred to as the Witczak 1-40D prediction model and it is shown in

Equation 2.11.

$$\log E^* = -0.349 + 0.754(G^{*-0.0052})x \begin{pmatrix} 6.65 - 0.032\rho_{200} + 0.0027\rho_{200}^2 \\ + 0.011\rho_4 - 0.0001\rho_4^2 + 0.006\rho_{38} \\ - 0.00014\rho_{38}^2 - 0.08V_a - 1.06\left(\dfrac{V_{beff}}{V_a + V_{beff}}\right) \end{pmatrix}$$
$$+ \frac{2.56 + 0.03V_a + 0.71\left(\dfrac{V_{beff}}{V_a + V_{beff}}\right) + 0.012\rho_{38} - 0.0001\rho_{38}^2 - 0.01\rho_{34}}{1 + e^{(-0.7814 - 0.5785\log G^* + 0.8834\log\delta)}}$$

<div align="right">**Equation 2.11**</div>

where,

E*   = dynamic modulus, psi

ρ_{200} = % passing #200 sieve

ρ_4 = cumulative % retained on #4 sieve

ρ_{38} = cumulative % retained on the 3/8 in. sieve

ρ_{34} = cumulative % retained on the 3/4 in. sieve

V_a = air voids, % by volume

V_{beff} = effective binder content, % by volume

G*   = dynamic shear modulus of binder, psi

δ   = phase angle of binder associated with G*, degree

The Witczak 1-40D Model was developed and then validated using the expanded

database of 7400 measured E* values from 346 different mixes. The measured values

were compared to the respective predicted E* values through a goodness of fit correlation and the R^2 value was approximately 0.90 for the logarithmic scale (Bari and Witczak, 2006).

2.3.2.1.3 Hirsch Model

The Hirsch model was developed by Christensen, Pellinen, and Bonaquist in 2003 to analyze the effect of changes in air void content, VMA, VFA, and binder stiffness. It is based on the law of mixtures which represents the mechanical response of two separate phases in parallel. It can also be derived for phases in series. T.J. Hirsch first developed a variation of the law of mixtures by combining the parallel and series arrangement of the phases in order to model the mechanical behavior of asphalt. Three versions of the Hirsch model were evaluated, consisting of a mastic version, a simple version, and a transition zone version. Ultimately, the simple version, which is a function of VMA, VFA, and G*, was chosen as the best model, which is shown in Equation 2.12 and 2.13 (Christensen, Pellinen, and Bonaquist, 2003).

$$E^* = P_C \left[4,200,000 \left(1 - \frac{VMA}{100} \right) + 3G^* \left(\frac{VFAxVMA}{10,000} \right) \right]$$
$$+ (1 - P_C) \left[\frac{1 - (VMA/100)}{4,200,000} + \left(\frac{VMA}{3(VFA)G^*} \right) \right]^{-1}$$

Equation 2.12

where,

$$P_C = \frac{\left(20 + \frac{VFAx3G^*}{VMA} \right)^{0.58}}{650 + \left(\frac{VFAx3G^*}{VMA} \right)^{0.58}}$$

Equation 2.13

E*   = dynamic modulus, psi

VMA = voids in mineral aggregate, %

28

VFA = voids filled with asphalt, %

G* = shear dynamic modulus of binder, psi

The model was developed using a database consisting of 206 E* values measured on 18 mixtures using 8 binders and 5 different gradations. A correlation of 0.98 was found between the measured and predicted values (Christensen et al., 2003).

2.3.2.1.4 Model Comparison

Christensen et al. evaluated the 1-37 A and Hirsch models using measured E* data collected by Witczak and his associates for a sensitivity study. Mixes were used from the Arizona DOT, which varied by air void and asphalt content. The standard error for the Hirsch model was 41% compared to the Witczak 1-37A model with 45%. However, the experimental standard error was only 20%. It was concluded that although the measured values were more accurate, both model predictions were suitable for practical design applications. In fact, when both predicted modulus values were plotted against each other, they were in close agreement. Since the agreement of the two models was so close, the simpler Hirsch model would be more effective in predicting E* values (Christensen, Pellinen, and Bonaquist, 2003).

In a study conducted by Dongré et al., the predicted E* values using the Hirsch model were found to be closer to the measured values when compared to the Witczak 1-37A model. This was attributed to the Hirsch model using G* of the binder as a direct input rather than using a second relationship to convert G* to viscosity as done in the Witczak 1-37A model (Dongré et al., 2005).

When the Hirsch model was reevaluated by Bari and Witczak in 2006 using the database containing 7400 data points from 346 mixes, the correlation decreased to 0.61

showing very poor prediction capabilities. However, correlation results have varied by research project. When the three models were evaluated with ten different mixes from the 2006 NCAT Test Track, the Hirsch model produced the highest correlation of 0.71 in log scale between the predicted and measured E* values. The Witczak 1-37A model was unreliable, showing a high amount of scatter in the data and the Witczak 1-40D model tended to over predict E* values, especially at the lower dynamic moduli values (Robbins, 2009).

The Hirsch model has been found to provide reasonable results in predicting E* values. The fact that it only requires three input parameters (VFA, VMA, and G*) makes this model very desirable for use in predicting E*. The simplicity of this model compared to both Witczak models also makes this model desirable for use in backcalculating G* using the mix modulus, E*. The following section will discuss the use of the Hirsch model for backcalculation techniques.

2.3.2.2 Backcalculation of G*

2.3.2.2.1 G* Definition

The shear modulus, G*, is the binder's resistance to deformation when repeatedly sheared. It is defined as the absolute value of the maximum shear stress amplitude divided by the maximum recoverable shear strain amplitude for a material subjected to shearing in a sinusoidal load form. Once G* data are obtained through either direct measurement or backcalculation techniques, a master curve should be developed to present the binder moduli. Christensen and Anderson developed a master curve for G* which is referred to as the Christensen-Anderson model (C-A). This model is shown as Equation 2.14 (Christensen and Anderson 1992).

$$G^* = G_g \left[1 + \left(\frac{\omega_c}{\omega_r} \right)^k \right]^{-1/k}$$

Equation 2.14

where,

G_g = glassy modulus, typically 1GPa

ω_c = crossover frequency, rad/s

ω_r = reduced frequency, rad/s

k = shape parameter

The temperature shift factors are incorporated into the equation above through the reduced frequency variable as shown in Equation 2.15,

$$\log(\omega_r) = \log(\omega) + \log[a(T)]$$

Equation 2.15

where,

ω = loading frequency, rad/s

$a(T)$ = shift factor as a function of temperature

The shift factor is calculated using the Williams-Landel-Ferry Equation 2.16 for temperatures above the reference temperature. For temperatures below the reference temperature, the Arrhenius equation is used shown in Equation 2.5.

$$\log[a(T)] = \frac{-C_1(T - T_r)}{(C_2 + T - T_r)}$$

Equation 2.16

where,

$a(T)$ = shift factor

C_1, C_2 = empirical constants (treated as fitting parameters)

T = test temperature, °K

T_r = reference temperature, °K

The fitting parameters (C_1, C_2, ω_C, and k) are obtained through numerical optimization using the Excel Solver function. The SSE should be calculated between the log of the measured G* values and the log of the G* values predicted from Equation 2.14. The Solver function then minimizes the SSE by changing the fitted parameters. The predicted G* can then be plotted against the log of the reduced frequency in order to obtain a fitted curve representing the G* at different loading rates for one referenced temperature.

The δ is also an important parameter to obtain to characterize the viscoelasticity of binder. Christensen and Anderson developed a prediction model for constructing δ master curves as shown in Equation 2.17.

$$\delta = \frac{90}{1 + \left(\dfrac{\omega_c}{\omega_r}\right)^k}$$
Equation 2.17

where,

δ = phase angle, deg

ω_C = cross over frequency, rad/s

ω_r = reduced frequency, rad/s

k = shape parameter

These functions can be input into an Excel spreadsheet to simplify the calculations. The Solver function can then be used for numerical optimization, adjusting the shape parameter and the crossover frequency to produce the best fit line.

2.3.2.2.2 Hirsch Model for Backcalculation of G*

Because of the simplicity of the Hirsch model, G* values can easily be obtained by using the Solver or Macro functions in Excel to backcalculate G* using VFA, VMA, and E*. A study conducted by Bennert and Dongré in 2009 evaluated the feasibility of using the

32

Hirsch model for backcalculation by predicting the G* from several virgin mixtures and comparing them to the G* measured by the DSR. A comparison of the master curves developed for both the predicted and measured G* were in close agreement with each other. When comparing the measured to predicted G*/sinδ, a difference of 14.5% was observed. This was considered reasonably accurate considering that the AASHTO T 315 specification, Standard Method of Tests for Determining the Rheological Properties of Asphalt Binder Using a Dynamic Shear Rheometer (DSR), allows a difference of 9% for two different results determined by a single operator.

The next phase of the Bennert and Dongré study evaluated the feasibility of using the Hirsch model to backcalculate G* of mixes containing RAP. The backcalculated G* results were higher when 15% and 20% RAP was included in the mix. However, the 25% RAP mixture had backcalculated G* values more similar to the 15% RAP mix and backcalculated δ values more similar to the 0% RAP mix. A comparison between the predicted G* to the measured G* for the RAP mixes indicated that the degree of blending for the 15% and 20% RAP mixes was not as thorough as the 25% RAP mix.

A study conducted by Tran et al. in 2009 also evaluated the use of the Hirsch model to backcalculate G*, and ultimately determine the binder critical high temperature. The critical high temperature is the temperature at which RTFO aged G*/sin(δ) = 2.2 kPa. The temperature at which the unaged G*/sin(δ) = 1.0 kPa is also required to determine the critical high temperature of the binder. Plant produced mixtures were sampled from the 2006 NCAT Test Track for this study. AMPT samples were made from 13 mixtures which varied in binder and aggregate type. The binder was also sampled during the same time so that DSR results could be compared to the

backcalculated binder properties. The analysis concluded that the Hirsch model tended to underestimate G* at higher testing temperatures. This was attributed to the fact that the Hirsch model was calibrated with E* data measured on laboratory produced mixtures and this study used plant produced mixtures. The errors caused by the backcalculation further influenced the determination of the binder high critical temperature with differences between the measured and backcalculated high critical temperatures ranging between 0.5 to 15.1°C, which is approximately 2.5 performance grades. The Hirsch model was calibrated using RTFO aged G* data. It was concluded that the Hirsch model should be recalibrated using unaged G* data, since the determination of the binder critical high temperature requires both unaged and RTFO aged binder properties. For mixtures containing RAP, it would be possible to base the critical high temperature on only RTFO aged binder properties, considering the variability of the RAP materials in the field (Tran, Taylor, West, Kvasnak, and Turner 2009).

2.4 Summary

When designing an asphalt mixture which contains RAP, the RAP has to be characterized in order to fully account for all of the material properties which contribute to the final blend. The first process in characterizing RAP is determining the asphalt content by means of either the ignition oven or solvent extraction. Although there are advantages and disadvantages to both methods, one research study mentioned previously by Kvasnak et al. in 2009 found that the ignition oven produced asphalt contents closest to the original asphalt content when evaluating laboratory produced RAP. For this reason, along with the benefit of being a quick method which does not require any chemical

solvents, the ignition oven method is the most practical extraction method for obtaining an accurate asphalt content of RAP.

The residual aggregate is retained after the extraction process to test the material properties of the RAP aggregate. These tests include a gradation analysis, consensus properties, and G_{sb}. Because it has been found that the ignition oven method can cause aggregate breakdown of certain types of aggregates, a study was conducted by Prowell et al. in 2000 to check the accuracy of aggregate tests on ignition oven extracted aggregates. The evaluation determined that aggregate recovered from the ignition oven resulted in accurate results in the gradation, FAA, and flat and elongated analysis. However, there were mixed results on determining the appropriate G_{sb} for calculating VMA. The Prowell et al. study concluded that the G_{sb} from the ignition oven extracted aggregate resulted in a more accurate calculation of VMA, whereas the study conducted by Kvasnak et al. in 2009 concluded that an estimation of G_{sb} using the G_{se} produced more accurate results when calculating VMA. The difference in results is most likely due to the different types of aggregates tested in the studies.

The final RAP characterization that must be performed is determining the RAP binder properties. At high RAP contents, the aged binder may significantly stiffen the final binder grade of the mixture. Therefore, it is necessary to determine the binder grade of the RAP asphalt when using more than 25% RAP. The binder grade is determined by testing the recovered RAP binder in the DSR at a high temperature as if it were original, unaged binder. The remaining binder is RTFO-aged and tested in the DSR and Bending Beam Rheometer (BBR). From these tests, the critical temperatures can be determined and blending charts can be used to obtain the appropriate virgin binder grade or

35

percentage of RAP to be used in the design. However, blending charts not only assume

that a linear relationship exists with increasing RAP percentages, but it also assumes that

100% blending occurs between the RAP binder and the virgin binder. Since many of the

studies mentioned previously have shown that 100% blending does not always occur, a

new method to determine the amount of blending has been proposed by other researchers,

which involves using mix properties and a predictive model to backcalculate the effective

binder properties.

Two mix tests were described in this literature review, along with several

predictive models used to backcalculate the binder properties. Due to the extensive

amount of parameters required in the two Witczak models, the Hirsch model seems ideal

in backcalculating G*. In the most recent evaluation of all three models by Robbins in

2009 using mixtures from the NCAT test track, the Hirsch model was found to produce

the highest correlation between measured and predicted E* values. When the Hirsch

model was used to backcalculate G* using the HMA mix properties in the study by

Bennert et al. in 2009, the predicted G* values were found to be reasonably similar to the

measured values. The Tran et al. study, however, found that the Hirsch model under

predicted G* at the higher test temperatures. The error was attributed to the fact that

plant produced mixtures were evaluated in the study and the Hirsch model was calibrated

using laboratory produced mixtures.

The Hirsch model shows promise in backcalculating binder properties based on

work performed by previous researchers. However, additional studies should be

conducted to further analyze any errors associated with this backcalculation procedure.

The remainder of this thesis outlines a research investigation of using the Hirsch model to

backcalculate binder properties for mixes containing 0% to 100% RAP.

CHAPTER 3
EXPERIMENTAL PLAN

3.1 Introduction

The main objective of this research was to develop a simple method of characterizing

RAP asphalt without directly testing recovered binder. Two approaches were

investigated. The first method used the dynamic modulus test on compacted mix

specimens and backcalculation of the binder shear modulus and phase angle using the

Hirsch and C-A model, respectively. The second method used the relaxation modulus

test.

There were two phases to this study. In the first phase, the two methods were

evaluated to determine if either resulted in reasonable backcalculated binder properties.

In the second phase, the selected method was used to evaluate plant and laboratory

produced mixes with varying percentages of RAP to assess the sensitivity of the method

to changes in the binder properties.

3.2 Phase I Experimental Plan

In Phase I, two mix tests were evaluated to determine if the resulting backcalculated

binder properties were acceptably similar to known binder properties. Six sources of

RAP and two virgin laboratory mixes were evaluated in Phase I. The RAP specimens

consisted of RAP compacted to target air voids. The two virgin mixes used the same

aggregate gradation with different virgin binder grades. Three specimens per mix were

prepared for E* testing and three specimens per mix were prepared for E(t) testing.

The E* data were used to determine the backcalculated binder properties using the Hirsch model. The C-A model was then used to predict the G* and δ at a specified reference temperature and frequency in order to calculate the critical temperature. This critical temperature was then compared to measured values.

Since the Hirsch model requires VMA as an input, the RAP aggregate bulk specific gravity (G_{sb}) must be determined or estimated from the effective specific gravity (G_{se}). A mini-study was conducted to determine if the method selected for calculating the RAP G_{sb} substantially affected the VMA. Four G_{sb} values were determined for each mix:

1. Measured G_{sb} from solvent extracted aggregate

2. Measured G_{sb} from ignition oven extracted aggregate

3. Estimation of G_{sb} from G_{se} and percent binder (P_b) from solvent extraction

4. Estimation of G_{sb} from G_{se} and P_b from ignition oven extraction

Comparisons between the calculated VMA values for each G_{sb} method were made. The VMAs were also used in the Hirsch model, along with VFA and G*, to compare the calculated E* for all four methods.

The E(t) test was also used to determine mix properties of the virgin and 100% RAP samples. The effective binder properties were determined and compared among the different mixes.

After completing the data analysis of the two methods, the method that was the most reasonable for backcalculating binder properties was chosen for phase II of the study.

3.3 Phase II Experimental Plan

The second phase of the study evaluated plant produced mixes to verify if the chosen mix test produced reasonable backcalculated binder properties. Five field mixes consisting of up to 25% RAP, with one mix having both RAP and reclaimed asphalt shingles (RAS), were collected for dynamic modulus testing. The E* of each field mix, along with volumetric properties, were then used in the Hirsch model to backcalculate G* values. The C-A model was used to predict the critical temperatures which were then compared to measured values.

The second phase also consisted of testing the sensitivity of the selected method to changes in the binder properties. E* testing was performed on laboratory produced mixes and the binder properties were backcalculated. The sensitivity analysis involved evaluating mixes that varied in RAP content and virgin binder grade. Three RAP sources were used in the mix designs. For each RAP source, nine mixes were designed with different combinations of three RAP percentages and three binder grades. The three RAP percentages used during the mix design process included 20%, 35%, and 50% RAP and the three binder grades included PG 58-28, PG 67-22, and PG 76-22. This provided a total of 27 separate mixes to evaluate. Three replicates of each mix were tested for E* which was used with the Hirsch model to backcalculate G*. The high critical temperatures of these mixtures were then predicted using the C-A model. The sensitivity analysis consisted of determining if the backcalculated critical temperature for mixes that only differ by binder properties or percentage of RAP were distinctive.

CHAPTER 4
MATERIALS

4.1 Phase I Materials

4.1.1 Virgin and RAP Properties

In Phase I, two virgin and six RAP mixes were evaluated. The materials for all of the

mixes were collected in Alabama. This section summarizes the properties of the mixes

evaluated as part of Phase I.

Two virgin mixes containing limestone aggregate were used in this evaluation.

The limestone aggregate was obtained from a quarry in Calera, Alabama and mixed with

either PG 67-22 asphalt or PG 76-22 asphalt. The same aggregate gradation with a

nominal maximum aggregate size (NMAS) of 12.5 mm, as well as an asphalt content of

5.0% were used for both mixes. The gradation for both virgin aggregate blends is shown

in Table 4.1

Table 4.1 Virgin Blend Gradation

Sieve Size (mm)	Sieve size (in)	Virgin Gradation % Passing
19	**3/4"**	100
12.5	**1/2"**	93.0
9.5	**3/8"**	78.0
4.76	**#4**	52.0
2.36	**#8**	38.0
1.18	**#16**	22.0
0.600	**#30**	14.0
0.300	**#50**	10.0
0.150	**#100**	7.0
0.075	**#200**	3.0

RAP from six sources collected throughout the state of Alabama were also used in

this study. The areas where these RAP sources were obtained are illustrated in Figure

4.1.
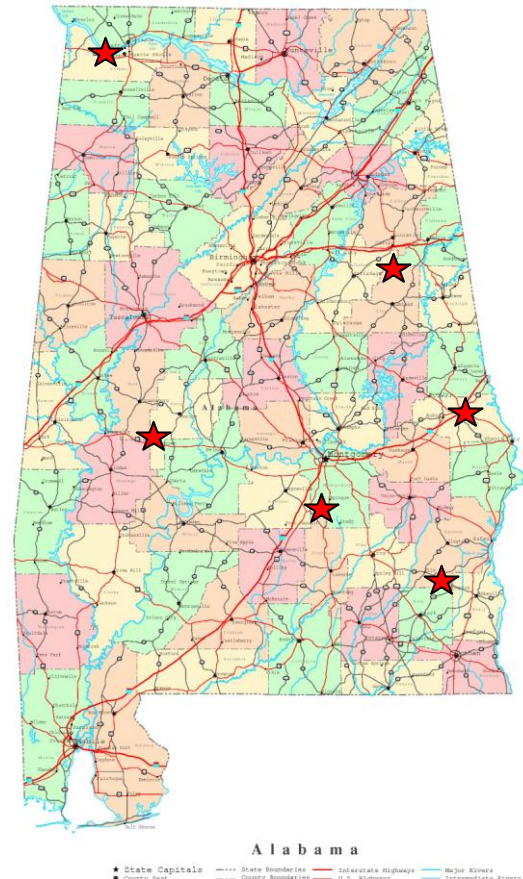
Figure 4.1 RAP Source Locations in Alabama

The aggregate from each RAP source was extracted using both the ignition

method and the solvent extraction method following AASHTO T 308 and AASHTO T

164 Method A, respectively. Asphalt contents were determined and gradation analyses of

the recovered aggregates were performed for both the ignition and solvent extracted

materials. It should be noted that correction factors were not used for the ignition oven

tests. After the solvent extraction was conducted, the Rotavapor method (AASHTO T 319) was used to recover the binder for testing. The gradations for all six RAP sources from the ignition and the solvent extraction methods, as well as the NMAS of each mix, are shown in Table 4.2 and Table 4.3, respectively.

Table 4.2 RAP Source Gradations (Ignition Method)

Sieve Size (mm)	Sieve size (in)	RAP 1	RAP 2	RAP 3	RAP 4	RAP 5	RAP 6
25	1.0"	100	100	100	100	100	100
19	3/4"	100	100	100	99.6	96.5	100
12. 5	1/2"	98.8	94.8	99.8	97.9	90.8	99.9
9. 5	3/8"	93.9	86.4	97.5	94.2	83.8	96.8
4. 76	#4	76.6	67.1	75.7	71.6	65.4	73.2
2. 36	#8	56.8	54.4	56.3	52.2	49.3	56.6
1. 18	#16	41.6	43.9	41.9	41.4	39.3	47.0
0. 600	#30	29.2	32.8	32.0	34.0	31.4	38.4
0. 300	#50	18.5	22.2	23.1	22.2	19.8	25.9
0. 150	#100	14.0	15.2	15.9	14.8	11.7	15.7
0. 075	#200	10.8	11.4	11.3	10.8	9.1	9.6
NMAS (mm)	-	**9.5**	**12.5**	**9.5**	**9.5**	**12.5**	**9.5**

Table 4.3 RAP Source Gradations (Solvent Method)

Sieve Size (mm)	Sieve size (in)	RAP 1	RAP 2	RAP 3	RAP 4	RAP 5	RAP 6
25	1.0"	100	100	100	100	100	100
19	3/4"	100	98.7	99.7	98.6	98.5	100
12. 5	1/2"	99.5	93.8	99.9	94.5	90.5	99.9
9. 5	3/8"	94.3	88.1	97.4	90.2	84.3	97.5
4. 76	#4	77.6	68.7	75.0	66.4	66.1	73.5
2. 36	#8	57.5	55.8	55.2	48.0	48.8	58.9
1. 18	#16	41.4	45.1	41.2	37.6	37.7	49.0
0. 600	#30	28.5	33.7	31.3	30.0	29.3	39.8
0. 300	#50	17.3	22.3	22.2	18.5	17.7	26.5
0. 150	#100	12.6	14.8	14.8	11.7	9.7	15.6
0. 075	#200	9.5	10.3	10.5	8.3	7.1	9.4
NMAS (mm)	-	**9.5**	**12.5**	**9.5**	**9.5**	**12.5**	**9.5**

The asphalt content, theoretical maximum specific gravity (G_{mm}), and the bulk specific gravity (G_{sb}) for the virgin blend and each RAP source are shown in Table 4.4. The asphalt content and the G_{sb} were determined from both the ignition and solvent extraction methods and are shown accordingly.

Table 4.4 Aggregate and Mix Properties of Virgin and 100% RAP Blends

Extraction Method	Property	Virgin PG 67-22	Virgin PG 76-22	RAP 1	RAP 2	RAP 3	RAP 4	RAP 5	RAP 6
	G_{mm}	2.551	2.549	2.642	2.520	2.548	2.421	2.511	2.573
Ignition Method	P_b	5.01	5.06	5.43	5.04	5.81	6.27	5.30	5.62
	G_{sb}	2.700	2.700	2.765	2.689	2.682	2.525	2.632	2.643
Solvent Method	P_b	4.67	4.77	4.64	4.98	5.11	5.28	4.69	5.18
	G_{sb}	2.730	2.730	2.719	2.647	2.650	2.481	2.61	2.573

4.2 Phase II Materials

4.2.1 Plant Produced Mixes

Five plant produced mixes from several locations in Alabama were evaluated in Phase II.

Each mix was sampled from a transfer truck at the plant, brought back to the lab, and

reheated for specimen fabrication. Table 4.5 shows information about the plant produced

mixes evaluated in this project. One plant mix contained a combination of RAP and RAS

as denoted in the table. It should also be noted that Mix 5 was an Open Graded Friction

Course (OGFC). An OGFC mixture is designed to have a high volume of air voids.

Therefore, it was necessary to use the corelok method, following AASHTO T 331, to

obtain the bulk specific gravity (G_{mb}). The corelok method uses a vacuum seal so that a

saturated surface dry weight can be obtained without losing water from the open pores.

Table 4.5 Plant Produced Mixes Evaluated

Mix	NMAS (mm)	Virgin Binder Grade	Total Binder (%)	RAP % by Mix Weight	RAS % by Mix Weight	RAP % by Binder Weight	RAS % by Binder Weight
1	25.0	PG 76-22	4.2	25	0	21.4	0
2	19.0	PG 67-22	4.5	20	0	24.4	0
3	19.0	PG 76-22	4.5	20	0	22.2	0
4	19.0	PG 67-22	5.0	15	5	15.0	20
5	19.0	PG 76-22	6.2	9	0	7.3	0

4.2.2 Laboratory Produced Mixes

Three sources of RAP were used in this evaluation. For each of the three RAP sources,

three RAP percentages and three binders were used in designing a total of 27 mixes. The

three RAP percentages used for each RAP source were 20%, 35%, and 50%. The three

binders used for each RAP source were PG 58-28, PG 67-22, and PG 76-22. Similar

gradations and effective asphalt contents were targeted to keep the mixes as similar as

possible. It was a goal to keep the effective asphalt contents within 0.5%. Mix design summaries are shown in the following sections.

4.2.1.1 RAP 1 Mix Designs

The aggregate used for the following designs was a combination of limestone, Shorter sand, and RAP 1. The design summaries for RAP 1 mixes are shown in, Table 4.6, Table 4.7, and Table 4.8.

Table 4.6 lists the gradations and combined G_{sb} and effective specific gravity (G_{se}) of the three different RAP percentages for the first RAP source. The NMAS for all three mixes was 19.0 mm. The G_{sb} was measured on each individual stockpile and then combined mathematically using the percentages of each type of aggregate used in the mixture. The G_{sb} of the RAP aggregate was measured on ignition extracted aggregate.

Table 4.6 Design Gradations for RAP 1 Mix Designs

		20% RAP	35% RAP	50% RAP
Sieve Size, in	Sieve Size, mm	% Passing Design Gradation	% Passing Design Gradation	% Passing Design Gradation
2"	50	100.0	100.0	100.0
1.5"	37.5	100.0	100.0	100.0
1"	25	100.0	100.0	100.0
3/4"	19	99.7	96.3	94.5
1/2"	12.5	90.0	87.2	87.0
3/8"	9.5	73.7	76.9	78.7
#4	4.75	51.3	51.6	60.0
#8	2.36	37.7	36.9	48.7
#16	1.18	28.3	27.6	37.5
#30	0.6	18.1	18.0	24.4
#50	0.3	8.3	8.7	11.6
#100	0.15	5.0	5.4	7.2
#200	0.075	3.5	3.9	5.0
Combined G_{sb} of Aggregates		2.703	2.730	2.755
Combined G_{sa} of Aggregates		2.755	2.794	2.827

All of the mixes were designed according to ALDOT Superpave specifications.

Table 4.7 lists the consensus properties of the aggregate blends for each mix along with

the ALDOT requirements.

Table 4.7 Consensus Properties for RAP 1 Mix Designs

Consensus Properties	ALDOT Requirements	20% RAP	35% RAP	50% RAP
Flat and Elongated, (Percent Maximum)	10	1.6	1.2	0
Fractured Faces, (Percent Minimum)	95/90[a]	100/100	100/100	100/100
Uncompacted Void Content of Fine Aggregate, (Percent Minimum)	45	45.3	45.4	45.5
Sand Equivalent, (Percent Minimum)	45	85.4	90.5	85.6

[a] denotes that 95% of the coarse aggregate has one fractured face and 90% has two or more fractured faces

Table 4.8 Design Summary for RAP 1 Mix Designs

	20% RAP	35% RAP	50% RAP
Max Aggregate Size, mm	25.0	25.0	25.0
Nominal Max. Agg. Size, mm	19.0	19.0	19.0
Anti-Strip Additive	0.75% LOF		
Optimum AC, %	4.8	4.7	4.9
AC from virgin binder, %	3.87	3.08	2.58
AC from RAP, %	0.93	1.62	2.32
RAP Binder as % of Total Binder	19.4	34.5	47.3
Va, %	4.0%	4.0%	4.0%
VMA, %	13.8%	13.5%	14.4%
VFA, %	71.6%	70.2%	71.3%
Effective AC, %	4.20%	4.73%	4.19%
Dust / Asphalt	0.80	0.99	1.20
G_{se}	2.751	2.790	2.811
TSR	0.90	0.96	0.91

Table 4.8 contains the design summaries, including the volumetrics of each mixture. It should be noted that an anti-strip additive was used in this mixture because the tensile strength ratio (TSR) for the 50% RAP mixture could not meet the minimum 0.80 specification without the additive. For consistency, an anti-strip additive was used in all three RAP percentage scenarios.

4.2.1.2 RAP 2 Mix Designs

The aggregate used for the following designs was a combination of limestone, granite, Shorter sand, coarse RAP 2, and fine RAP 2. The design summaries for RAP 2 mixes are shown in Table 4.9, Table 4.10, and Table 4.11.

All three mixtures were finer than the RAP 1 mixtures with a NMAS of 9.5 mm. The gradations are listed in Table 4.9. Again, the G_{sb} of the RAP aggregate was measured on ignition extracted aggregate.

Table 4.9 Design Gradations for RAP 2 Mix Designs

		20% RAP	35% RAP	50% RAP
Sieve Size, in	Sieve Size, mm	% Passing Design Gradation	% Passing Design Gradation	% Passing Design Gradation
3/4"	19	100.0	100.0	100.0
1/2"	12.5	100.0	99.9	99.9
3/8"	9.5	98.8	97.4	96.4
#4	4.75	68.0	66.6	64.3
#8	2.36	55.3	54.4	52.6
#16	1.18	43.7	43.0	43.2
#30	0.6	29.3	29.5	29.2
#50	0.3	14.3	14.4	14.3
#100	0.15	8.1	8.5	8.1
#200	0.075	5.1	5.6	5.1
Combined Gsb of Aggregates		2.648	2.650	2.636
Combined Gsa of Aggregates		2.707	2.705	2.690

All of the mixtures passed the ALDOT Superpave specifications for the consensus properties. These values are shown in Table 4.10.

Table 4.10 Consensus Properties for RAP 2 Mix Designs

Consensus Properties	ALDOT Requirements	20% RAP	35% RAP	50% RAP
Flat and Elongated, (Percent Maximum)	10	0	0	0
Fractured Faces, (Percent Minimum)	95/90[a]	100/99	99/98	99/97
Uncompacted Void Content of Fine Aggregate, (Percent Minimum)	45	45.7	45.8	45.4
Sand Equivalent, (Percent Minimum)	45	88.2	87.2	87.3

[a] denotes that 95% of the coarse aggregate has one fractured face and 90% has two or more fractured faces

Table 4.11 Design Summary for RAP 2 Mix Designs

	20% RAP	35% RAP	50% RAP
Max Aggregate Size, mm	12.5	12.5	12.5
Nominal Max. Agg. Size, mm	9.5	9.5	9.5
Optimum AC, %	6.3	5.9	6.16
AC from virgin binder, %	5.27	4.31	3.87
AC from RAP, %	1.03	1.59	2.29
RAP Percentage by % of Binder	16.3	26.9	37.2
V_a, %	4.0%	4.0%	4.0%
VMA, %	16.7%	15.9%	16.3%
VFA, %	75.9%	74.2%	76.4%
Effective AC, %	5.5%	5.1%	5.4%
Dust / Asphalt	0.94	1.10	0.94
G_{se}	2.709	2.706	2.693
TSR	0.86	0.96	0.81

The design summary, including the volumetrics of each mix, is shown above in Table 4.11. An anti-strip additive was not necessary for these mixtures.

4.2.1.3 RAP 3 Mix Designs

The aggregate used for the following designs was a combination of limestone, Shorter sand, baghouse fines, coarse RAP 3, and fine RAP 3. The design summary for RAP 3 mixes are shown in Table 4.12, Table 4.13, and Table 4.14.

The gradation for each design is listed in Table 4.12. Each mix had a NMAS of 12.5 mm. The G_{sb} of the RAP was measured on ignition extracted aggregate.

Table 4.12 Design Gradations for RAP 3 Mix Designs

		20% RAP	35% RAP	50% RAP
Sieve Size, in	Sieve Size, mm	% Passing Design Gradation	% Passing Design Gradation	% Passing Design Gradation
1"	25	100.0	100.0	100.0
3/4"	19	99.7	99.6	99.4
1/2"	12.5	94.5	94.9	92.9
3/8"	9.5	84.5	85.0	80.9
#4	4.75	64.4	62.9	58.8
#8	2.36	48.2	48.8	47.8
#16	1.18	37.0	38.4	38.6
#30	0.6	24.2	25.6	26.2
#50	0.3	11.8	12.9	13.4
#100	0.15	7.2	8.0	8.4
#200	0.075	5.3	5.7	6.0
Combined Gsb of Aggregates		2.675	2.679	2.685
Combined Gsa of Aggregates		2.735	2.736	2.739

All of the mixtures using the RAP 3 source met the ALDOT Superpave consensus properties specification. These values are listed in Table 4.13.

Table 4.13 Consensus Properties for RAP 3 Mix Design

Consensus Properties	ALDOT Requirements	20% RAP	35% RAP	50% RAP
Flat and Elongated, (Percent Maximum)	10	0.46	0.14	0.11
Fractured Faces, (Percent Minimum)	95/90[a]	100/100	100/100	100/99
Uncompacted Void Content of Fine Aggregate, (Percent Minimum)	45	45.2	45.3	45.4
Sand Equivalent, (Percent Minimum)	45	82.9	84.8	86.3

[a] denotes that 95% of the coarse aggregate has one fractured face and 90% has two or more fractured faces

Table 4.14 Design Summary for RAP 3 Mix Designs

	20% RAP	35% RAP	50% RAP
Max Aggregate Size, mm	19	19	19
Nominal Max. Agg. Size, mm	12.5	12.5	12.5
Anti-Strip Additive	0.75% LOF		
Optimum AC, %	5.10	5.10	5.10
AC from virgin binder, %	4.48	3.56	2.94
AC from RAP, %	0.62	1.54	2.16
RAP Percentage by % of Binder	12.2	30.2	42.4
Va, %	4.0%	4.0%	4.0%
VMA, %	14.4%	15.2%	14.6%
VFA, %	72.4%	72.7%	71.8%
Effective AC, %	4.40%	4.80%	4.50%
Dust / Asphalt	1.20	1.20	1.20
G_{se}	2.722	2.733	2.731
TSR	1.00	0.90	0.80

The design summary for RAP 3 mixtures are listed above in Table 4.14. The 50%

RAP mixture could not meet the TSR specification without using an anti-strip additive.

Therefore, 0.75% LOF was added to each design mix for consistency.

CHAPTER 5
TEST PROCEDURES

5.1 Phase I

5.1.1 RAP Characterization

The first step of this study was to characterize the RAP in terms of asphalt contents and aggregate properties. This information is required, not only for mix design purposes, but also to calculate the VMA which was used in the Hirsch Model to backcalculate G*.

5.1.1.1 Binder Properties

There are several different methods of obtaining asphalt contents. The two methods that were used in this evaluation were the centrifuge solvent method (AASHTO T-164 Method A) and the ignition oven method (AASHTO T-308).

Centrifuge Solvent Extraction. The AASHTO T-164 Method A (Centrifuge Method) procedure was followed for extracting the asphalt from the RAP. Each RAP source was split into two samples, weighing approximately 2000g each. Each RAP sample was then placed into a bowl and covered with Trichloroethylene (TCE) for no more than one hour allowing the chemical to dissolve the asphalt. A filter ring and cover were clamped to the top of the bowl, and the centrifuge began spinning at a maximum of 3600 rpm. A large flask was placed under the drain to collect the extract. Once the solvent had stopped flowing from the drain, another 200 mL of TCE was added to the bowl and the centrifuge was run again. This process was repeated at least three times until the extract that drained from the bowl was a light straw color. Figure 5.2 depicts a typical centrifuge used for solvent extractions.

Figure 5.2 Centrifuge Extractor

All of the extract and washings that were collected in the flask were placed in a continuous flow, high speed centrifuge that revolved at 9000 rpm or more. A container was used to collect the solvent from the centrifuging operation and the remaining mineral matter was collected in a bowl. The asphalt content was then calculated by subtracting the mass of the extracted mineral aggregate and mineral matter from the initial mass of the test portion divided by the initial mass of the test portion.

The binder from the collected solvent was recovered for additional testing. The procedure followed ASTM D5404, Standard Practice for Recovery of Asphalt from Solution Using the Rotary Evaporator. Figure 5.3 depicts a typical rotary evaporator used for this process. The binder was then graded according to AASHTO M 320 Standard Specification for Performance Graded Asphalt Binder. These results were later used to compare to backcalculated binder properties.

Figure 5.3 Rotary Evaporator

Ignition Oven Extraction. The procedure from AASHTO T 308 was followed for
extracting the asphalt from the RAP aggregate by means of the ignition oven. Each RAP
source was split into two samples, weighing approximately 1500g each. The samples
were then placed in the sample basket, which is composed of two stainless steel mesh
trays stacked one on top of the other. An ignition oven sample basket is illustrated in
Figure 5.4. The basket and sample was placed into the ignition oven, which has a built-in
scale that weighs the sample continuously during the process.

Figure 5.4 Ignition Oven Baskets

Typically, a calibration factor is determined prior to running an ignition test. This is required because aggregates tend to lose mass when exposed to extreme temperature encountered during the test. Since the amount of mass loss can vary depending on the types of aggregates and gradation, a calibration factor is determined by burning a lab prepared sample with a known asphalt content. Since the asphalt content of RAP is not known, a calibration factor cannot be determined. For this evaluation, no calibration factor was used in determining asphalt contents.

The temperature of the ignition oven was set to 538°C (1000°F) before the sample was placed inside. During the test, the asphalt was burned off the aggregate. The process was considered complete after the sample achieved a constant weight. The asphalt content was then calculated as the difference between the initial mass of the RAP sample and the mass of the residual aggregate.

5.1.1.2 Aggregate Properties

Specific Gravity. Another property that needed to be determined for this study was the aggregate bulk specific gravity, G_{sb}, of each RAP source. This information is required for both mix design purposes and in the calculation of the VMA. Just as in determining asphalt contents, several different methods can be used in determining the RAP G_{sb}. Four methods were utilized and evaluated in this study. Two of those methods involved measuring the RAP G_{sb} from ignition-extracted aggregate and solvent extracted aggregate following AASHTO T-84 and AASHTO T-85, Specific Gravity and Absorption of Fine and Coarse Aggregates. The other two methods involved estimating the G_{sb} using either the ignition oven binder content or the solvent extraction binder content with the corresponding effective specific gravity, G_{se}, shown in Equation 5.1:

$$G_{sb_{est}} = \frac{G_{se}}{\dfrac{G_{se} * P_{ba}}{100 * G_b} + 1}$$

Equation 5.1

where,

G_{se} = effective specific gravity of the aggregate

P_{ba} = percent asphalt absorbed

G_b = asphalt binder specific gravity

A site-specific P_{ba} is required for the estimation process. For this research, the average P_{ba} was calculated based on the measured G_{sb} from both the ignition oven and solvent extraction methods. The average P_{ba} for each RAP source was then verified with the contractor. Also, the G_b was assumed to be 1.028 since this is the typical specific gravity of asphalt.

The G_{se} was calculated using Equation 5.2:

$$G_{se} = \frac{100 - P_b}{\dfrac{100}{G_{mm}} - \dfrac{P_b}{G_b}}$$

Equation 5.2

where,

P_b = percentage of asphalt (determined by ignition oven or solvent extraction)

G_{mm} = maximum specific gravity of RAP

After the RAP had been characterized, the mixture property testing was conducted. Two mix property tests, dynamic modulus and relaxation modulus, were evaluated in phase I of this study. The following sections outline the testing procedures.

5.1.2 Dynamic Modulus

The dynamic modulus test measures the stiffness of an asphalt mixture. There are several procedures available. The following subsections detail the procedures used in this study.

5.1.2.1 Specimen Preparation

Six sources of RAP and two virgin laboratory prepared mixes were evaluated in Phase I. For the virgin mixes, the aggregate was heated for approximately four hours at 180°C (355°F) and mixed with 5% of either PG 67-22 or PG 76-22 asphalt. The mix was then short-term oven aged for two hours at 157°C (315°F).

For the 100% RAP samples, the RAP was heated for approximately one hour at 180°C (355°F) and then dry mixed without any virgin binder. The 100% RAP mix was aged for one hour at 157°C (315°F) to minimize additional hardening of the recycled asphalt.

Once the aging process was finished, samples were tested to determine maximum specific gravity (G_{mm}) following AASHTO T 209. Separate aged samples were compacted in a gyratory compactor to a height of 170 mm following AASHTO TP 62. The compacted specimens were then cored and cut to approximately 100 mm in diameter and 150 mm in height. Three replicates were made for each mix, resulting in 24 specimens for testing in the Asphalt Mixture Performance Tester (AMPT). For each specimen, bulk specific gravity (G_{mb}) and air voids were then determined following AASHTO T 166 and T 269, respectively. The target air voids for all AMPT samples was 7±0.5%.

5.1.2.2 Dynamic Modulus Testing

Following AASHTO TP 62 specifications, mounting studs were glued to the sides of

each specimen 120° apart for the three axial linear variable differential transducers

(LVDTs). A rubber membrane was then placed over the specimen and attached

mounting studs. A prepared dynamic modulus sample that has studs attached is shown in

Figure 5.5.

Figure 5.5 Dynamic Modulus Sample

The dynamic modulus test was performed at four different temperatures;

therefore, the specimens had to be conditioned at each temperature for a specified time.

The conditioning time for each temperature is shown in Table 5.15.

Table 5.15 Specimen Conditioning Criteria

Specimen Temp., °C (°F)	Time from Room Temp., hours	Time from Previous Test Temp., hours
4.4 (40)	Overnight	4 hours or overnight
21.1 (70)	1	3
37.8 (100)	2	2
54.0 (130)	3	1

Specimens were placed into the AMPT loading frame after temperature conditioning. The AMPT loading frame consists of hardened steel platens placed on the bottom and top of the specimen. Discs cut from a rubber membrane were placed between the top and bottoms of the specimen and the platens to minimize friction. The LVDTs were then placed between the mounting studs and adjusted to near the end of its linear range to allow the full range to be available for the accumulation of compressive permanent deformation. A confining pressure of 138 kPa was applied to the specimen and then sinusoidal loading began in a cyclic manner. Although rubber membranes were used, the specimens in Phase I had essentially no confinement due to the way the specimens were prepared. However, the mistake was corrected and the specimens in Phase II were fully confined. Figure 5.6 illustrates a dynamic modulus specimen in the AMPT loading device.

Figure 5.6 Dynamic Modulus Specimen in AMPT

The specimens were tested at four different temperatures; 4.4°C (40°F), 21.1°C (70°F), 37.8°C (100°F), and 54°C (130°F). The lowest test temperature of -10°C from AASHTO TP 62 was not used due to limitations of the AMPT environmental chamber. At each temperature, the test was run at six frequencies; 25 Hz, 10 Hz, 5 Hz, 1 Hz, 0.5 Hz, and 0.1 Hz. This provided a wide range for simulating fast to slow traffic speeds. The specimens were tested from the lowest to highest temperature. At each temperature, testing was conducted from the highest to lowest frequency. These testing conditions were performed to minimize damage accumulation on the specimen. The AMPT software calculated the dynamic modulus and the phase angle for each of the temperature and frequency combinations.

The dynamic moduli, along with volumetric properties, were used in the Hirsch model to backcalculate G*. The backcalculated values were used in the Christensen Anderson Model (C-A) to predict the phase angle (δ), and subsequently the critical temperature at which G*/sin δ equaled 2.2 kPa. This was then compared to the measured

60

critical temperatures for the virgin binders and the recovered RAP binders following

AASHTO M320.

5.1.3 Relaxation Modulus

The relaxation modulus test measures the ability of an asphalt mixture to relax under an

applied strain. Relaxation modulus, E(t), is the reciprocal of creep compliance where the

time-dependent strain is measured from an applied static load. Methods have been

developed to directly measure E(t) by applying a known strain to the specimen for a

designated time limit and measuring the stress as the specimen relaxes. Because of the

viscoelastic behavior of asphalt concrete, a target strain must first be determined so that

the specimen is not damaged during testing.

5.1.3.1 Specimen Preparation

For the virgin samples, the virgin aggregate was heated for approximately four hours at

180°C (355°F) and mixed with 5% of either PG 67-22 or PG 76-22 asphalt. The mix was

then aged for two hours at 157°C (315°F). For the 100% RAP samples, the RAP was

heated for approximately one hour at 180°C (355°F) and then dry mixed. The 100%

RAP mix was aged for only one hour at 157°C (315°F) to minimize additional hardening

of the recycled asphalt.

Once the aging process had finished, the mix was compacted to a height of 115

mm in a gyratory compactor. At least 6 mm were sawed from both sides of the

compacted specimens and the remainder was sawed into two cut halves following

AASHTO T 322, yielding specimens that were approximately 150 mm in diameter and

38 to 50 mm in height. Three replicates were made for the two virgin mixes and the six

100% RAP mixes. The G_{mb} and air voids were then determined for each sample

61

following AASHTO T 166. The target air voids for all relaxation modulus samples was 4±1%.

A paint pen was used to mark three points around the circumference of each specimen. The points were approximately 30° apart and labeled 0, 30, and 60°. Three additional points were marked at 180° from the three labeled points so that the position of the specimen in the loading device would be lined up directly across the diameter. A picture of a relaxation modulus specimen is shown in Figure 5.7.
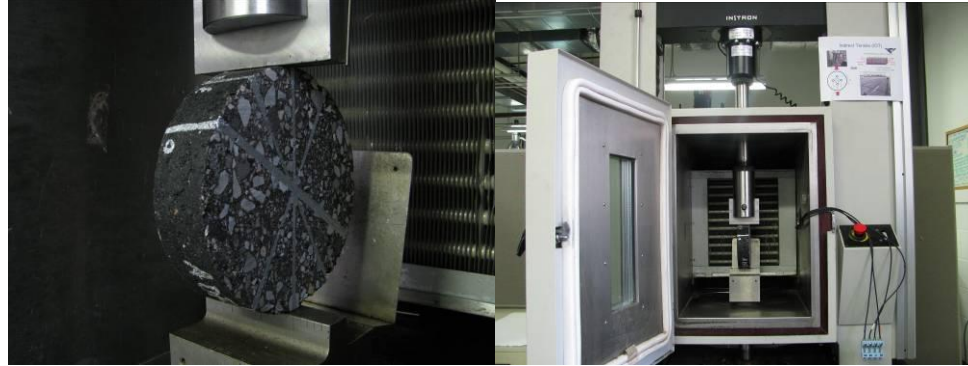

Figure 5.7 Relaxation Modulus Specimen

5.1.3.2 Relaxation Modulus Testing

The target strain for 100% RAP specimens and virgin specimens was established prior to relaxation modulus testing so that the specimen would not be damaged. In order to perform this task, a 100% RAP specimen and a virgin specimen were randomly selected for this initial testing. These two specimens were conditioned in an environmental chamber for a minimum of one hour at 25°C (77°F). Once the specimens were conditioned for one hour, they were removed from the chamber and immediately placed on the lower platen of a diametral testing jig, commonly used for indirect tension testing. This particular diametral testing jig was enclosed in an environmental chamber also set to

25°C (77°F) so that the testing temperature never fluctuated. The top and bottom loading

strips were aligned with the 0° point on the circumference of the specimen. The loaded

testing device is illustrated in Figure 5.8.

Figure 5.8 Relaxation Modulus Testing Device

The loading frame was moved down so that no more than 45 kN of seating load

was applied to the specimen. The seating load was applied for two seconds. After that

initial two seconds, a vertical strain of 1000 microstrain (με), which corresponds to a ram

displacement of approximately 0.146 mm, was quickly applied to the specimen and firm

contact was maintained for 45 seconds. The load was recorded as it peaked at the given

strain and then relaxed over the duration of the test. Once the test completed, the load

was released and the specimen was allowed to sit for approximately 10 minutes before

further testing was performed. After the specimen had set for 10 minutes, the same

procedure was performed, only the step strain was increased by 500 με. This process was

repeated up to a final strain of 4000 με had been reached.

Once the data had been collected at each strain level, the tensile stress was

calculated at each time increment from the recorded load and the specimen dimensions

using Equation 5.3.

$$T = \frac{2P}{\pi l d}$$

<div align="right">**Equation 5.3**</div>

where,

T = tensile stress, kPa

P = applied load by the testing machine, kN

l = length of the specimen, m

d = diameter of specimen, m

      The horizontal strain was calculated using Equation 5.4.

$$\varepsilon_h = \varepsilon_v \mu$$

<div align="right">**Equation 5.4**</div>

where,

ε_h = horizontal strain

ε_v = vertical strain (target strain)

μ = Poisson's Ratio (0.35 @ 25°C)

      The relaxation modulus, E(t), was then calculated at each time increment using the tensile stress and the horizontal strain, as shown in Equation 5.5.

$$E(t) = \frac{T}{\varepsilon_h}$$

<div align="right">**Equation 5.5**</div>

      E(t) was plotted against time and a power function trend line was fit to the data at each strain level with an R^2 above 0.9. The initial relaxation modulus is considered the maximum modulus as time approaches zero. The exponent of the power curve is considered the degree of curvature and it represents the mix's ability to relax. The higher the degree of curvature, the more the mix will relax over time. Using the fitted power function, E(t) was determined at two seconds which is when the strain was actually applied. The ratio of $E(t)_{(2sec)}$ at the various tested $\mu\varepsilon$ to $E(t)_{(2sec)}$ at 1000 $\mu\varepsilon$ was determined. This value was then plotted against the strain levels used during testing. An

<div align="center">64</div>

example of this plot for a 100% RAP specimen is shown in Figure 5.9. The strain level with the highest ratio value that was still in the linear viscoelastic range was chosen as the target strain. The linear viscoelastic range is the strain that a specimen can endure and still return to its original condition once that strain is removed. In order to determine the limits of this range, the specimen must be tested at different strain levels until it no longer returns to its original state.
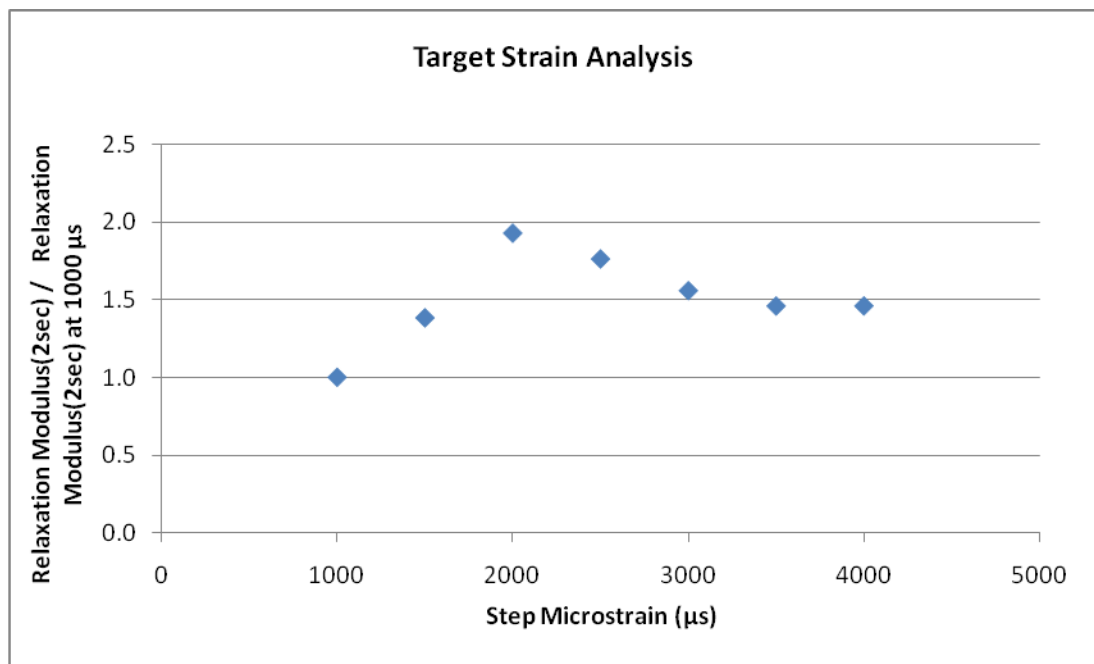
Figure 5.9: Example of Determining Target Strain for 100% RAP Specimens

It was determined from the plot in Figure 5.9 that the target strain for the RAP specimen was 1500 με. The target strain for the virgin specimen was determined to be 2000 με in the same manner that the target strain was determined for the RAP specimen. Once the target strains were determined for both RAP and virgin specimens, the relaxation modulus testing was performed.

65

Each specimen was conditioned in an environmental chamber for a minimum of one hour at 25°C (77°F). Once the specimen was removed from the chamber, it was immediately placed in the jig and tested in the same manner as just described, only the determined target strain was used for each specimen. The load was recorded as it peaked at the given strain and then relaxed over the duration of the test. Once the test was complete, the load was released and the specimen was allowed to sit for approximately 10 minutes before further testing was performed on the rotated diameters. The software recorded the load for every 0.01 seconds.

5.2 Phase II

After the analysis for Phase I was complete, the dynamic modulus test was selected as the most appropriate method for backcalculating binder properties due to inconsistencies in the relaxation modulus test. The second phase of the study consisted of verifying the backcalculation procedure with plant produced mixes and evaluating the sensitivity of the dynamic modulus to changes in the binder properties on laboratory produced mixes.

5.2.1 Plant Produced Mixes

Five plant produced mixes from several locations in Alabama were used to verify the backcalculation method using dynamic modulus test results. The materials ranged from a 19.0 mm to a 25.0 mm mix and contained either RAP or RAS, contributing to a maximum binder replacement of 35%. The mix properties are detailed in Chapter 4.

The plant mixes were reheated in an oven until the mix temperature reached 157°C (315°F). Once the mix had achieved this temperature, dynamic modulus specimens were prepared the same way as in Phase I of this study following AASHTO TP 62. The specimens were also tested in the same manner at the same four temperatures

and six frequencies. The E* of each plant mix, along with volumetric properties, were

then used in the Hirsch model to backcalculate G* values. The backcalculated values

were used in the C-A model to predict the phase angle (δ), and subsequently the critical

temperature at which G*/sin δ equaled 2.2 kPa. This was then compared to the measured

critical temperature.

5.2.2 Laboratory Produced Mixes

The sensitivity analysis consisted of evaluating laboratory produced mixes that varied in

RAP content and virgin binder grade. Three RAP sources were used in the mix designs.

For each RAP source, nine mixes were designed with different combinations of three

RAP percentages and three binder grades. The three RAP percentages used during the

mix design process included 20%, 35%, and 50% RAP and the three binder grades

included PG 58-28, PG 67-22, and PG 76-22. This provided a total of 27 separate mixes

to evaluate as shown in Table 5.16.

Table 5.16 Mix Design Variables for Phase II

	RAP 1			RAP 2			RAP 3		
PG 58-28	20%	35%	50%	20%	35%	50%	20%	35%	50%
PG 67-22	20%	35%	50%	20%	35%	50%	20%	35%	50%
PG 76-22	20%	35%	50%	20%	35%	50%	20%	35%	50%

For the 27 mix designs, the virgin aggregate was heated for approximately four

hours and the RAP was heated for 30 minutes at the target mixing temperature plus 30°F

to account for heat loss. Each blend was first dry mixed with the RAP, then mixed with a

virgin binder, and aged for approximately four hours at the designated compaction

temperature. The mixing and compacting temperature for each binder is shown in Table

5.17.

Table 5.17 Mixing and Compacting Temperatures for PG Binders

Binder	Mixing Temperature, °F	Compaction Temperature, °F
PG 58-28	289-297	268-276
PG 67-22	310-325	295-315
PG 76-22	330-340	310-320

Following the aging process, the mix was either used for the determination of the maximum specific gravity, G_{mm}, following AASHTO T 209 or compacted to a height of 170 mm in a gyratory compactor following AASHTO TP 62. The compacted specimens were then cored and cut to approximately 100 mm in diameter and 150 mm in height. Three replicates were made for each of the 27 mixes, resulting in 81 AMPT specimens. The mix bulk specific gravities (G_{mb}) and air voids were then determined for each sample following AASHTO T 166. The target air voids for all AMPT samples was 7±0.5%.

The specimens were tested according to AASHTO TP 62 at the same four temperatures and six frequencies. The resulting E* was used with the Hirsch model and C-A model to backcalculate G* and δ. The critical high temperature grades were then compared between each binder source and each RAP percentage.

CHAPTER 6
RESULTS AND DISCUSSION

6.1 Phase I

6.1.1 RAP Characterization

One of the mix tests performed in this study included measuring E* and then

backcalculating G* using the Hirsch model. Two of the variables required in the Hirsch

model are VMA and VFA. In order to calculate VMA and VFA, the RAP aggregate bulk

specific gravity (G_{sb}) had to be determined or estimated from the effective specific

gravity (G_{se}). A mini-study was conducted to determine if the method selected for

calculating the RAP G_{sb} substantially affected the VMA. The four methods for

determining G_{sb} values are listed below:

1. Measured G_{sb} from solvent extracted aggregate

2. Measured G_{sb} from ignition oven extracted aggregate

3. Estimation of G_{sb} from G_{se} and percent binder (P_b) from solvent extraction

4. Estimation of G_{sb} from G_{se} and P_b from the ignition method

The G_{sb} values determined from the four different methods are shown in Figure 6.10.
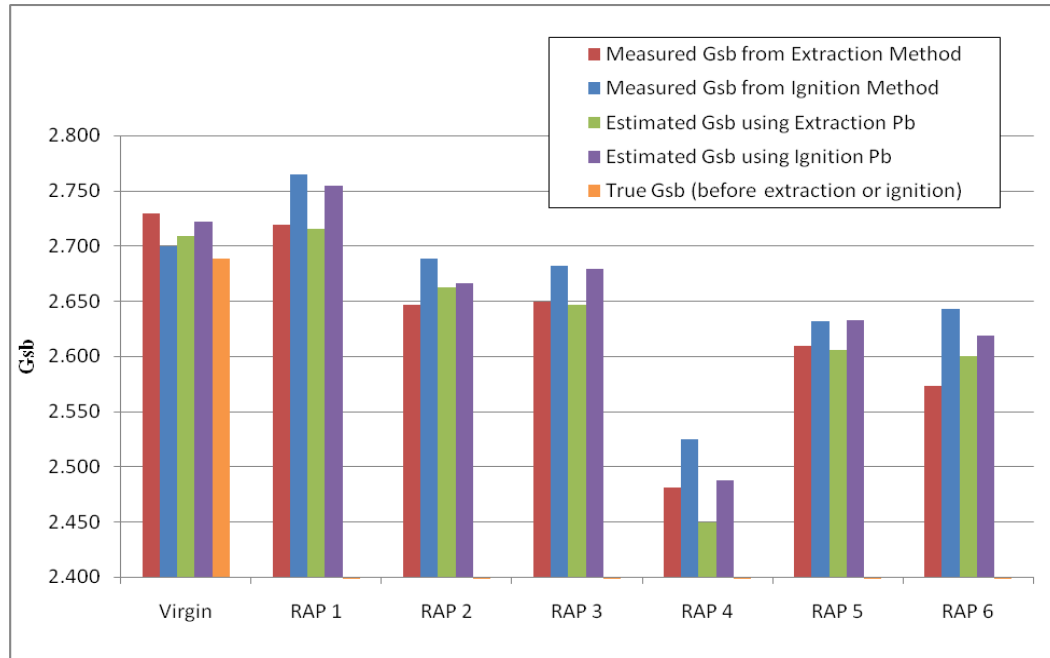
Figure 6.10 G$_{sb}$ Comparison

The estimated G$_{sb}$ values were calculated based on typical absorption values observed at each plant where the RAP was sampled. It is important that these absorption values are similar to site-specific absorption values; otherwise, it will give a poor representation of the actual G$_{sb}$.

The G$_{sb}$ of the virgin aggregate was also determined before the aggregate was mixed with binder in order to compare a 'True G$_{sb}$' to the four methods. The G$_{sb}$ of the RAP can only be determined by one of the four methods listed above so there is no 'True G$_{sb}$' for comparison. However, the 'True G$_{sb}$' of the virgin aggregate was most similar to the G$_{sb}$ measured from the ignition extracted aggregate, which is shown in Figure 6.10.

After the G$_{sb}$ values were determined, the VMA was calculated using Equation 6.1

$$VMA = 100 - \frac{G_{mb} * P_s}{G_{sb}}$$

Equation 6.1

70

where,

VMA = voids in mineral aggregate

G_{sb} = bulk specific gravity of total aggregate

G_{mb} = bulk specific gravity of compacted mixture

P_s = aggregate content, percent by total mass of mixture

In the case of the estimated values, the G_{sb} in Equation 6.1 would be replaced with the

estimated G_{sb}.

Figure 6.11 compares the average VMA of the virgin specimens for each

method. The error bars represent the standard deviation between three replicate

specimens. The VMA comparison of each RAP source is depicted in Figure 6.12.
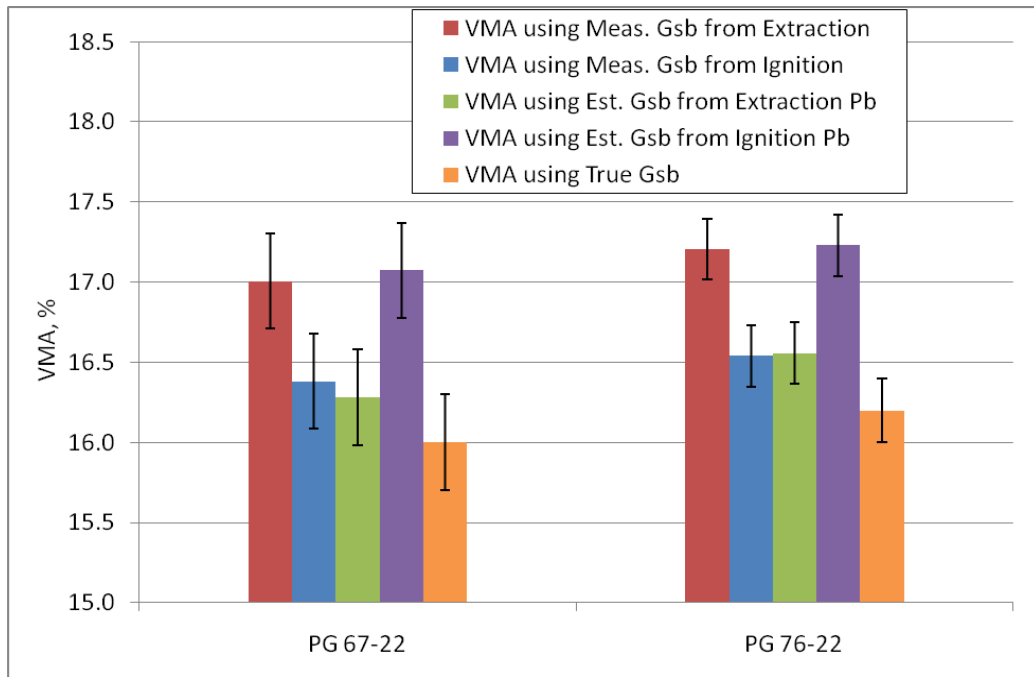
Figure 6.11 VMA Comparison of Virgin Specimens
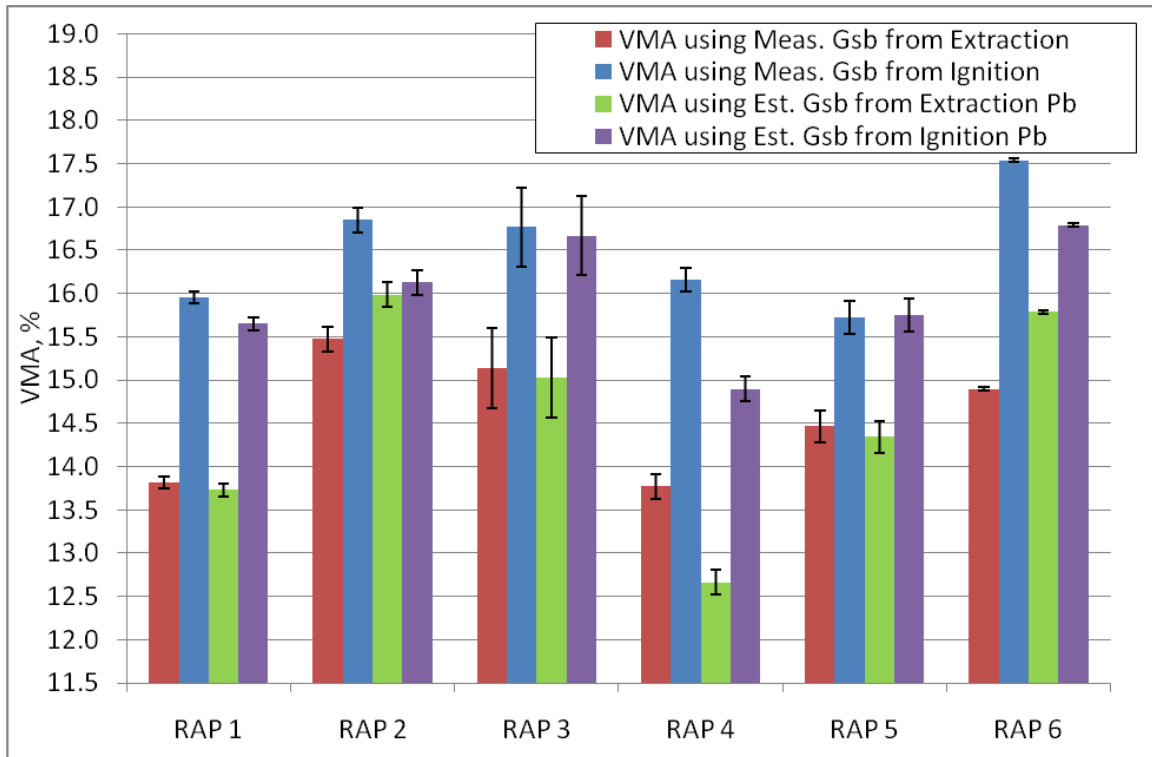
Figure 6.12 VMA Comparison of RAP Specimens

Similar trends were seen in the VMA as in the G_{sb} values. However, the VMA differences appear greater since these specimens were made with 100 percent RAP. The four methods were compared statistically using a Student's t-test. The ANOVA, shown in Table 6.18, suggests that all of the methods for determining G_{sb} values produce statistically different VMA results using a significance level of 0.05. The Student's t-test, shown in Table 6.19, also shows the statistical differences. The cells that are colored green denote that the *p*-value was greater than 0.05 and that the methods were not statistically different.

Table 6.18 ANOVA of VMA Values

ANOVA of All Mixes				
Factors	Degree of Freedom	Mean Square	F Value	p-value
Source	7	10.15	177.14	<0.0001
Methods	3	12.72	222.09	<0.0001

72

Table 6.19 p-values from Student's t-Test Comparison of VMA Values

RAP Source	Meas Ext vs. Meas Ign	Meas Ext vs. Est Ext	Meas Ext vs. Est Ign	Meas Ign vs. Est Ext	Meas Ign vs Est Ign	Est Ext vs. Est Ign
RAP 1	0.0000	0.2118	0.0000	0.0000	0.0064	0.0000
RAP 2	0.0003	0.0122	0.0053	0.0018	0.0035	0.3046
RAP 3	0.0123	0.7844	0.0154	0.0099	0.7937	0.0122
RAP 4	0.0000	0.0007	0.0007	0.0000	0.0004	0.0000
RAP 5	0.0012	0.4698	0.0011	0.0008	0.8678	0.0008
RAP 6	0.0000	0.0000	0.0000	0.0000	0.0000	0.0000
Virgin 67-22	0.0977	0.0675	0.8242	0.7528	0.0752	0.0526
Virgin 76-22	0.0140	0.0152	0.8860	0.9207	0.0124	0.0135

Although the four methods were found to be statistically different for some of the combinations, it was necessary to determine the effect of those differences on calculations of E*. The Hirsch model, shown in Equation 6.2 and Equation 6.3 was used to calculate E* using the VMA and VFA determined from each method. The other parameter required for the Hirsch model was the shear modulus of the binder, G*. G* was determined using a Dynamic Shear Rheometer (DSR) at six frequencies and three temperatures. The six frequencies coincided with the E* testing; 25, 10, 5, 1, 0.5, and 0.1 Hz. Due to temperature limitations on the DSR, the binder was only tested at 21.1°C (70°F), 37.8°C (100°F), and 54°C (130°F). The low temperature of 4.4°C (40°F) was excluded from the binder testing.

$$E*_{mix} = Pc\left[4{,}200{,}000\left(1-\frac{VMA}{100}\right)+3G*\left(\frac{(VMA)(VFA)}{10{,}000}\right)\right]+\frac{(1-Pc)}{\left(\frac{1-\frac{VMA}{100}}{4{,}200{,}000}+\frac{VMA}{VFA(3G*)}\right)}$$ **Equation 6.2**

where,

$$Pc = \frac{\left(20 + \dfrac{VFA(3G*)}{VMA}\right)^{0.58}}{650 + \left(\dfrac{VFA(3G*)}{VMA}\right)^{0.58}}$$

<div align="right">**Equation 6.3**</div>

$E*_{mix}$ = Dynamic Modulus of Asphalt Mixture

VMA = Voids in Mineral Aggregate

VFA = Voids Filled with Asphalt = $\dfrac{VMA - VTM}{VMA}$, where VTM is the air voids in total mix

$G*$ = Shear Modulus of Asphalt Binder

 Using the VMA and VFA for each of the four methods, E* was calculated at each frequency and temperature used for testing G*. The calculated E* values based on VMA and VFA determined from G_{sb} from the four methods were compared statistically against the measured E* using a *t-test* and significance level of 0.05. The *t-test* compared each calculated E* to the measured E* for six frequencies, three temperatures, and eight mixes. This resulted in 144 comparisons per method. The results are summarized in Table 6.20.

Table 6.20 Summary of E* *t-tests*

	Hirsch E* (Ext) vs. Meas. E*	Hirsch E* (Ign) vs. Meas. E*	Hirsch E* (Est Ext) vs. Meas. E*	Hirsch E* (Est Ign) vs. Meas. E*
Number of Comparisons Not Significantly Different	82	91	83	90
Total Number of Comparisons	144	144	144	144
Percent that is Not Significantly Different	56.9%	63.2%	57.6%	62.5%

Although the differences between the VMA using the four tested methods were significant, the differences did not affect the calculated E*. Since the number of comparisons that were not significantly different were similar among the different methods, it was concluded that the calculated E* from the Hirsch model is insensitive to VMA.

A master curve was developed for each mix comparing the four methods against the measured E*. Master curves use the principle of time-temperature superposition. The measured data at different temperatures are shifted to a reference temperature with respect to the loading frequency until a single smooth curve is constructed. This describes the material's dependency on the loading rate and temperature. The modulus is expected to increase as the loading rate increases. The higher frequencies also represent low temperatures. At lower frequencies, or high temperatures, the material will be less stiff due to the viscoelastic nature of the binder.

The master curves were constructed following AASHTO PP 61, Standard Practice for Developing Dynamic Modulus Master Curves for Hot Mix Asphalt Using the Asphalt Mixture Performance Tester. The master curve for RAP 1, at a reference temperature of

21.1°C (70°F), is shown in Figure 6.13. This graph illustrates the similarities between each method. The other RAP sources and the virgin samples are shown in Figure 6.14 to Figure 6.20. The four different calculated E* master curves are very similar to each other, as well as to the measured E*. RAP 1, 2, and 3 has some deviation at the intermediate frequencies. The measured E* master curve deviates from the calculated E* on the low frequencies for RAP 4 and RAP 5. Both of the virgin mixes have a different trend on the lower frequencies of the master curve, exhibiting a 'tail' on the calculated E* values using the Hirsch model. The measured E* values did not have a 'tail'. This is most likely due to the sensitivity of the binder at high temperatures when measuring G*. The measured E* values are not as sensitive because the stiffness is attributed more to the aggregate than the binder at this point.
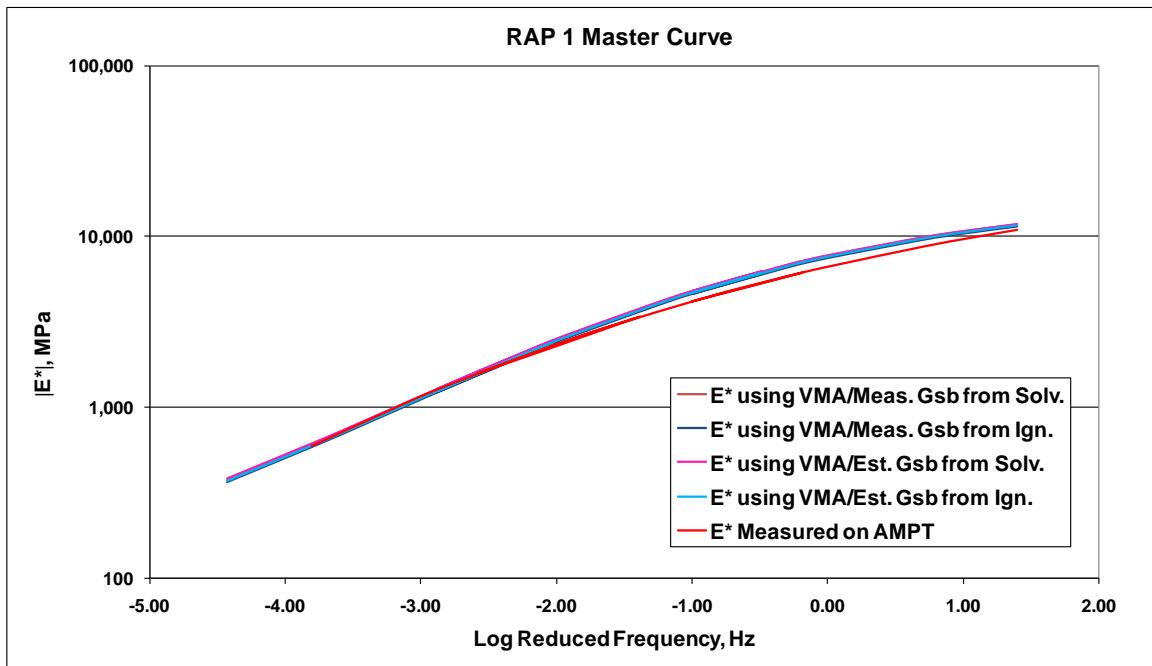
Figure 6.13 E* Master Curve for RAP 1
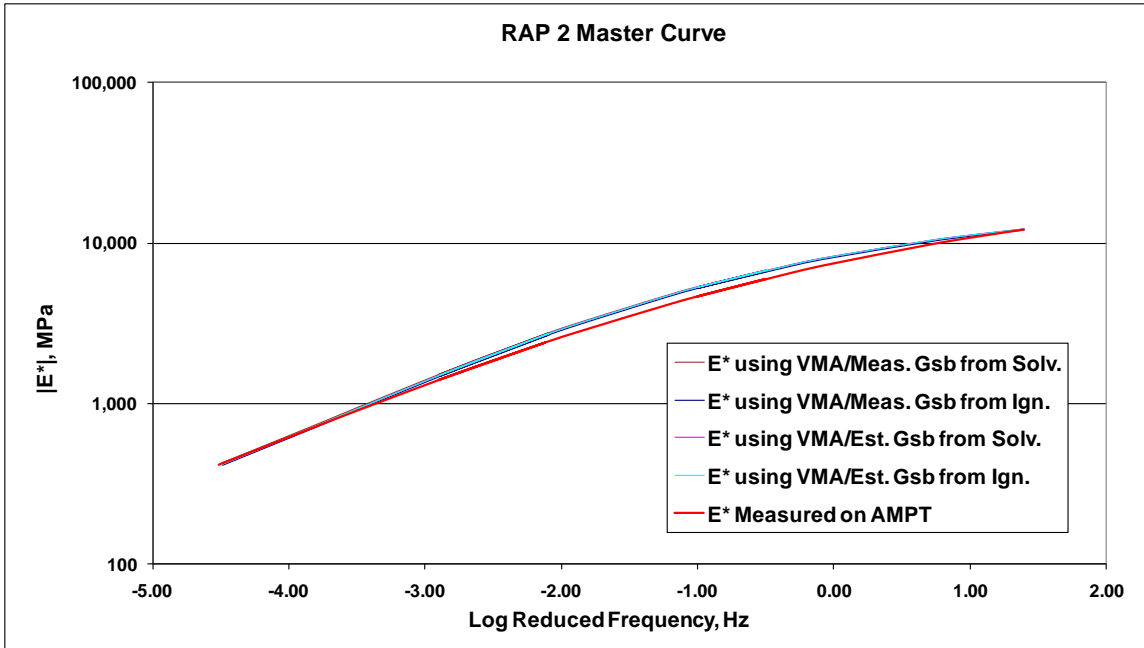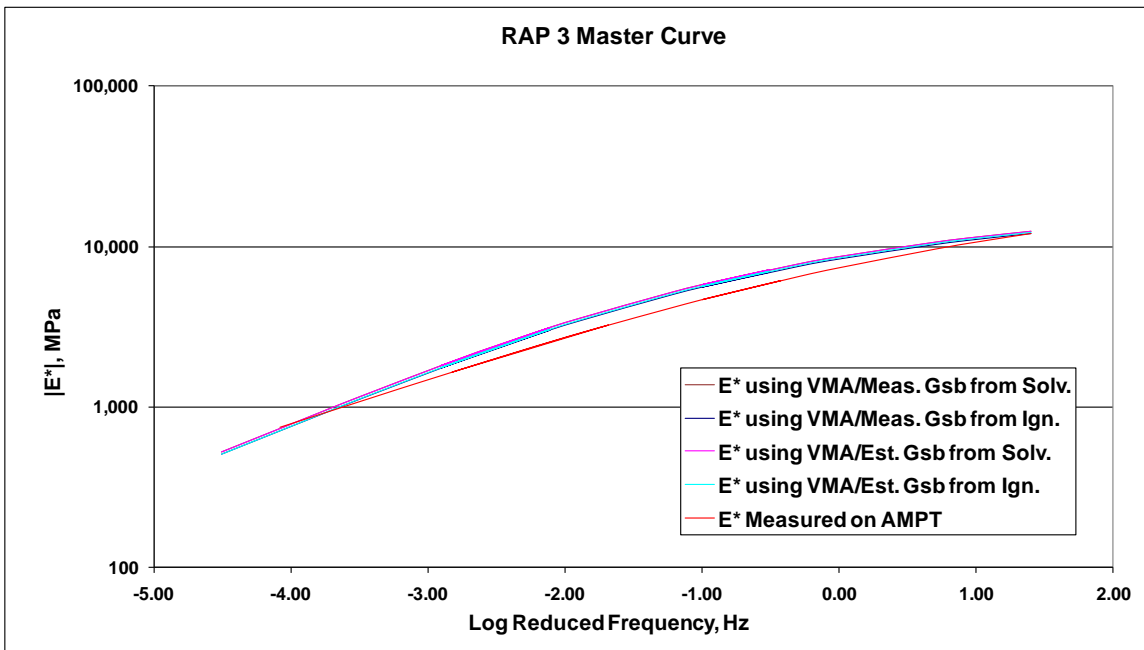
Figure 6.14 E* Master Curve for RAP 2

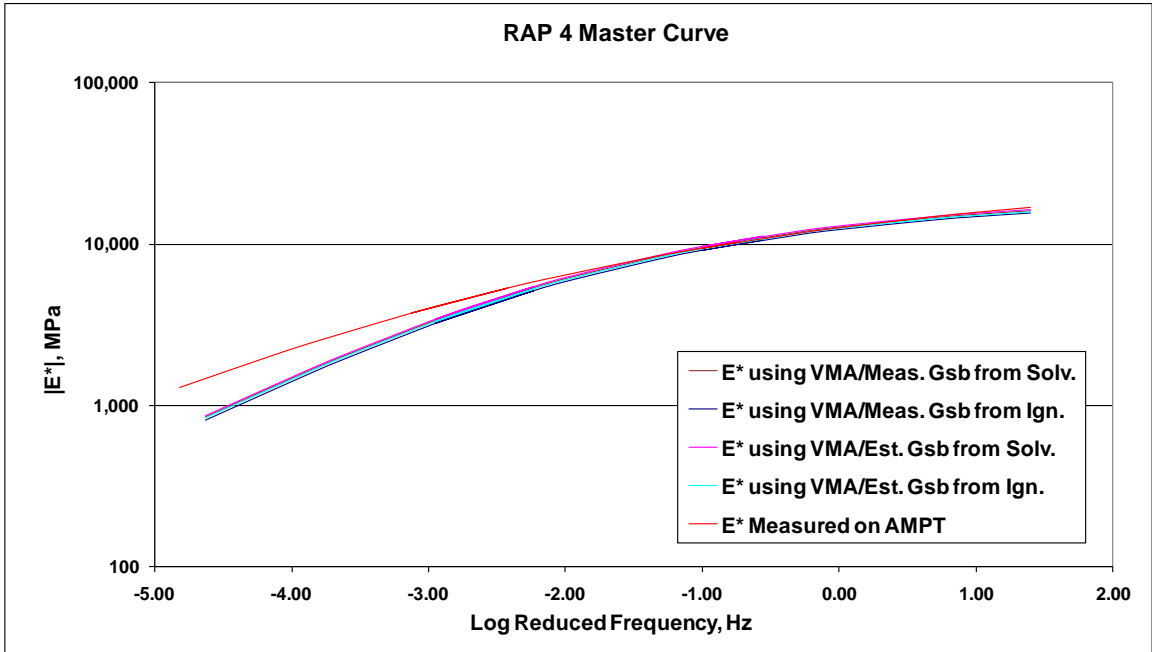**Figure 6.15 E* Master Curve for RAP 3**

77

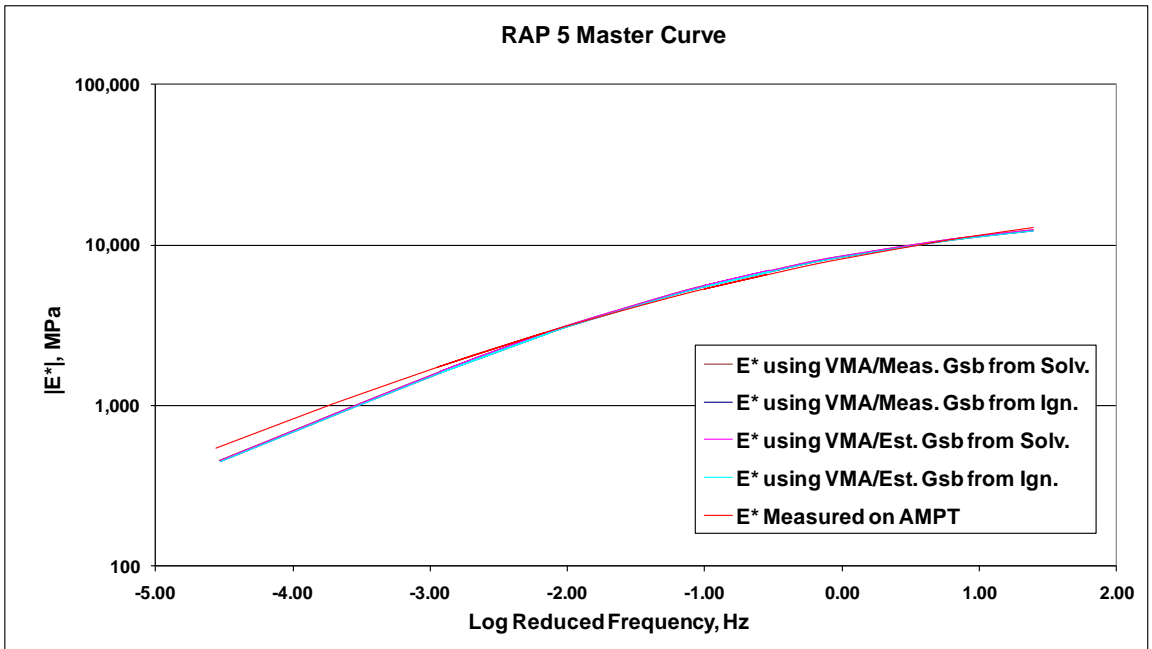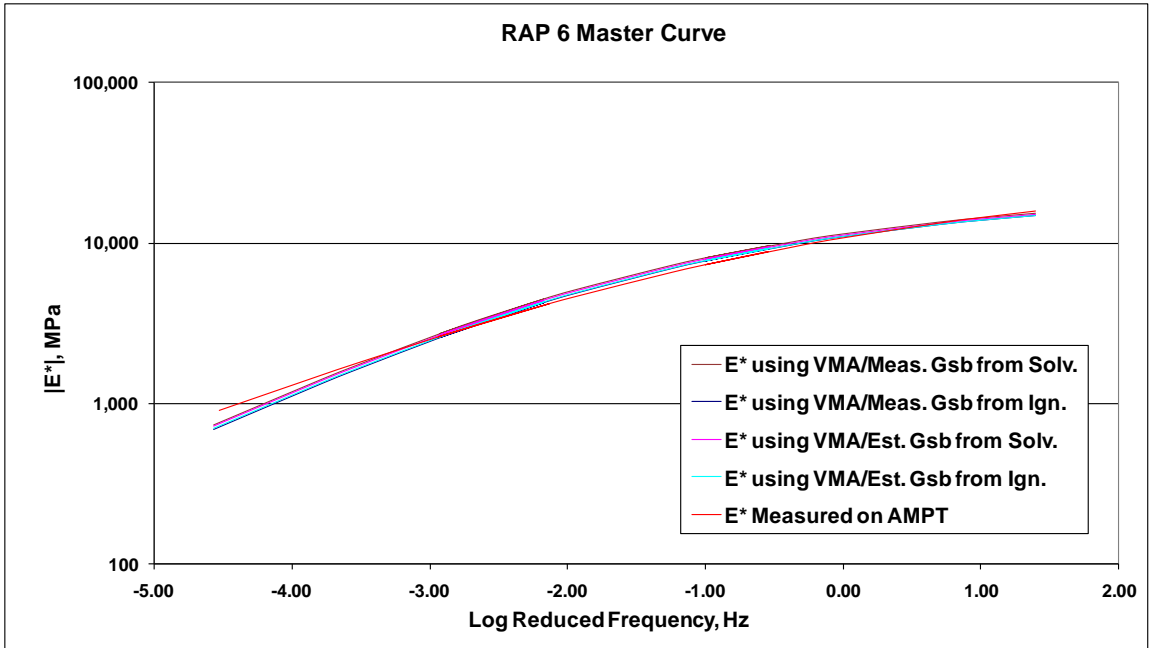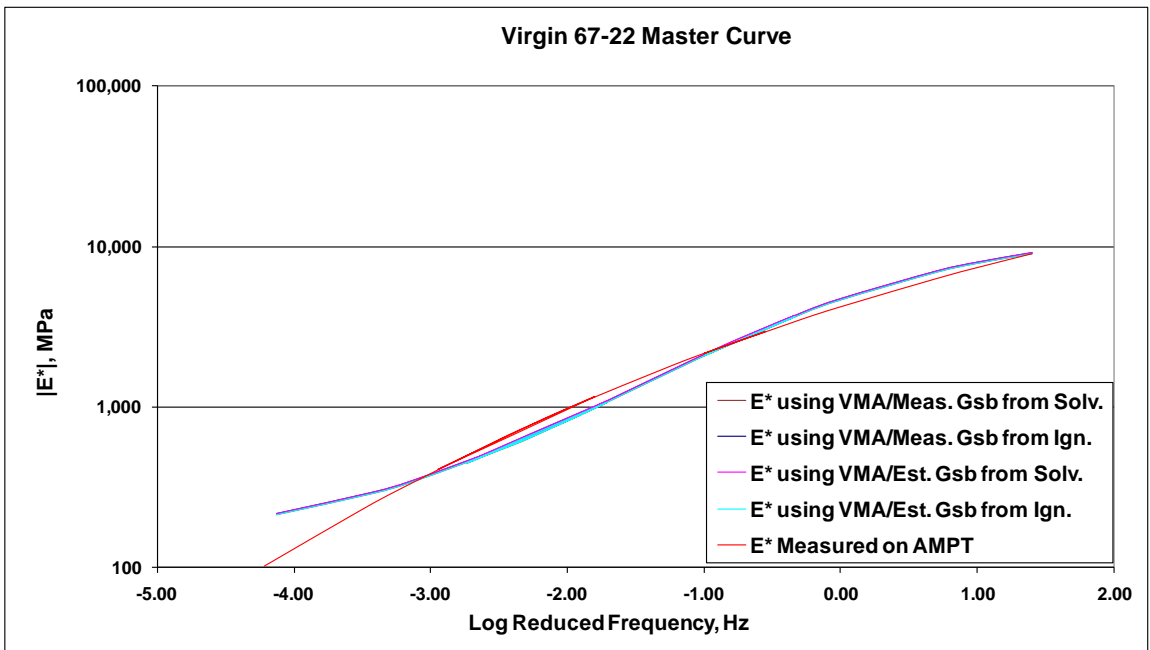**Figure 6.16 E* Master Curve for RAP 4**

Figure 6.17 E* Master Curve for RAP 5

Figure 6.18 E* Master Curve for RAP 6

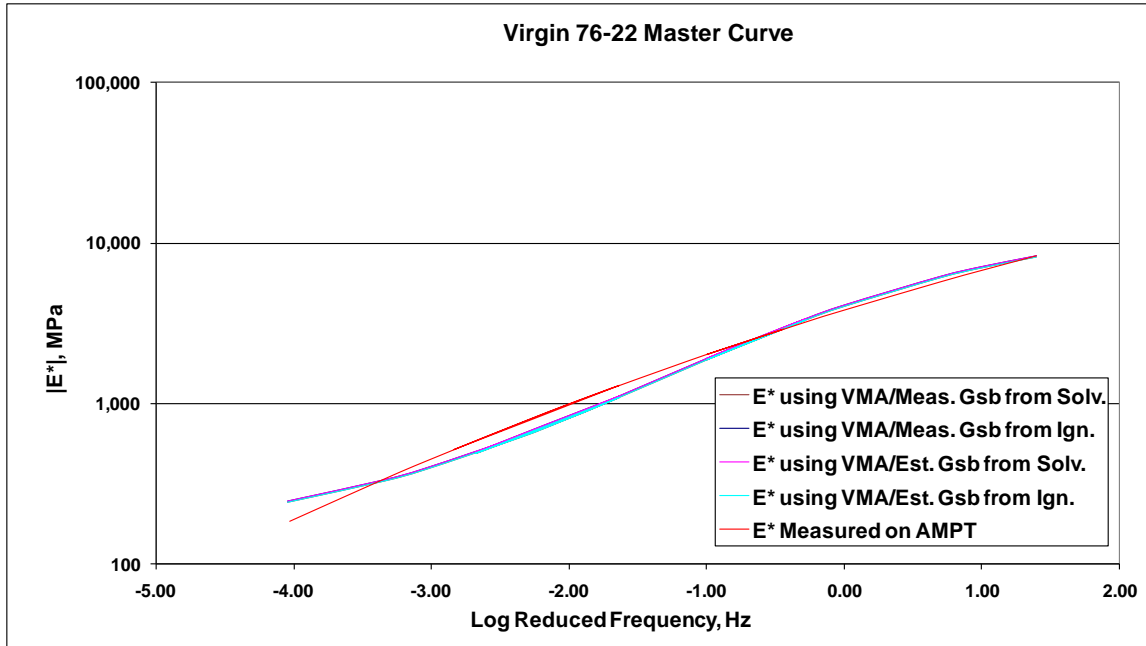**Figure 6.19 E* Master Curve for Virgin 67-22**

79

Figure 6.20 E* Master Curve for Virgin 76-22

Since it was determined that E* calculated from the Hirsch model is insensitive to VMA, any of the four methods to determine VMA can be utilized. Since the overall objective of this study was to determine a non-solvent method of characterizing RAP, the ignition method was used for further analysis.

6.1.2 Dynamic Modulus

Six sources of RAP and two virgin laboratory mixes were tested in the AMPT. The RAP specimens consisted of 100% RAP compacted to target air voids. The two virgin mixes consisted of the same aggregate gradations as one another but differed in the virgin binder grade. Three specimens per mix were prepared and tested in the AMPT at 25, 10, 5, 1, 0.5, and 0.1 Hz. These frequencies were duplicated at four temperatures; 4.4°C (40°F), 21.1°C (70°F), 37.8°C (100°F), and 54°C (130°F)   A master curve was developed from the average E* of the three replicates, following AASHTO PP 61 using a

80

reference temperature of 21.1°C (70°F). The master curve shown in Figure 6.21

illustrates the differences between the RAP and virgin materials. It is apparent that the

100% RAP specimens were much stiffer than the virgin specimens, especially at the
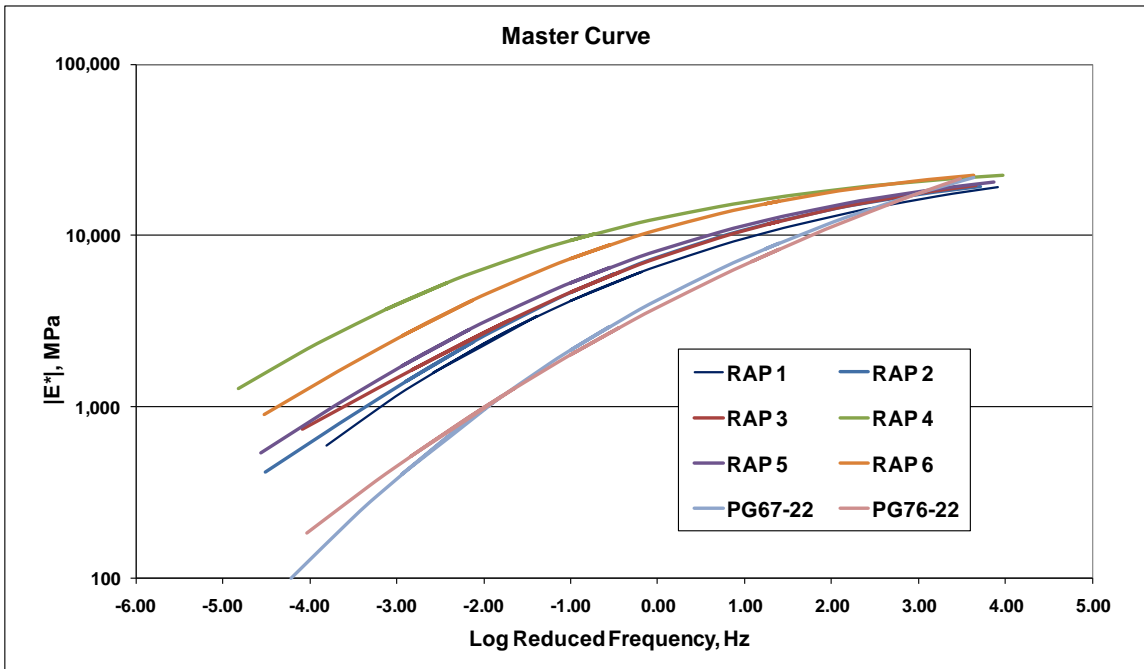
lower frequencies.

Figure 6.21 E* Master Curve of 100% RAP and Virgin Mixes

Using the measured E*, the calculated VMA from the ignition method G_{sb}, and

the VFA, the Hirsch model was employed to backcalculate G* at each of the four

temperatures and six frequencies. Master curves were then developed for the G* values

using the C-A model. This model works on the same principle as the E* master curves.

The measured data at different temperatures are shifted to a reference temperature with

respect to the loading frequency until a single smooth curve is constructed. The predicted

G* master curve at a reference temperature of 25°C, shown in Figure 6.22, compares the

different virgin and RAP sources. The G* master curve follows the same trend as the E*

master curve shown in Figure 6.21.
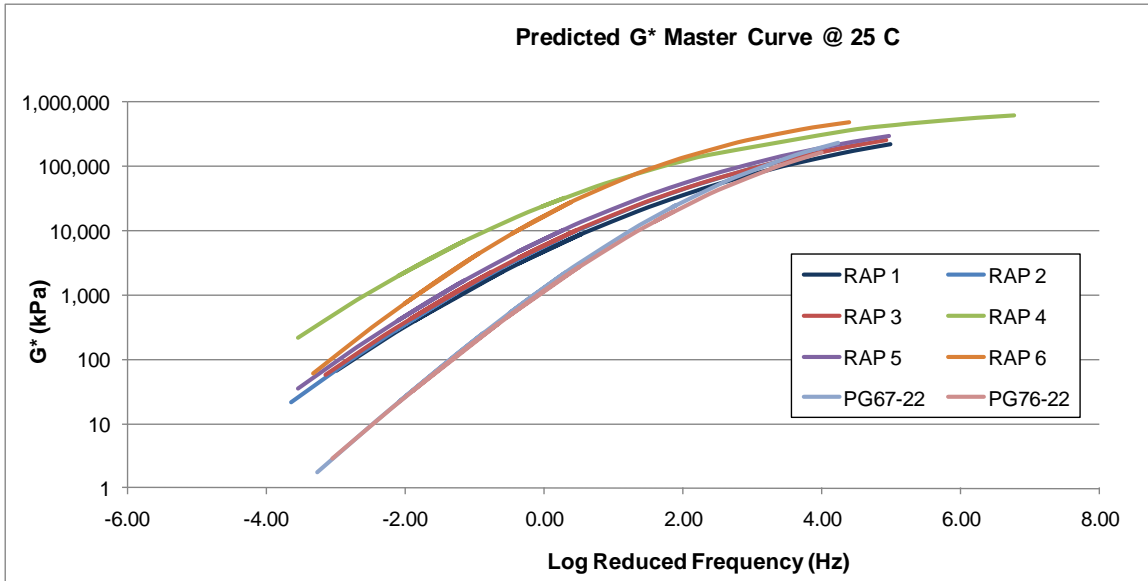
Figure 6.22 Predicted G* Master Curve

The C-A model also employs a method to predict the phase angle (δ) of the binder. The δ is an important parameter to obtain to characterize the viscoelastic behavior of binder. It is defined as the lag between the applied shear stress and the resulting shear strain. A purely elastic material has a δ equal to 0° while a purely viscous material has a δ equal to 90°.

At a chosen reference temperature for constructing the master curves, the G* and δ were extrapolated at 1.59 Hz. This is the frequency that is used to determine the high and intermediate critical temperature grades, according to AASHTO M 320 Standard Specification for Performance Graded Asphalt Binder. The high critical temperature grade is determined as the temperature in which G*/sinδ is equal to 2.2 kPa for binders aged in a Rolling Thin Film Oven (RTFO). Two master curves were developed with the first reference temperature producing a G*/sinδ > 2.2 kPa. The second master curve used a reference temperature that was 6°C higher so that G*/sinδ < 2.2 kPa. The critical temperature was then determined from Equation 6.4.

$$T_C = T_1 + \frac{Log(2.2) - Log\left(\frac{G^{\cdot}}{sin\delta}\right)_1}{Log\left(\frac{G^{\cdot}}{sin\delta}\right)_1 - Log\left(\frac{G^{\cdot}}{sin\delta}\right)_2} * (T_1 - T_2)$$

Equation 6.4

where,

T_C = critical temperature

T_1 = reference temperature 1

T_2 = reference temperature 2

$(G^*/sin\delta)_1$ = high temperature property at reference temperature 1

$(G^*/sin\delta)_2$ = high temperature property at reference temperature 2

The intermediate critical temperature was determined in the same manner, only the intermediate critical temperature is defined as the temperature at which $G^*sin\delta = 5000$ kPa for binders aged in a Pressure Aging Vessel (PAV). The critical temperature was determined from Equation 6.5.

$$T_C = T_1 + \frac{Log(5000) - Log(G^{\cdot}sin\delta)_1}{Log(G^{\cdot}sin\delta)_1 - Log(G^{\cdot}sin\delta)_2} * (T_1 - T_2)$$

Equation 6.5

The extrapolated critical temperatures were compared to the true critical temperatures measured on the DSR. The average values are listed in Table 6.21 for both the intermediate and high temperatures. The graphical comparison is shown in Figure 6.23 and Figure 6.24. The error bars represent the standard deviations based on three data points per source for the predicted critical temperatures. There were no replicate specimens to determine the true critical temperatures and therefore, the standard deviation is based on the maximum coefficient of variation specified in AASHTO M 320.

Table 6.21 True vs. Predicted Intermediate and High Critical Temperatures

	Intermediate Temperature		High Temperature	
	PREDICTED	TRUE	PREDICTED	TRUE
RAP 1	24.1	26.0	100.7	85.7
RAP 2	25.9	29.2	85.7	84.8
RAP 3	26.6	32.2	96.7	95.0
RAP 4	38.4	39.0	97.3	91.2
RAP 5	27.8	29.5	91.5	88.3
RAP 6	36.2	39.0	92.9	98.4
PG67-22	20.1	23.9	69.9	67.5
PG76-22	17.5	22.4	71.1	78.7
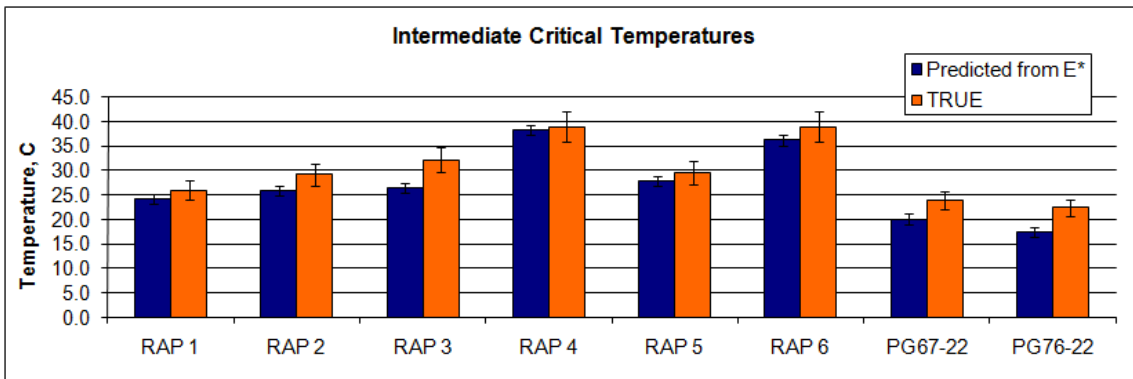
Figure 6.23 True vs. Predicted Intermediate Critical Temperatures
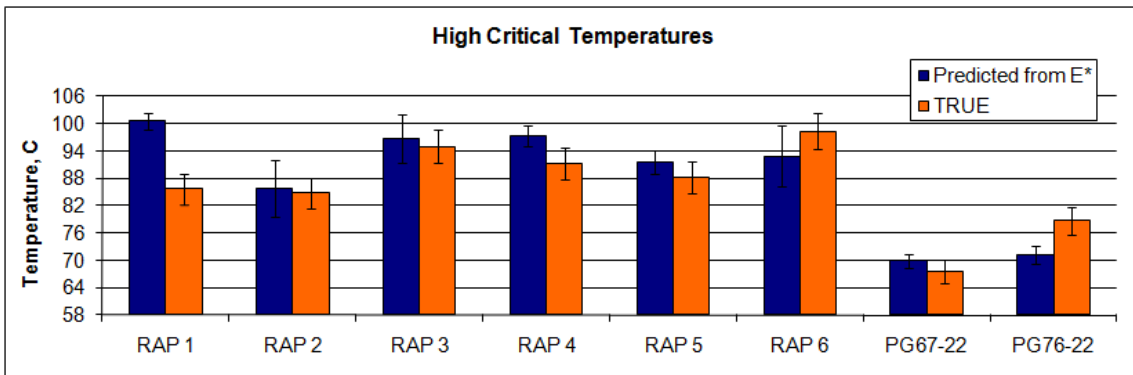
Figure 6.24 True vs. Predicted High Critical Temperatures

In comparing the intermediate critical temperatures, all of the predicted values were close to the true temperatures except for RAP 3 and PG 76-22. The predicted values were slightly lower than the true values. For the high critical temperatures, most of the predicted values were comparable to the true temperatures except for RAP 1 and PG 76-22. Most of the sources had a slightly higher predicted value compared to the true values.

A *t-test* was performed using a significance level of 0.05. This test revealed that only the true vs. predicted intermediate temperatures of RAP 3 and PG 76-22 were significantly different. RAP 1 and PG 76-22 also were significantly different when comparing the high critical temperatures. These differences could possibly be a result of binder extraction and testing issues with polymer modified binder. The p-values are shown in Table 6.22, along with the notation "Y" for significantly different and "N" for not significantly different.

Table 6.22 Statistical Analysis (t-test of True vs. Predicted Critical Temperatures)

	Intermediate Temperature		High Temperature	
Source	p-value	Significantly Different	p-value	Significantly Different
RAP 1	0.32	N	0.01	Y
RAP 2	0.14	N	0.84	N
RAP 3	0.04	Y	0.67	N
RAP 4	0.78	N	0.08	N
RAP 5	0.43	N	0.26	N
RAP 6	0.26	N	0.31	N
PG67-22	0.05	N	0.26	N
PG76-22	0.02	Y	0.04	Y

6.1.3 Relaxation Modulus

The same six sources of RAP and two virgin laboratory mixes were tested in an Instron 8501 Indirect Tensile Tester. Three specimens were prepared per mix and tested to determine the relaxation modulus, E(t).

Although all of the tests were run by the same individual, the repeatability of the test was very poor. The largest contributor to the variability was the application of the seating load. Once the specimen was placed on the testing jig, the load frame was lowered to apply no more than 45 kN. However, once the load was placed on the specimen, it began to immediately relax and the load would decrease. It was difficult to ensure that the relaxation test began with the same seating load on each specimen. This factor affected the initial relaxation modulus of the different mixes. Figure 6.25 illustrates the differences between the relaxation modulus curves for the three testing points of one specimen. Figure 6.26 illustrates the differences between the relaxation modulus curves for three specimens from one RAP source. Each curve shown in Figure 6.26 is the average of the three testing points of one specimen. It is obvious that there was a lot of variability for any single specimen.
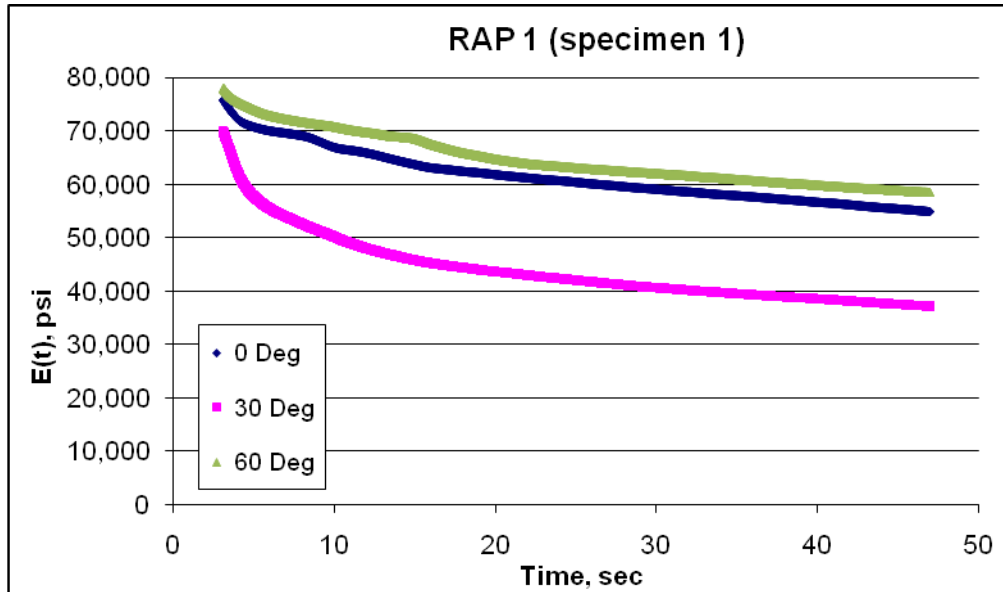
Figure 6.25 Relaxation Modulus of One Specimen at 0, 30, 60 Degrees Apart
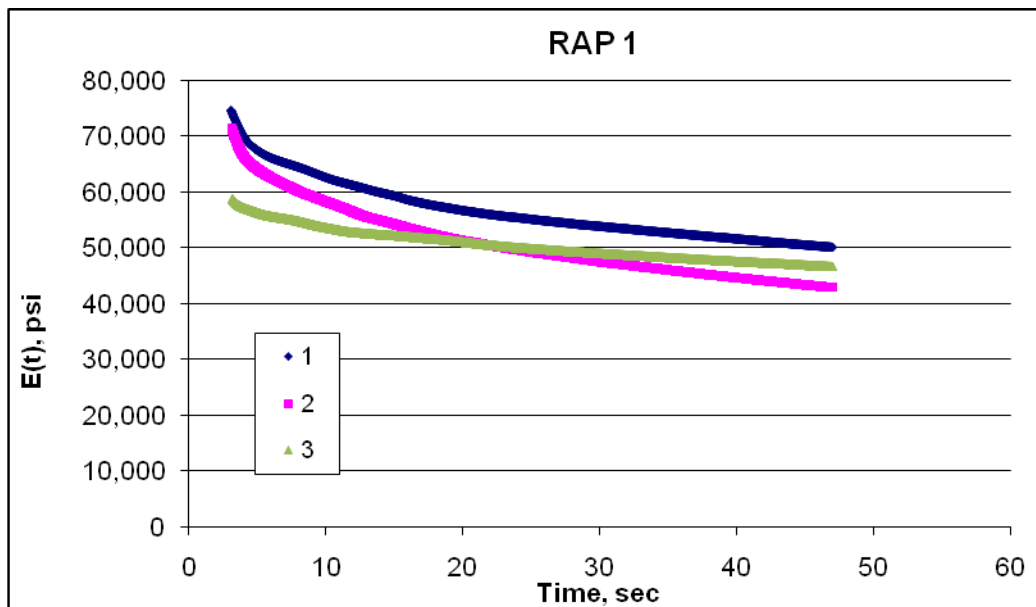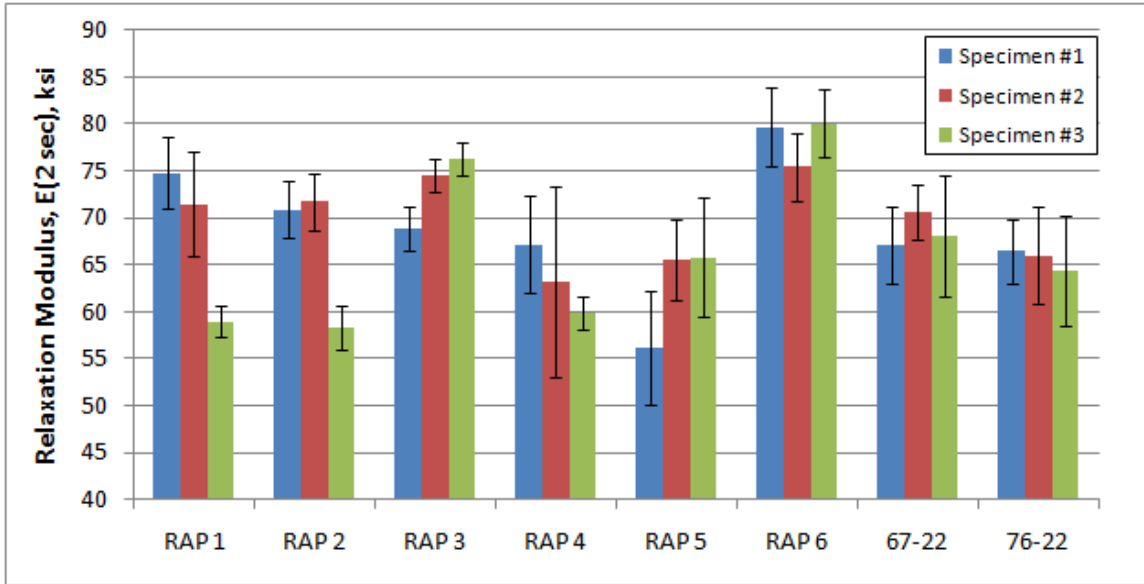

Figure 6.26 Relaxation Modulus of Three Specimens from the RAP 1 Mix

A power curve was fit to each relaxation modulus curve. The relaxation modulus and degree of curvature was determined from the power function at a time of two seconds. The first two seconds was an initial lag time before the actual test began.

Figure 6.27 shows the average relaxation modulus at two seconds for each specimen of the six RAP and two virgin mixes. The error bars represent the standard deviation between the three testing points located 30° apart.
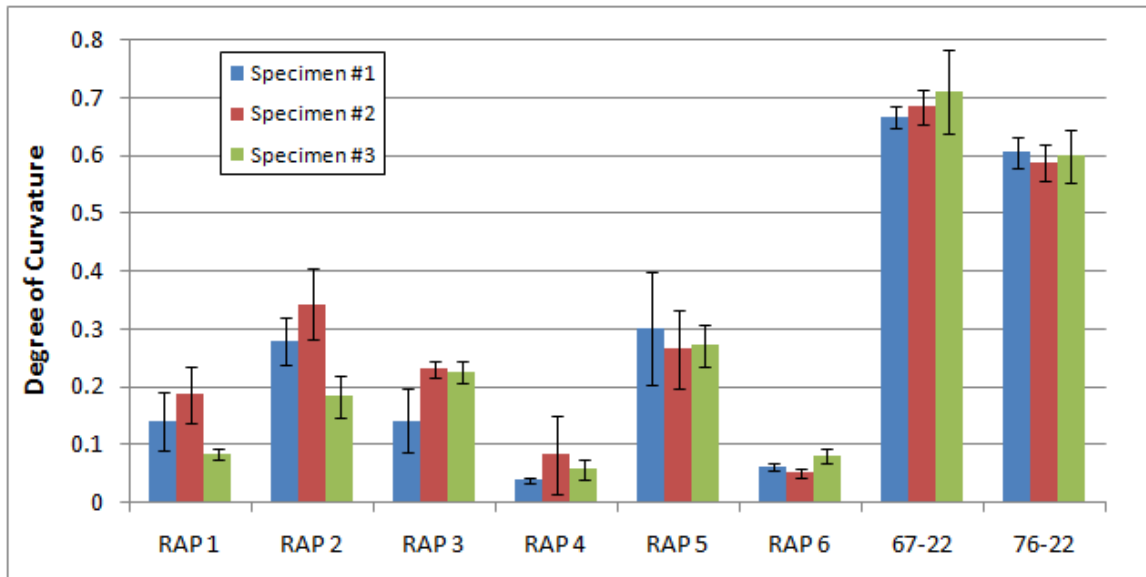

Figure 6.27 Relaxation Modulus of Each RAP and Virgin Source

It is clear that there is some variability, not only between the three testing points, but also the three specimens within a single RAP or virgin source. Table 6.23 lists the coefficient of variation (COV) between the different specimens and testing locations. The COV is defined as the standard deviation divided by the average, represented as a percentage. The COV ranges between 2.39% and 16% within one specimen. It ranges between 1.63% and 12.22% within one RAP or virgin source. The variation is even greater in the degree of curvature which is shown in Figure 6.28 and listed in Table 6.24.

Table 6.23 COV of Relaxation Modulus

Source	Specimen	COV (between testing locations)	COV (between specimens)
RAP 1	1	5.14	12.22
	2	7.90	
	3	2.82	
RAP 2	1	4.22	11.23
	2	4.19	
	3	4.07	
RAP 3	1	3.35	5.35
	2	2.47	
	3	2.39	
RAP 4	1	7.58	5.80
	2	16.00	
	3	2.87	
RAP 5	1	10.69	8.71
	2	6.55	
	3	9.64	
RAP 6	1	5.30	3.27
	2	4.75	
	3	4.47	
67-22	1	6.11	2.61
	2	4.03	
	3	9.45	
76-22	1	5.07	1.63
	2	7.87	
	3	9.06	

Figure 6.28 Degree of Curvature of Each RAP and Virgin Source

89

Table 6.24 COV of Degree of Curvature

Source	Specimen	COV (between testing locations)	COV (between specimens)
RAP 1	1	35.62	38.01
	2	25.61	
	3	10.48	
RAP 2	1	14.74	28.81
	2	18.17	
	3	19.91	
RAP 3	1	38.26	35.45
	2	5.98	
	3	8.42	
RAP 4	1	12.25	57.19
	2	81.57	
	3	30.14	
RAP 5	1	32.62	6.38
	2	25.32	
	3	12.94	
RAP 6	1	10.63	25.79
	2	13.99	
	3	16.60	
67-22	1	2.63	3.23
	2	4.52	
	3	10.23	
76-22	1	4.57	1.50
	2	5.50	
	3	7.63	

The COV ranged between 2.63% and 81.57% within one specimen, and between 1.50% and 57.19% within one RAP or virgin source. The virgin samples did have a higher degree of curvature, indicating that this softer mix relaxes quicker than a stiffer RAP mix.

It was difficult to minimize the variation within even one sample. Although the same technician followed the same method on each specimen and testing location, the seating load had a large effect on the relaxation modulus. Further analysis and test method development should occur before the relaxation test is adopted as a viable mix

test. Because of the difficulties with this particular test method, the dynamic modulus test was chosen for Phase II.

6.2 Phase II

After the analysis for Phase I was complete, the dynamic modulus test was selected as the most appropriate method for backcalculating binder properties for RAP materials. The second phase of the study consisted of verifying the backcalculation procedure with plant produced mixes and evaluating the sensitivity of the dynamic modulus to changes in the binder properties on laboratory produced mixes.

6.2.1 Plant Produced Mixes

Five plant produced mixes from several locations in Alabama were used to verify the backcalculation method using dynamic modulus test results.   The plant mixes were sampled from the transfer truck, brought back to the lab, and reheated in an oven until the mix temperature reached 157°C (315°F). Once the mix had achieved this temperature, dynamic modulus specimens were prepared and tested the same way as in Phase I, only the specimens in Phase II were confined during testing. As mentioned earlier, the specimens in Phase I were unconfined due to a mistake in specimen preparation with the membrane. This mistake was corrected in Phase II and the specimens were confined during testing. However, this ultimately may have resulted in error since the Hirsch model was developed with unconfined specimens.

The master curve shown in Figure 6.29 illustrates the differences between the different plant mixtures. It should be noted that Mix 5 was actually an Open Graded Friction Course (OGFC). An OGFC mixture is designed to have a high volume of air voids. For this reason, it was not as stiff as the other plant mixes. Mix 1 contained both

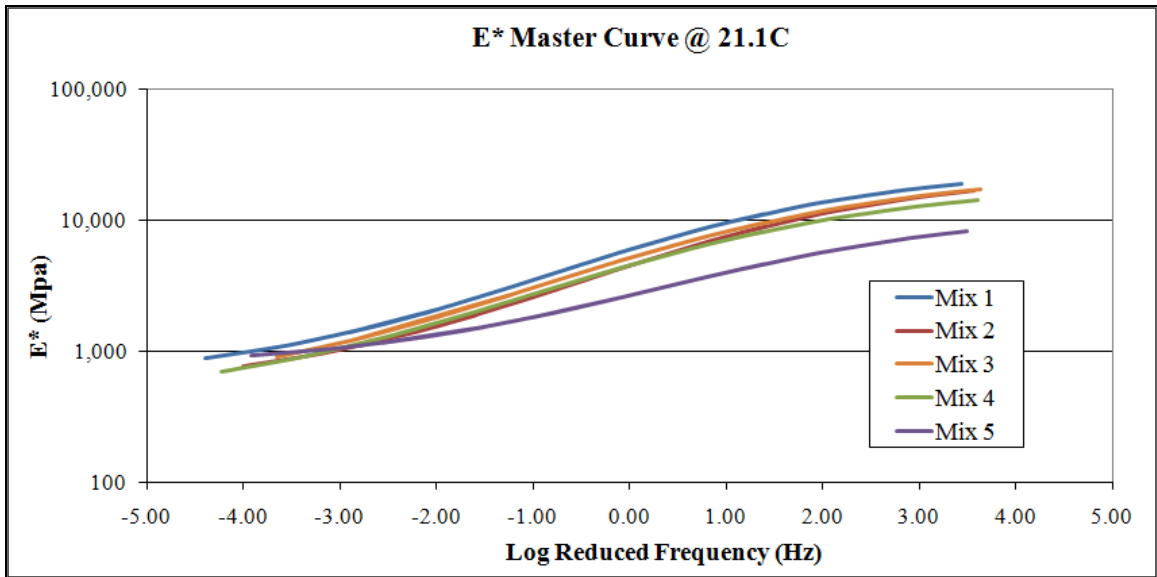RAP and RAS which produced a much stiffer mix than the other plant mixes containing only RAP.


Figure 6.29 E* Master Curve of Plant Mixes

The E* of each plant mix, along with volumetric properties, were then used in the Hirsch model to backcalculate G* values. The backcalculated values were used in the C-A model to predict the phase angle (δ), and subsequently the critical temperatures at which G*/sin δ = 2.2 kPa and G*sinδ = 5000 kPa. This was then compared to the critical temperatures measured on the DSR of extracted binder.

The average critical temperatures are listed in Table 6.25 for both the intermediate and high temperatures. The graphical comparisons are shown in Figure 6.30 and Figure 6.31. The error bars represent the standard deviations based on three data points from the E* predicted values. The standard deviations for the 'True' values are based on the maximum COV specified in AASHTO M 320.

Table 6.25 True vs. Predicted Critical Temperatures

|	Intermediate Temperature		High Temperature	
	PREDICTED	TRUE	PREDICTED	TRUE
1	20.9	23.3	84.8	90.1
2	15.3	24.1	87.7	87.2
3	19.8	26.7	96.7	93.5
4	16.0	24.1	90.9	86.4
5	17.9	21.2	102.1	84.1
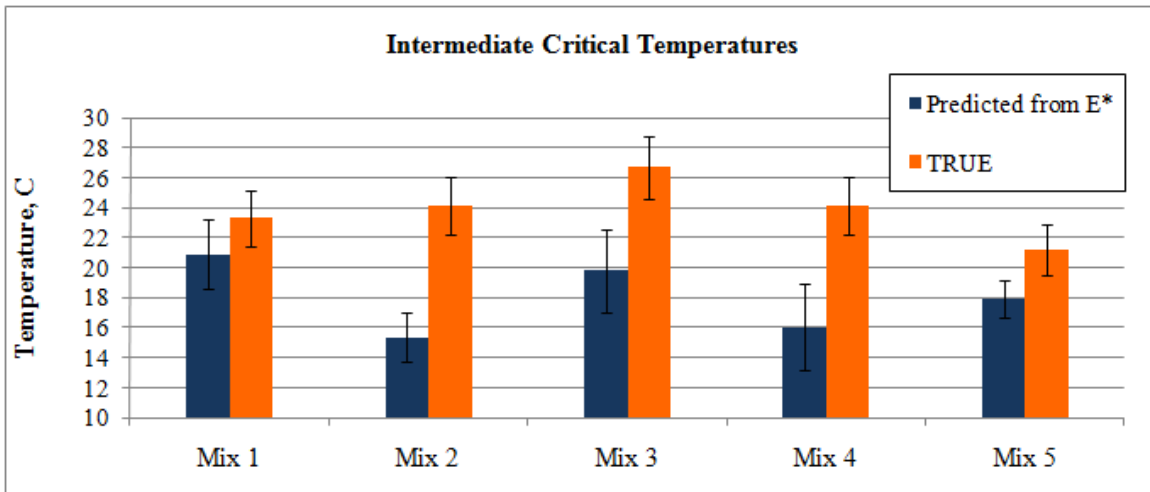
Figure 6.30 True vs. Predicted Intermediate Critical Temperatures

All of the predicted intermediate critical temperatures were much lower than the intermediate critical temperatures from the tests on the recovered binders. However, Mix 1 and Mix 5 were only about 2 or 3°C less. A *t-test* revealed that Mix 1 and Mix 5 were the only ones that were not significantly different, using a significance level of 0.05. However, Mix 5 was almost significantly different with a *p*-value of 0.05. The *p*-values are shown in Table 6.26, along with the notation "Y" for significantly different and "N" for not significantly different.

A possible reason as to why the correlation between predicted and 'true' is so low is that the 'true' intermediate critical temperatures were determined from binder aged in a

pressure aging vessel. The predicted values were based off field mix that had only undergone plant aging and not long term aging. That is why all of the predicted intermediate temperatures are lower than the 'true' temperatures.
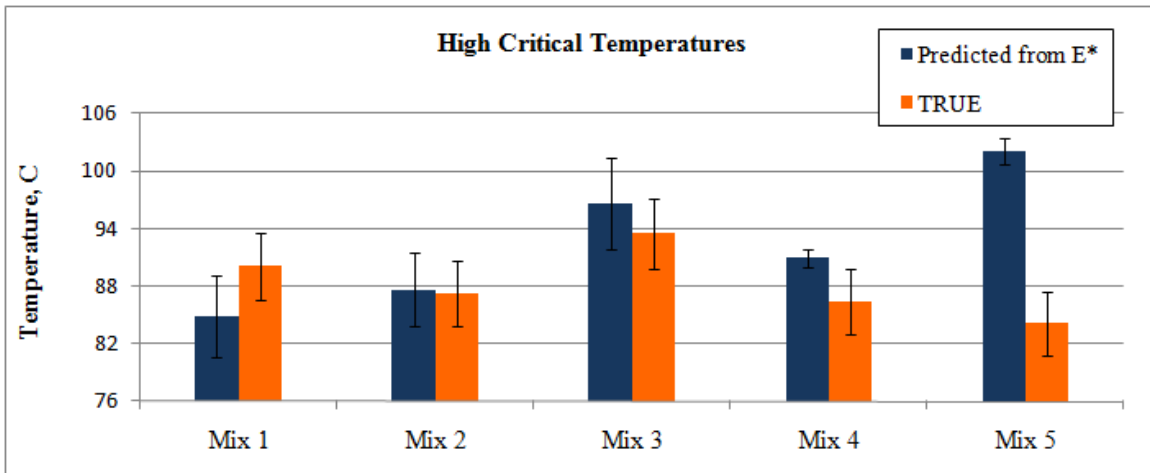
Figure 6.31 True vs. Predicted High Critical Temperatures

When comparing the high critical temperatures, most of the predicted temperatures were slightly higher than the true temperatures except for Mix 1. One theory as to why the predicted values were higher is that at high testing temperatures, the mixture stiffness is attributed mainly to the aggregate structure. This would then cause the predicted values to be higher than the true values which were determined from only binder tests.

Although most of the predicted temperatures were higher than the true temperatures, the values were the same grade or only one grade higher. In fact, none of the mixtures were significantly different except for Mix 5 using a significance level of 0.05. The *p*-values for the high critical temperatures are shown in Table 6.26.

As noted previously, Mix 5 was an OGFC mix. OGFC mixes have very high VMA values which in turn affects the backcalculation of G^* in the Hirsch Model. The statistical differences seen in Mix 5 are most likely caused from using the Hirsch model, which was not developed for OGFC mixes.

Table 6.26 Statistical Analysis (t-test of True vs. Predicted Critical Temperatures)

Source	Intermediate		High	
	p-value	Statistically Different	p-value	Statistically Different
1	0.24	N	0.17	N
2	0.004	Y	0.88	N
3	0.03	Y	0.42	N
4	0.03	Y	0.15	N
5	0.05	N	0.003	Y

6.2.2 Laboratory Produced Mixes

The sensitivity analysis consisted of evaluating laboratory produced mixes that varied in RAP content and virgin binder grade. Three RAP sources were used in the mix designs. For each RAP source, nine mixes were designed with different combinations of three RAP percentages and three binder grades. The three RAP percentages used during the mix design process included 20%, 35%, and 50% RAP and the three binder grades included PG 58-28, PG 67-22, and PG 76-22. This provided a total of 27 separate mixes to evaluate.

Dynamic modulus specimens were tested according to AASHTO TP 62 at the same four temperatures and six frequencies. The E^* master curves of each RAP source and binder type at a reference temperature of 21.1°C are shown in Figure 6.32 – Figure 6.40.
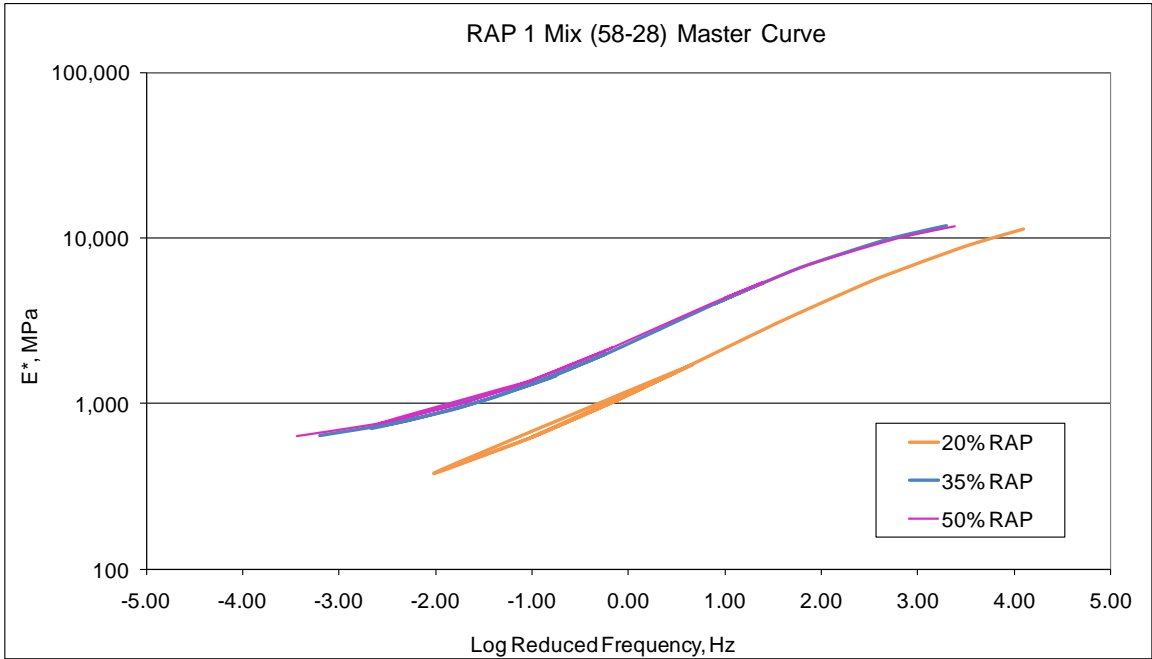
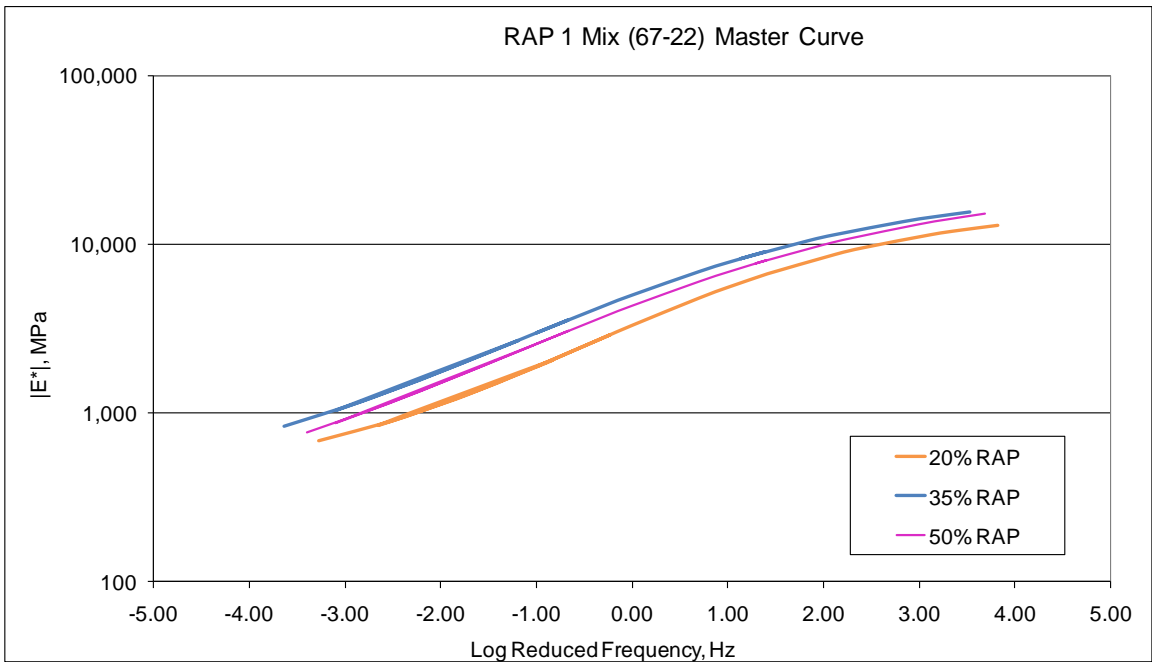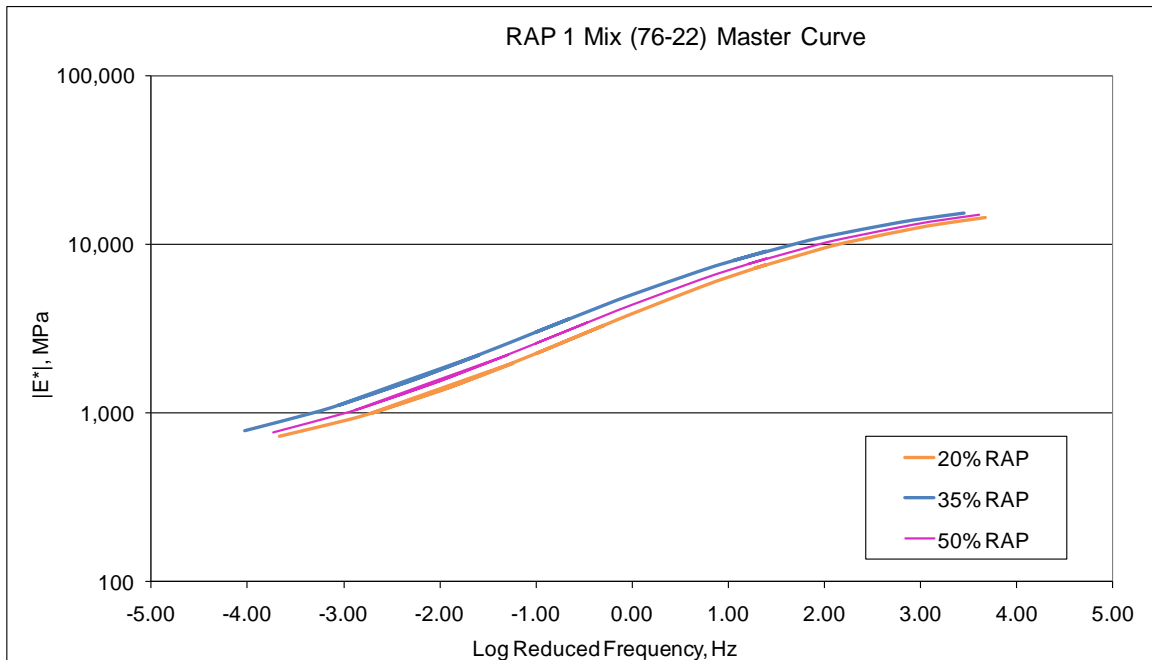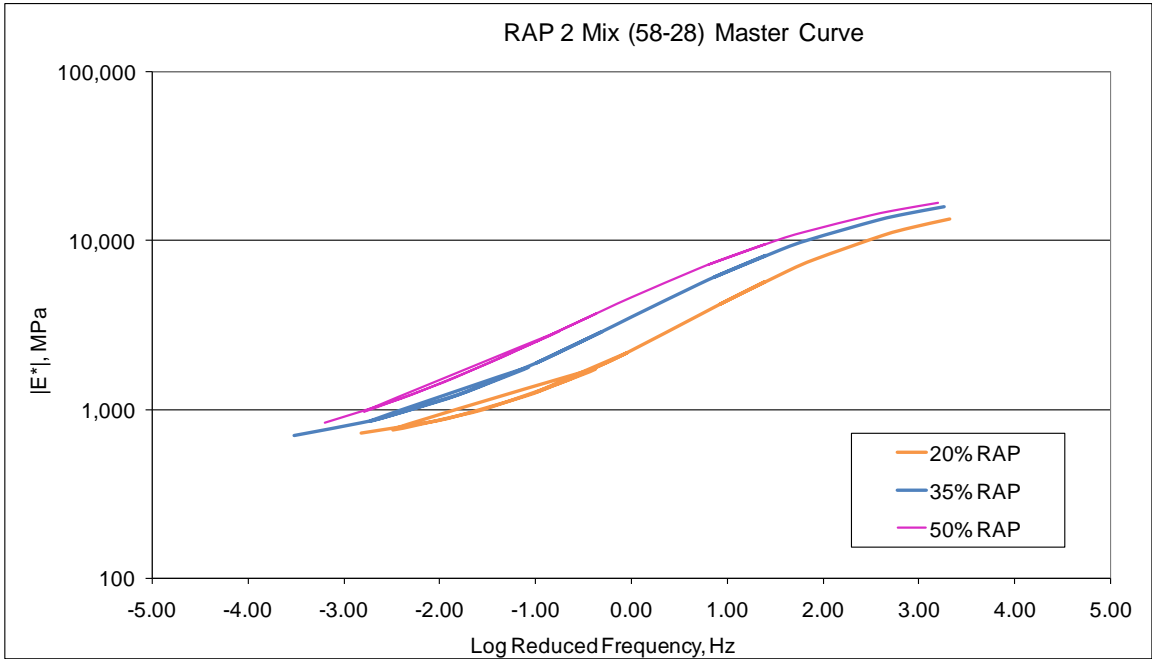**Figure 6.32 E* Master Curve Comparing RAP Percentage (RAP 1 Mix, 58-28)**

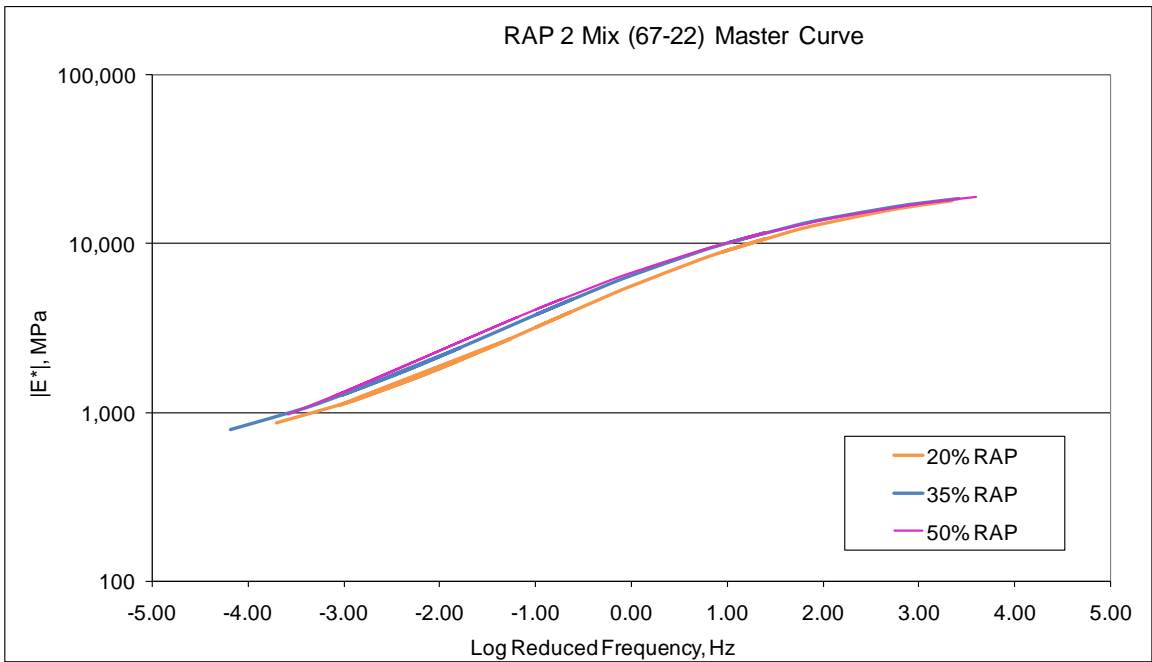**Figure 6.33 E* Master Curve Comparing RAP Percentage (RAP 1 Mix, 67-22)**

96

Figure 6.34 E* Master Curve Comparing RAP Percentage (RAP 1 Mix, 76-22)

For the RAP 1 mixes, the 20% RAP designs were the least stiff for all three binder types. However, the 35% RAP mix was stiffer than the 50% RAP for the 67-22 and 76-22. This could possibly suggest that the 50% RAP mixes were not fully blending compared to the 35% RAP mixes.

Figure 6.35 E* Master Curve Comparing RAP Percentage (RAP 2 Mix, 58-28)

Figure 6.36 E* Master Curve Comparing RAP Percentage (RAP 2 Mix, 67-22)
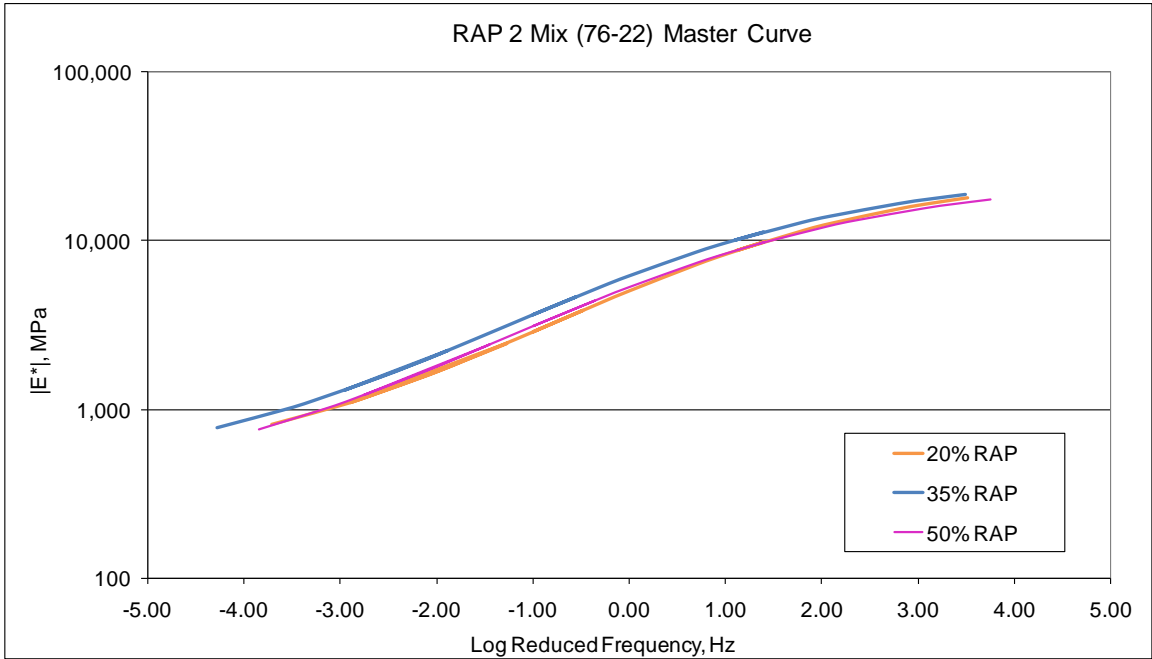
RAP 2 Mix (76-22) Master Curve

Figure 6.37 E* Master Curve Comparing RAP Percentage (RAP 2 Mix, 76-22)

For the RAP 2 mixes, the 35% RAP mix was stiffer than the 50% RAP for only the 76-22. The stiffness was the same between the 35% and 50% RAP when using a 67-22.

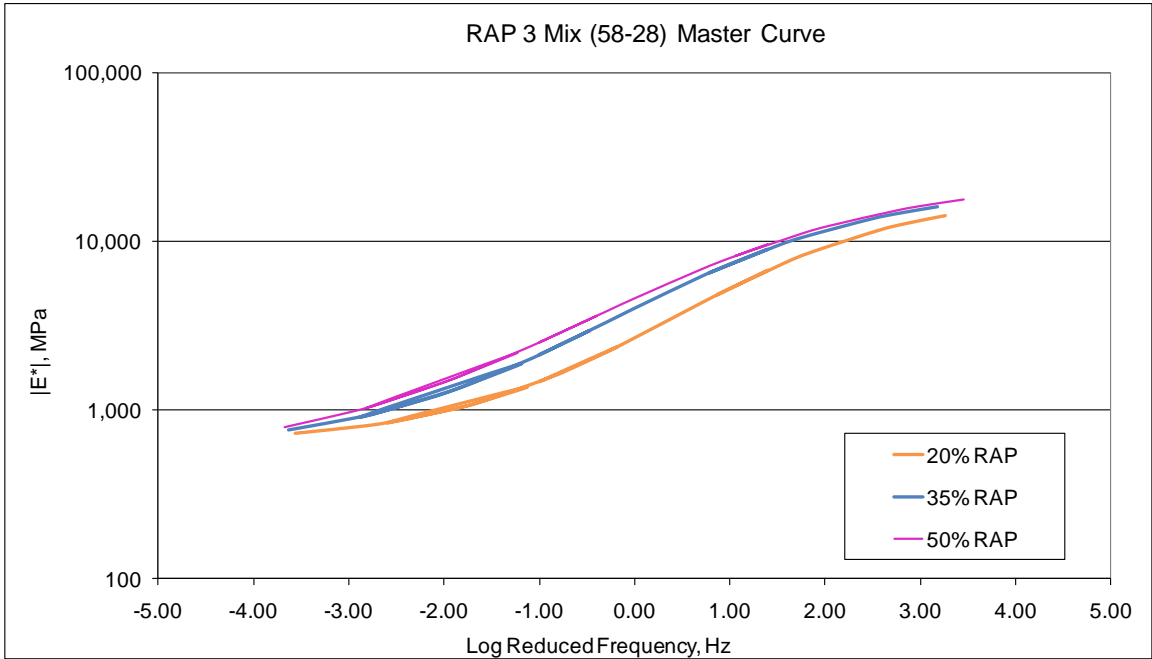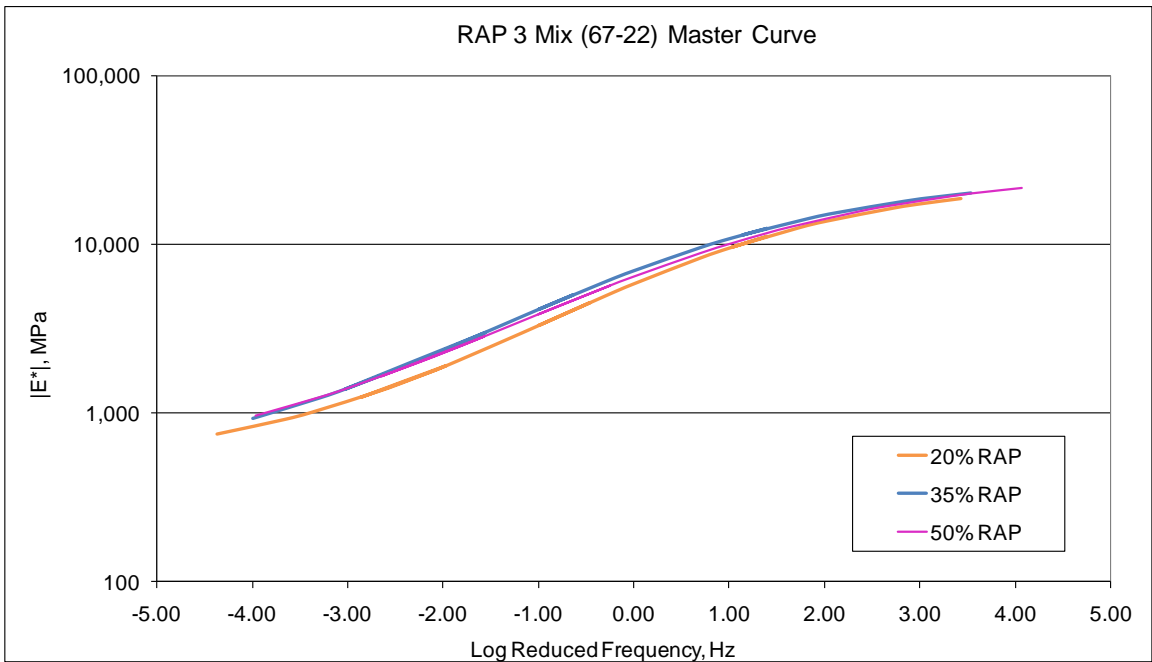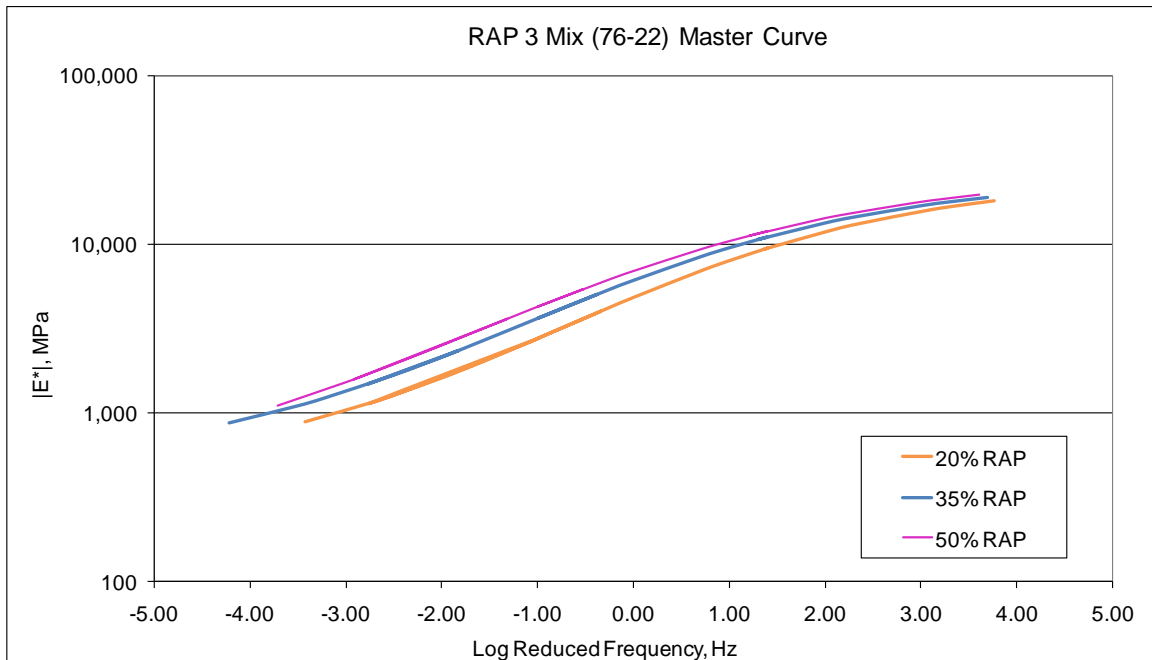**Figure 6.38 Master Curve Comparing RAP Percentage (RAP 3 Mix, 58-28)**

Figure 6.39 E* Master Curve Comparing RAP Percentage (RAP 3 Mix, 67-22)

Figure 6.40 E* Master Curve Comparing RAP Percentage (RAP 3 Mix, 76-22)

Similar to the RAP 2 mixes, RAP 3 mixes had almost identical master curves with both 35% and 50% RAP using a 67-22. This would imply that a mixture would exhibit the same stiffness regardless of whether or not the higher RAP percentage was utilized.

The measured E* for each mixture was used with the Hirsch model and C-A model to backcalculate G* and δ. The critical high temperature grades were then predicted and compared between each binder source and each RAP percentage. It is expected that as the RAP percentage increases, the high temperature grade should also increase. This same trend is expected when increasing the virgin binder grade from a 58-28 to a 67-22 and then to a 76-22.

For comparison purposes, a linear blending equation shown in Equation 6.6 was used to determine what the expected high temperature grade of the blended mixture should be. This equation assumes 100% blending between the RAP and virgin binders.

In order to determine the expected high temperature grade of the blended mixture, the high critical temperature was measured on the extracted RAP binder and also on extracted virgin binder that had been mixed with virgin aggregate and aged at the determined compaction temperature for four hours. This four hour age of the virgin mixes was conducted to simulate the same aging process that the E* specimens of the 27 mixtures had undergone. The high critical temperatures of these extracted binders are shown in Table 6.27. It should be noted that the %RAP in Equation 6.6 is the percent RAP by weight of binder.

$$T_{Blend} = \% RAP \left(T_{RAP} - T_{Virgin} \right) + T_{Virgin}$$ **Equation 6.6**

Table 6.27 Measured High Critical Temperatures of Extracted RAP Binder and Aged Virgin Binder

	PG 58-28	PG 67-22	PG 76-22	RAP 1	RAP 2	RAP 3
Measured High Critical Temperatures, °C	64.6	80.1	91.9	85.7	91.6	92.2

The predicted results for the nine RAP 1 mixes are illustrated in Figure 6.41 as solid bars. The expected results from the linear blending equation are also illustrated in this figure as hatched bars of the same corresponding color. Note that the percentage of RAP is labeled as percent by binder weight.

The backcalculation method over predicts the high critical temperature for the PG 58-28 mixes in comparison to the expected temperatures using the linear blending equation by about three temperature grades. The difference between the predicted and expected values for the PG 67-22 and PG 76-22 mixes are much less. Although the predicted and expected temperatures are not the same for all mixes, the general trend of

increasing high temperature with increased RAP binder percentage was observed for the PG 58-28 and PG 67-22. This would suggest that lower virgin binder grades are more sensitive to changes in RAP percentage as compared to a stiffer PG 76-22.
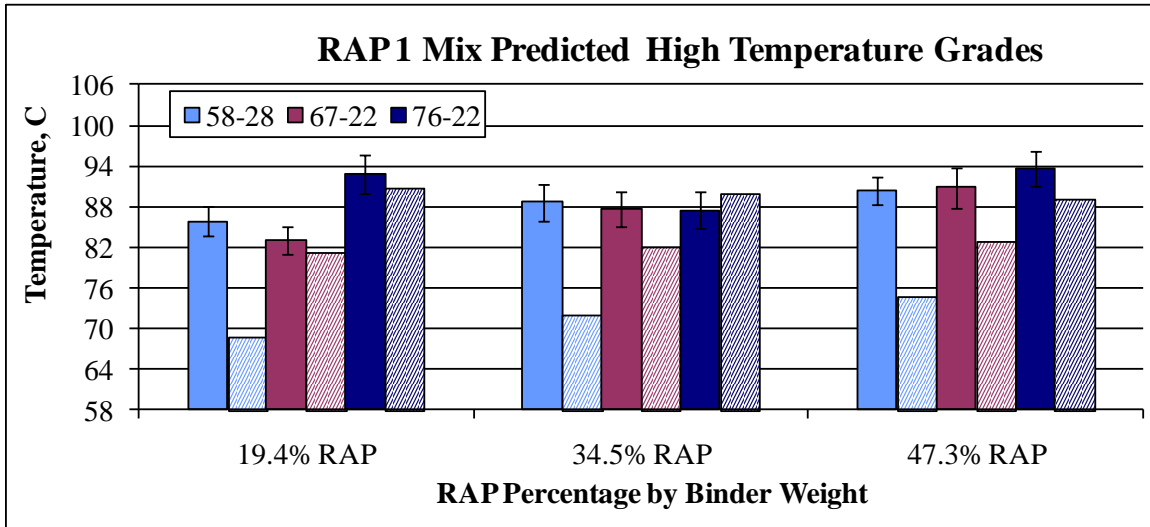

Figure 6.41 RAP 1 Mix – High Critical Temperature

The predicted high temperature grades of the RAP 2 mixes, along with the corresponding expected temperatures from linear blending calculations, are shown in Figure 6.42. Again, the backcalculation method grossly over predicted the high critical temperature of the PG 58-28 mixes. The temperatures of the PG 67-22 mixes were also over predicted, especially at the higher RAP percentages. It is interesting to see that the expected high critical temperatures calculated from the linear blending equation shows little increase from 16.3% RAP to 37.2% RAP by weight of binder for the PG 67-22 and PG 76-22 mixtures. However, an increase in high temperature with increasing RAP percentage is observed in the predicted values for the PG 67-22 mixes.
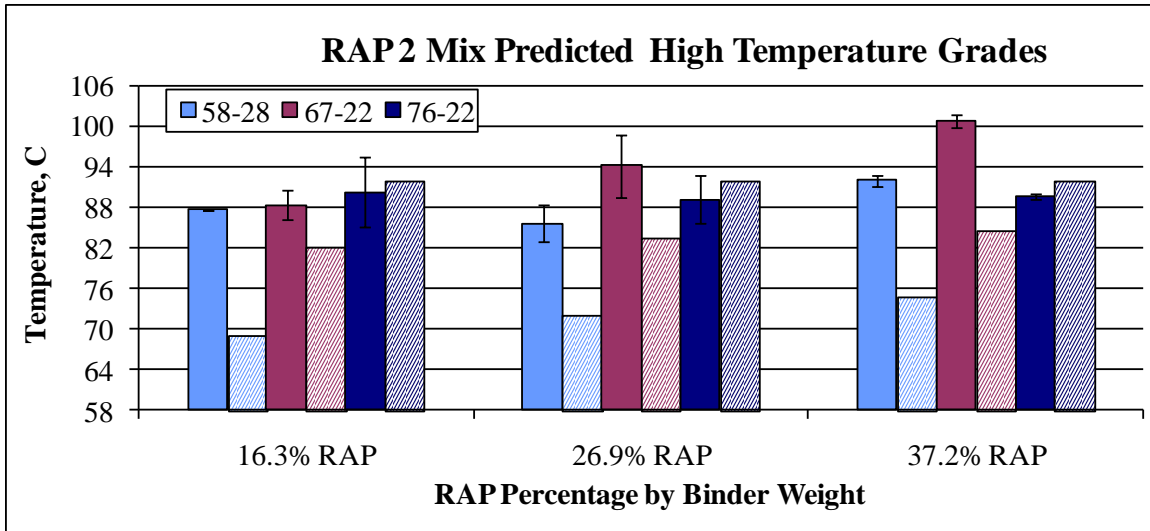
Figure 6.42 RAP 2 Mix - High Critical Temperature

The high temperature grades of the RAP 3 mixes, along with the corresponding expected temperatures from linear blending calculations, are shown in Figure 6.43. The predicted critical temperatures of the 15.5% RAP mixtures were much larger than the expected values for all three virgin binder types. This suggests that even low percentages of this particular RAP source greatly stiffens the mixture, in terms of E* testing. However, the 30.2% RAP mixtures had lower predicted high critical temperatures than the 15.5% RAP mixtures.
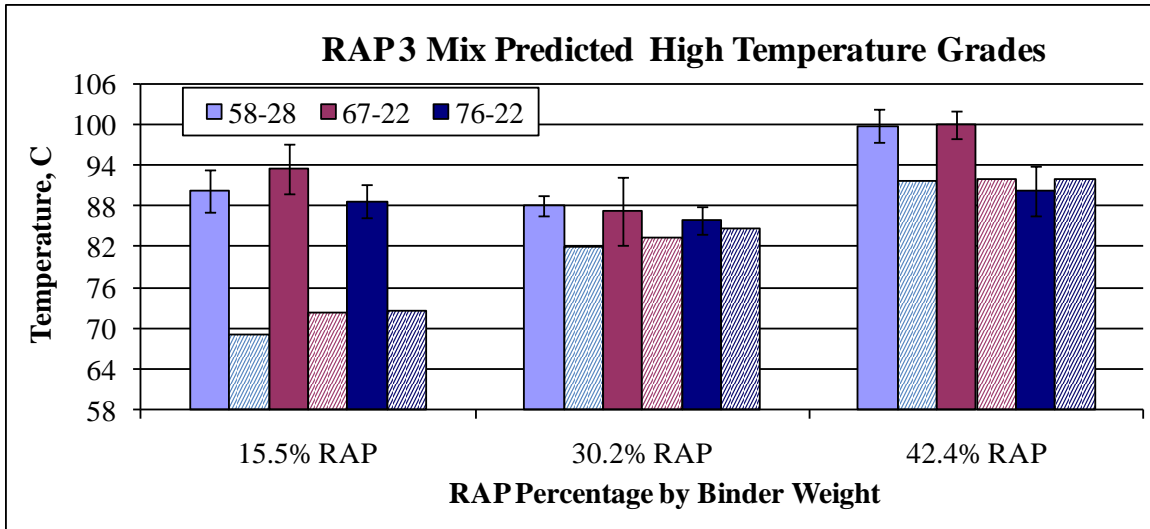
Figure 6.43 RAP 3 Mix - High Critical Temperature

There are obviously some discrepancies in the expected trends of binder stiffness. It is expected that as the RAP percentage increases, the high binder grade will also stiffen. It is possible that the backcalculation method is not predicting the precise critical high temperature grade. However, there are other factors that could result in these differences including specimen preparation and testing. Based on the 100% RAP data from Phase I and the plant mix from Phase II, the backcalculation method is plausible for estimating the high critical temperature grade without running actual binder tests, although additional testing should be conducted before implementing this method into standard mix design.

CHAPTER 7
CONCLUSIONS AND RECOMMENDATIONS
7.1 Summary

The main goal of this research was to evaluate a simple method of characterizing RAP asphalt without directly testing recovered binder. To accomplish this goal, a literature review was conducted to evaluate current mix design practices for RAP mixtures, the effect of those practices, and the development and analysis of new methods for characterizing RAP mixtures without using solvents.

In Phase I of this study, two mix tests were evaluated to determine if the resulting backcalculated binder properties were similar to known binder properties. Six sources of RAP and two virgin laboratory mixes were evaluated. Due to variability in the measured data for the E(t) test, the E* test was chosen for additional analysis. With the E* data and volumetric properties, the Hirsch model was used to backcalculate G*. The C-A model was used to predict G* and δ at a specified reference temperature and frequency in order to determine the critical temperatures of the mixture, which were then compared to measured values.

Since the Hirsch model requires VMA as an input, the RAP aggregate G_{sb} was measured or estimated using four different methods. An analysis was conducted to determine if the method selected for calculating the RAP G_{sb} substantially affected the VMA in the Hirsch model. The VMAs were also used in the Hirsch model, along with VFA and G*, to compare the calculated E* for all four methods.

106

The second phase of the study evaluated plant produced mixes to verify if the E* mix test produced reasonable backcalculated binder properties. Five field mixes consisting of up to 25% RAP, with one mix having both RAP and RAS, were collected for dynamic modulus testing. The E* of each field mix, along with volumetric properties, were then used in the Hirsch model to backcalculate G* values. The C-A model was used to predict the critical temperatures, which were compared to measured values.

The second phase also consisted of testing the sensitivity of the selected method to changes in the binder properties. This investigation involved evaluating mixes that varied in virgin binder grade, RAP source, and RAP content (20%, 35%, and 50%). The analysis consisted of determining if the backcalculated critical temperature was distinctive for mixes that only differ by binder properties or percentage of RAP.

7.2 Conclusions

7.2.1 RAP Characterization

Two of the variables required in the Hirsch model are VMA and VFA. In order to calculate VMA and VFA, the RAP aggregate G_{sb} must be determined through either measurement or estimation from G_{se}. Since the method chosen may have an impact on the final results, it was necessary to examine this impact. Four methods used for determining RAP G_{sb} values are listed below:

1. Measured G_{sb} from solvent extracted aggregate
2. Measured G_{sb} from ignition oven extracted aggregate
3. Estimation of G_{sb} from G_{se} and percent binder (P_b) from solvent extraction
4. Estimation of G_{sb} from G_{se} and P_b from the ignition method

The G_{sb} of the virgin aggregates compared in this study were also measured prior to mixing with virgin binder. Based on the results found for the virgin aggregates, the measured G_{sb} from ignition oven extracted aggregate was the closest to the 'true' G_{sb}. Unfortunately, a 'true' G_{sb} cannot be determined on RAP aggregate, so there is not a direct comparison between the four methods with RAP. Therefore, the G_{sb} from the four methods was used to calculate VMA and subsequently E* using the Hirsch model.

A statistical analysis determined that all four methods were significantly different for calculations of VMA. However, when comparing the four calculated E* methods to measured E* values, those differences between methods were not observed. Out of the E* data analyzed, more than 50% of the test values were significantly different from the measured E* values. However, each method had approximately the same percentage of differences between the calculated and measured values. Therefore, it can be concluded that the Hirsch model used for calculating E* is insensitive to VMA so any of the four methods can be used in this application.

7.2.2 Dynamic Modulus

The E* tests that were conducted on the two virgin and six 100% RAP mixes were used with the Hirsch model to backcalculate G*. The C-A model was then used to predict G* and δ in order to determine the intermediate and high critical temperatures. These predicted values were then compared to true critical temperatures measured during standard binder grading tests.

The predicted intermediate temperatures were in close agreement with the true values, except for the PG 76-22 and one of the RAP sources. The prediction method

tended to slightly under predict the critical temperatures, although only two of the eight mixes tested were significantly different.

The predicted high critical temperatures were also similar to the true values, except for the PG 76-22 and a different RAP source. The prediction method for the high critical temperatures tended to over predict the values. However, only two of the eight mixes were significantly different.

It was thought that since only virgin materials or 100% RAP materials were tested and there were no blending issues involved in this phase of the study that the measured and true critical temperatures would align. In both the intermediate and high critical temperature comparisons, the predicted values of the PG 76-22 mix were found to be significantly different than the true values. This difference could be a result of issues related to the solvent extraction process of polymer modified binder. Based on the findings from the RAP mixes, the Hirsch model, accompanied by the C-A model, is fairly accurate in predicting the critical temperatures of RAP. Therefore, differences found using a blend of virgin and RAP materials in Phase II may be a result of the actual interaction between the aged and fresh binders during mixing.

7.2.3 Relaxation Modulus

The same virgin and 100% RAP materials were used to test E(t). However, the repeatability of the test using a single operator was very poor. The largest contributor to the variability was the application of the seating load. When the seating load was placed on the specimen, it began to immediately relax and the load would decrease. It was difficult to ensure that each specimen was subjected to the same initial loading. This factor affected the initial relaxation modulus and especially the coefficient of curvature

for the different mixes. Due to the variability in this test method, it was not used for further analysis.

7.2.4 Plant Produced Mixes

Five plant produced mixes were evaluated using E* and volumetric properties to backcalculate G* using the Hirsch model. The C-A model was then employed to determine the intermediate and high critical temperatures. These predicted values were compared to true critical temperatures measured from standard binder grading tests.

Almost all of the mixes were determined to have a significant difference between the predicted and the true intermediate critical temperatures with the predicted values being much lower than the measured values. One possible reason as to why the correlation between predicted and 'true' values are so low is that the 'true' intermediate critical temperatures were determined from binder aged in a pressure aging vessel. The predicted values were based off field mix that had only undergone plant aging and not long term aging. That would explain why all of the predicted intermediate temperatures are lower than the 'true' temperatures. Another possible reason why the correlation is so low, is that the plant produced E* specimens were tested under a confinement pressure of 138 kPa and the Hirsch model was developed using unconfined E* test data. Therefore, this difference could be the result of confinement issues.

Most of the predicted high critical temperatures were slightly higher than the true temperatures but only one mix was significantly higher. This could be due to the fact that at high testing temperatures, the aggregate structure contributes more to mixture stiffness than the binder alone. This would then cause the predicted values to be higher than the true values which were determined from only binder tests. The confinement issues may

also have contributed to these slight differences. It should also be noted that since the predicted values were not lower than the measured values, the blending between the virgin and RAP binders that occurred during the mixing process was sufficient.

One of the plant produced mixes tested was an OGFC mixture. The high critical temperature was predicted to be about three grades higher than the actual grade. Because the Hirsch model did not include OGFC mixtures in the database used for development, this is most likely the reason as to why it did not accurately predict the binder properties. For this reason, the OGFC data generated in this study should be disregarded until further analysis of the model using an extended database is completed.

7.2.5 Laboratory Produced Mixes

Twenty seven different mixes comparing three RAP sources, three RAP percentages, and three binder grades were tested. Comparisons were made between E* master curves. The E* data from these mixtures were then used with the Hirsch and C-A models to predict the critical high temperatures. These values were also compared to the expected high critical temperatures of the blended mixtures calculated from a linear blending equation.

Except for the RAP 2 mixes with PG 76-22, all of the predicted high critical temperatures were higher than the expected temperatures. This suggests that complete blending is occurring but that the stiffer RAP binder is actually the controlling factor in the mixture's stiffness properties. This is especially noticeable in the softer PG 58-28 mixes.

Although there seem to be some inconsistencies with the predicted high critical temperatures compared to the expected critical temperatures, similar inconsistencies were

observed in the E* master curves with the 35% RAP often being stiffer than the 50% RAP. These mixtures did not follow the expected trend in either the E* testing or the backcalculation method. It is possible that the backcalculation method is not predicting the precise critical high temperature grade. However, there are other factors that possibly resulted in these differences including material properties, specimen preparation, and specimen testing.

7.3 Recommendations

Based on the findings from Phase I of this investigation, using the E* mix test along with the Hirsch and C-A models to predict both the intermediate and critical temperatures of RAP will result in reasonably accurate results. When using this model to test asphalt mixtures containing RAP, it is advisable to only predict the high critical temperatures since the intermediate temperatures will only be based on short term aging of the specimens. However, further analysis should be conducted to test laboratory mixtures with varying amounts of RAP and different binder types since the results from the sensitivity study were not as expected.

This research has shown that the backcalculation technique of predicting the high critical temperatures of a RAP mixture may be a better alternative to characterizing RAP than through solvent extractions and using linear blending charts. Additional research is recommended to assess the feasibility of backcalculating the high critical temperature of a RAP mixture to determine if the virgin binder grade should be adjusted. A mix test to determine the low critical temperatures would also be required to use this practice. Using a mix test in place of standard binder tests on extracted RAP binders will provide

properties that are more closely related to what the blended mixture will exhibit in the

field.

REFERENCES

AASHTO M320-10, *Standard Specification for Performance Graded Asphalt Binder.* AASHTO, 2010.

AASHTO M 323-07, *Superpave Volumetric Mix Design*. AASHTO, 2007.

AASHTO PP 61-09. *Determining Dynamic Modulus Master Curves for Hot Mix Asphalt (HMA) Using the Asphalt Mixture Performance Tester (AMPT)*. AASHTO, 2009.

AASHTO TP 62-07. *Standard Test Method for Determining Dynamic Modulus of Hot-Mix Asphalt (HMA)*. AASHTO, 2007.

AASHTO T 164-10, *Quantitative Extraction of Asphalt Binder from Hot-Mix Asphalt*. AASHTO, 2010.

AASHTO T 170-00, *Recovery of Asphalt Binder from Solution by Abson Method.* AASHTO, 2009.

AASHTO T 308-05, *Determining the Asphalt Binder Content of Hot-Mix Asphalt by the Ignition Method.* AASHTO, 2005.

AASHTO T 315-06. *Standard Test Method for Determining the Rheological Properties of Asphalt Binder Using Dynamic Shear Rheometer (DSR)*. AASHTO, 2006.

AASHTO T 319-08, *Quantitative Extraction and Recovery of Asphalt Binder from Asphalt Mixes.* AASHTO, 2008.

AASHTO T 331-10, B*ulk Specific Gravity and Density of Compacted Asphalt Mixtures Using Automatic Vacuum Sealing Method*, AASHTO, 2010.

Bari, J., and Witczak, M.W. (2006). Development of a new revised version of the Witczak *E** predictive model for hot mix asphalt mixtures. *Journal of the Association of Asphalt Paving Technologists,* Vol.75, pp. 381–423.

Bennert, T. and Dongré, R. (2009). A Backcalculation Method to Determine "Effective" Asphalt Binder Properties of RAP Mixtures. *Transportation Research Record: Journal of the Transportation Research Board, No. 2179,* Transportation Research Board of the National Academies, Washington, D.C., pp 75-84.

Carter, A. (2004). *Development of a Non-Solvent Based Test Method for Evaluating Reclaimed Asphalt Pavement Mixes*. (Doctoral Dissertation, Auburn University).

Christensen and Anderson (1992). Interpretation of Dynamic Mechanical Test Data for Paving Grade Asphalt Cements. *Journal of the Association of Asphalt Paving Technologist*, Vol. 61, pp. 67-116.

Christensen, Jr., D.W., T. Pellinen, and R.F. Bonaquist (2003). Hirsch Model for Estimating the Modulus of Asphalt Concrete. *Journal of the Association of Asphalt Paving Technologists from the Proceedings of the Technical Sessions,* Vol. 72, pp 97-121, Lexington, KY.

Collins-Garcia, H., Tia, M., Roque, R. and Choubane, B. (2000). Alternative Solvent for Reducing Health and Environmental Hazards in Extracting Asphalt: An Evaluation. *Transportation Research Record: Journal of Transportation Research Board, No.1712*, Transportation Research Board of the National Academies, Washington, D.C., pp. 79-85.

Daniel, J. and Lachance, A. (2005). Mechanistic and Volumetric Properties of Asphalt Mixtures with Recycled Asphalt Pavement. *Transportation Research Record: Journal of the Transportation Research Board, No. 1929,* Transportation Research Board of the National Academies, Washington, D.C., pp 28-36.

Dongre, R., L. Myers, J. D'Angelo, C. Paugh, and J. Gudimettla (2005). Field Evaluation of Witczak and Hirsch Models for Predicting Dynamic Modulus of Hot-Mix Asphalt. *Journal of the Association of Asphalt Paving Technologists from the Proceedings of the Technical Sessions,* Vol. 74.

Enviro Tech International, Inc. (2008). EnSolv Technical Data Sheet. Document No. 6000.

Hall, K.D. and Williams, S.G. (1999). Effects of the Ignition Method on Aggregate Properties. *Journal of the Association of Asphalt Paving Technologists, No. 68*, pp. 574.

Halogenated Solvent Industry Alliance, Inc. (2001). Trichloroethylene White Paper.

Huang, B., Li, G., Vukosavljevic, D., Shu, X., and Egan, B. (2005). Laboratory Investigation of Mixing Hot-Mix Asphalt with Reclaimed Asphalt Pavement. *Transportation Research Record: Journal of Transportation Research Board, No.1929*, Transportation Research Board of the National Academies, Washington, D.C., pp. 37-45.

Kvasnak, A., West, R., Michael, J., Loria, L., Hajj, E., and Tran, N. (2009). Evaluation of the Effect of Reclaimed Asphalt Pavement Aggregate Bulk Specific Gravity on Voids in Mineral Aggregate. *Transportation Research Record: Journal of Transportation Research Board, No.2170*, Transportation Research Board of the National Academies, Washington, D.C., pp. 30-35.

Li, X., Marasteanu, M., Williams, R.C. and Clyne, T. (2008). Effect of Reclaimed Asphalt Pavement (Proportion and Type) and Binder Grade on Asphalt Mixtures. *Transportation Research Record: Journal of the Transportation Research Board, No.*

2051, Transportation Research Board of the National Academies, Washington, D.C., pp 90-97.

McDaniel, R., Soleymani, H., Anderson, R.M., Turner, P., and Peterson, R. (2000). Recommended Use of Reclaimed Asphalt Pavement in the Superpave Mix Design Method. *NCHRP Web Document 30 (Project D9-12): Contractor's Final Report*

McDaniel, R. and Anderson, R.M. (2001). Recommended Use of Reclaimed Asphalt Pavement in the Superpave Mix Design Method: Technician's Manual. *NCHRP Report 452, Transportation Research Board-National Research Council*. Transportation Research Board of the National Academies, Washington, D.C.

McDaniel, R. and Nantung, T. (2005). *Designing Superpave Mixes with Locally Reclaimed Asphalt Pavement: North Central States Jointly Fund Study*. Research Pays Off: TR News 239, July-August 2005

Occupational Safety and Health Guideline for Trichloroethylene Potential Human Carcinogen, U.S. Department of Health and Human Services, Centers for Disease Control, 1988.

Prowell, B. and Carter, C. (2000). Interim Report: Evaluation of the Effect on Aggregate Properties of Samples Extracted Using the Ignition Furnace. *Virginia Transportation Research Council*, Charlottesville, VA.

Robbins, M. (2009). *An Investigation into Dynamic Modulus of Hot-Mix Asphalt and Its Contributing Factors.* (Master's Thesis, Auburn University).

Shah, A., McDaniel, R., Huber, G., and Gallivan, V. (2007). Investigation of Properties of Plant-Produced Reclaimed Asphalt Pavement Mixtures. *Transportation Research Record: Journal of the Transportation Research Board, No. 1998,* Transportation Research Board of the National Academies, Washington, D.C., pp 103-111.

Stroup-Gardiner, M. and Nelson, J.W. (2000). Use of Normal Propyl Bromide Solvents for Extraction and Recovery of Asphalt Cements. *NCAT Report* No. 00-06

Tran, Taylor, West, Kvasnak, and Turner (2009). Evaluation of Predictive Models for Determination of Binder Critical High Temperature from Mixture Properties. *Transportation Research Record: Journal of the Transportation Research Board, No. 2332,* Transportation Research Board of the National Academies, Washington, D.C.

Trichloroethylene MSDS (2010). Retrieved August 13, 2011, from http://www.phy.duke.edu/research/photon/qelectron/trichloroethylene_msds.pdf